



ILLINOIS

---

UNIVERSITY OF ILLINOIS AT URBANA-CHAMPAIGN

**PRODUCTION NOTE**

University of Illinois at  
Urbana-Champaign Library  
Large-scale Digitization Project, 2007.



DOC  
IL NHS  
CWE  
1994

**Natural History Survey  
Library**

# ILLINOIS NATURAL HISTORY SURVEY



## CENTER FOR WILDLIFE ECOLOGY

### **NEXRAD Algorithm for Bird Hazard Warning**

Contract No. 14-16-009-87-1221

**Final Report**  
**to U.S. Fish and Wildlife Service**  
1 June 1990 - 31 December 1992

Prepared by:

Ronald P. Larkin, Principal Investigator  
Illinois Natural History Survey

3 November 1994



## **Executive Summary**

The NEXRAD (WSR-88D) Doppler weather radar system is being installed throughout the United States, replacing the current generation of weather radars. Extensive computerization of the WSR-88D permits it to perform sophisticated and sometimes automated processing of the echoes it receives. Although designed to detect and warn of dangerous weather, the WSR-88D also receives echoes from flying birds, as determined by a preliminary study completed in 1983. This final report describes the results of research carried out at the Illinois Natural History Survey in 1984-1991 to develop a capability for the WSR-88D to process bird echoes. Three algorithms (or computer programs), described here, are the product of this research. They would permit the WSR-88D to process, quantify, and issue real-time information on bird echoes received by the radar, without human intervention.

Such capability is desired by military aviation safety authorities such as the U.S. Air Force Bird-Aircraft Strike Hazard (BASH) Team, because of continuing annual loss of lives and heavy dollar losses due to collisions between high-performance military aircraft and flying birds. Real-time warning of concentrations of flying birds, supplied by WSR-88D radars, would reduce this annual loss. In addition, use of these powerful instruments, which together nearly blanket the nation, as research tools will be beneficial to wildlife and agriculture as well as to aviation.

Research was carried out before quantitatively-accurate WSR-88D data became available; therefore, data from research weather radars were adapted to resemble WSR-88D data as closely as possible. Algorithm capability and skill were assessed by comparing algorithm results with separate visual and tracking radar observations and with various simulations and trial runs. Parameters in the algorithms that can be adjusted to suit new species or local conditions are defined in an Appendix.

The Migrating Birds Algorithm concentrates on broad-front migration of

mixed species of birds, most of which takes place at night in North America. Internally, it uses a knowledge matrix (expert system) approach to sort bird echoes from weather, insects, and clutter in widespread echo regions moving at night. The operation of this algorithm, which could not be verified to the degree that the other two algorithms were verified due to unavailability of data, is largely described in earlier interim reports.

The Roosting Birds Algorithm finds locations where large numbers of various species of birds, especially “blackbirds”, gather nightly and marks the area surrounding such roosts as hazardous for low-level operations, takeoffs, and landings. Internally, the algorithm uses a computer vision technique called the Hough Transform to recognize specific patterns generated by waves of birds departing a roost in the morning. The algorithm located about 75% of test roosts accurate to 2 km of their actual location and yielded a function relating echo strength to numbers of birds that was significant at  $p = 0.03$ . Larger roosts were located more accurately.

The Flocks of Waterfowl Algorithm focuses on particular days of the year when spatially-extensive flocks of large birds migrate *en masse* both day and night. Internally, a multidimensional track-while-scan operates on successive radar sweeps, taking advantage of known properties of the species of birds. Algorithm-generated paths of individual flocks were biologically accurate, corresponded to spot-observations in the field and to results of a limited hand-analysis, and were highly consistent among three migration events in three years. An extensive discussion of the kinds of errors to which such an algorithm is subject is presented.

## Executive summary

I. Introduction and general methods

II. Migrating birds

III. Roosting birds

IV. Following flocks of waterfowl

## Acknowledgements

## Literature Cited

Appendix I: Glossary and acronyms

Appendix II. English and scientific names of animals

Appendix III. The radar equation

Appendix IV. EMULATE\_NEXRAD subprogram

Appendix V. Adaptable parameters

## **I. Introduction and general methods**

Birds pose to military aviation a risk that is costly in dollars and in human lives (Blokpoel 1976, Gauthreaux 1974, United States General Accounting Office 1989). One way to reduce these costs is to reduce or avoid operations where hazardous birds are in the air. This can be accomplished on an actuarial basis, by forecasting the annual or daily statistical likelihood of the presence of birds and avoiding scheduling flight operations at those locations, times, and heights. It can also be accomplished on a real-time basis, by detecting the presence of hazardous birds on an hour-by-hour basis and rerouting, rescheduling, or canceling flight operations based on observed hazard. A preliminary study (Larkin 1982) established that large weather radars have a potential role both in providing better data for the actuarial approach and real time to warn pilots of birds.

The present study describes basic research behind the development and testing of weather radar algorithms to exploit this potential contribution of weather radars to military air safety. Many aspects of the project have been described in previous reports and papers (Defusco, et al. 1986, Larkin and Quine 1988, Larkin 1982, Larkin 1990, Larkin 1991b, Larkin and Quine 1987, Larkin and Quine 1989, Quine and Larkin 1987), whose contents will not be repeated here except where necessary e.g. to provide further data from those available earlier or to provide updated descriptions of algorithms.

Weather radars include a variety of different kinds of radars designed to detect echoes from moisture, particulate matter, and refractivity gradients and to aid in studying and forecasting air motion, rain, and other meteorological phenomena. The general characteristics of and principles behind weather radars are described in several books (Doviak and Zrnic 1984, Rinehart 1991, Skolnik 1970). Also, some technical radar terminology is briefly defined in Appendix I of this report. The weather radars discussed in the present report are all similar,



long-range radars sharing many characteristics: They have large antennas, resulting in great sensitivity and long-range detection capability and “narrow” beams on the order of  $1^\circ$ . They emit short pulses of microwave frequencies corresponding to wave lengths of about 10 cm (S-band) or sometimes 5 cm (C-band). They usually rotate slowly and continuously through  $360^\circ$  (a “sweep”) while changing angle above the horizon (elevation) more slowly. They record the amount of echo that returns to the radar (reflectivity, see Appendix III), the phase shift of that echo that results from motion, if any, toward or away from the radar (Doppler speed), and usually the amount of variation in Doppler speed (Doppler spectral width or sometimes variance), which is often attributable to variable motion by several scatterers at nearly the same range or to different motions by different parts of the scatterer.

The heretofore-standard U.S. operational weather radar, the model WSR-57, (Gauthreaux 1992) is being replaced by more a modern Doppler radar initially known as the Next Generation Weather Radar and now officially known as the WSR-88D (Crum and Alberty 1993, Crum, et al. 1993, Klazura and Imy 1993). The WSR-88D has better electronic specifications than its predecessors but more important attributes for the present application include:

- Doppler ability.
- Sophisticated data delivery and display capability .
- Computer-controlled operation and processing of weather echoes.

Importantly, this radar system contains enough computer power at each radar unit that it will be feasible for the WSR-88D to function as a bird-warning device at those (many) times when severe weather does not exercise the full capacity of the WSR-88D. Because the operators of the WSR-88D will not be trained as radar biologists, it is desirable to build as much intelligence as possible into WSR-88D bird-recognition capabilities. Therefore, the present research sought to

design computer algorithms that can distinguish between bird echoes and other echoes in real time or near-real-time and report the presence of birds hazardous to aviation, without human intervention. The project does not address the primarily military problem of using such information to convey warnings to pilots or other personnel. A second goal of the project, that of developing the potential of automated weather radars to help in understanding the movements of flying animals, has been partly accomplished in the course of pursuing the more encompassing goal of automated bird recognition.

Initially, workers on the project envisioned a two-step process: (1) distinguishing bird echoes from other echoes and (2) processing the bird echoes to determine the nature, height, and magnitude of the hazard. As the magnitude of the overall problem became visible and as the echoes began to sort themselves out over the landscape, the investigators realized that different classes of bird echoes differ from one another as much as they differ from non-bird echoes; therefore, several different algorithms would be needed to handle several very different kinds of bird movements. Eventually there evolved a Migrating Birds Algorithm (Chapt. II) to handle broad-front, mainly nocturnal migration of mixed species of songbirds, waterfowl, shorebirds, and other birds; a Roosting Birds Algorithm (Chapt. III) to handle resident birds that congregate together every night and disperse again in the morning; and a Flocks of Waterfowl Algorithm (Chapt. IV) to handle well-oriented mass movements of spatially-extensive flocks at any time of day. Undoubtedly, modern weather radar can detect other kinds of hazardous bird movements for which further algorithms could be developed or for which the present algorithms could be adapted.

Although the three algorithms share some logic, they differ in fundamental ways. The Flocks of Waterfowl algorithm is somewhat similar to track-while-scan (TWS) techniques in radar engineering. The Roosting Birds Algorithm is

derived from pattern-recognition techniques in computer vision. The Migrating Birds Algorithm is a simplified expert system that relies on a knowledge matrix designed to permit discrimination of different kinds of diffuse echoes on weather radar. The former two algorithms' computations depend on an earth-based inertial Cartesian coordinate system (Bogler 1990) but the Migrating Birds algorithm operates directly in the weather radar's polar coordinate system.

Each of the algorithms uses numerical parameters (constants or data values) essential to discrimination of wanted from unwanted echoes, processing of bird echoes, and quantification of numbers of birds and other indicators of the degree of hazard. Much of the research behind the algorithms was devoted to determining the best values for these parameters. Nevertheless, some of the parameters will require changing for different sites and different mixtures of species of birds, for WSR-88D radars *per se* (see below), and as our knowledge of the appearance of bird echoes on weather radars advances. These parameters are listed in Appendix V as adaptable parameters to emphasize their developmental nature.

Even though designed for meteorological purposes, weather radar is useful as a research tool in better understanding the movements of birds and other flying animals (Eastwood 1967, Gauthreaux 1992). The issue of whether birds can be detected on radar was settled long ago (Lack and Varley 1945) and will not be argued here. If animals fly high enough above the ground clutter, they can be detected on radar. English and scientific names (American Ornithologists' Union, 1983) mentioned in this report are listed in Appendix II.

Bats are known to be a significant hazard to aviation only in the special circumstance of mass emergence from daytime roosts (Williams and Williams 1969). Such emergence has been detected on the WSR-88D weather radar (T. O'Bannon, pers. comm.), but bats have not been studied in connection with the

present project. It is possible that the Roosting Birds Algorithm (Chapt. III) could be adapted for evening use with colonies of bats.

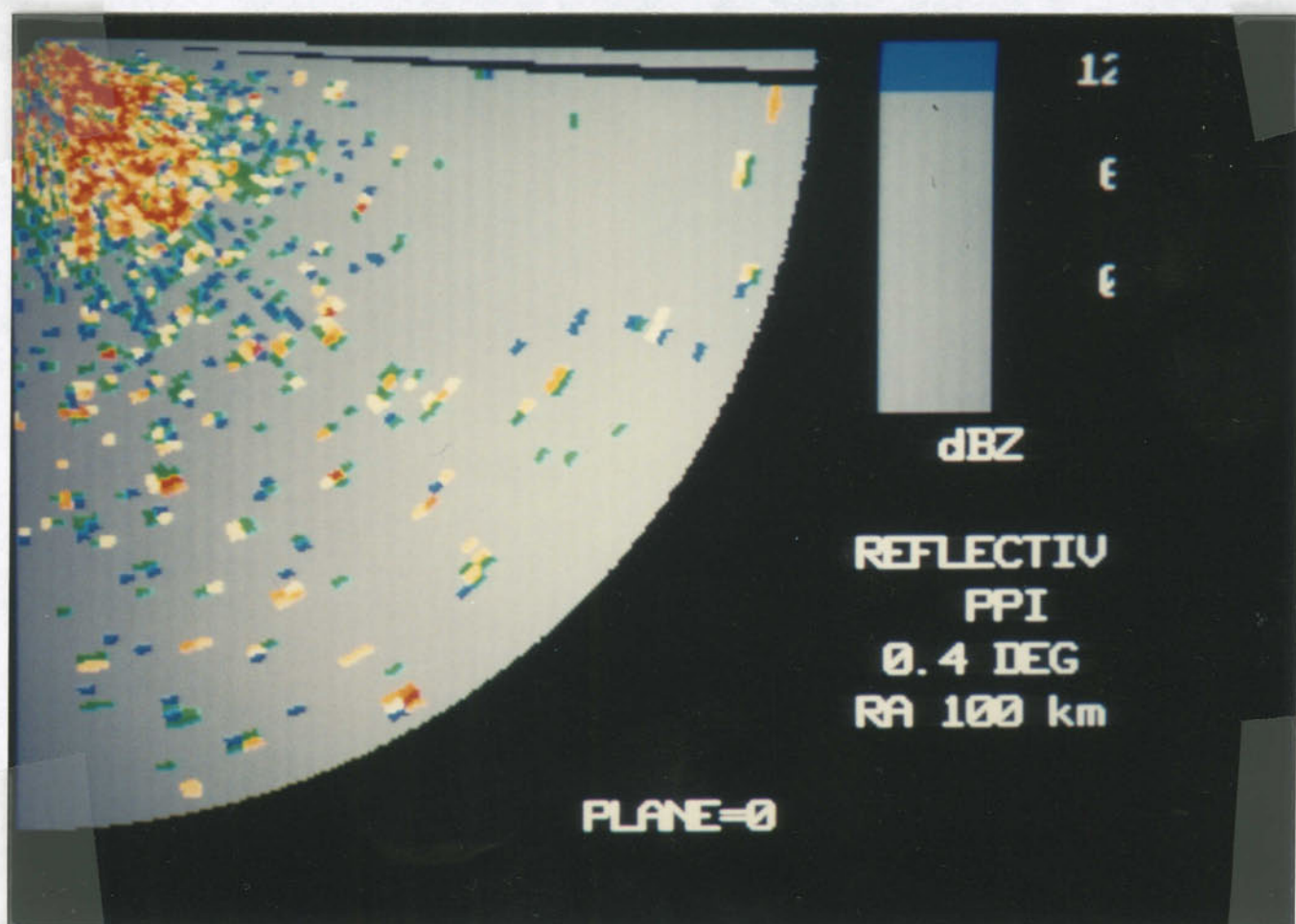
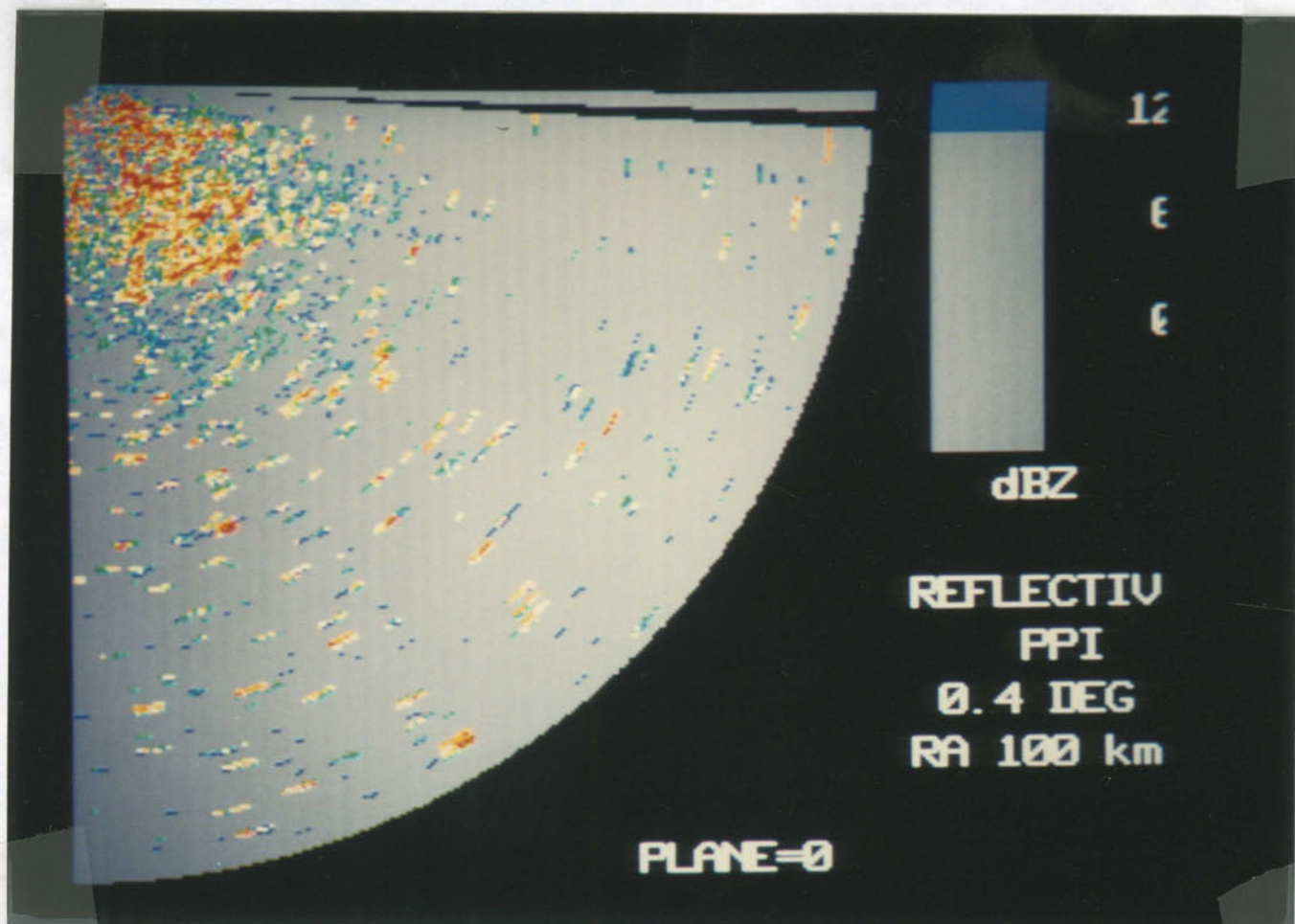
Insects (Achteemeier 1992, Larkin 1991a, Mueller and Larkin 1985, Rabb and Kennedy 1979, Riley 1989, Vaughn 1985, Wolf, et al. 1993) and arachnids (spiders) (Greenstone 1990, Greenstone 1991) can be detected and studied with radar. Because aerial spiders are usually a minor source of radar echo compared to insects, because "radar entomology" has become a subdiscipline in itself, because "insect" is a better-known term than "arthropods", and with apologies for taxonomic inaccuracy, "insects" will be used in this report instead of "arthropods". Insects are not important in North America as a hazard to aircraft, but their similarity on search radars to low-intensity migration of songbirds presents problems for the Migrating Birds Algorithm (Chapt. II).

The present project was coming to termination just as the WSR-88D was starting to be deployed but before useful data from WSR-88D's were available for study. In addition, early WSR-88D's operated in a mode known as circular polarization, which introduces poorly-understood complexities into the interpretation of animal echoes on radar. Although all current WSR-88D's have simpler and much better-understood linear polarization, this was not the case during the field research for this project. Therefore the project used quantitative data gathered from several linear-polarized research radars whose characteristics are summarized in previous reports (Larkin and Quine 1987, Mueller, et al. 1989) but not from WSR-88D's. Chief among these by far is the CHILL radar (acronym standing approximately for "CHicago University, University of ILLinois"), operated until 1990 by the Illinois State Water Survey under the direction of Dr. Eugene Mueller. CHILL clutter suppression is described in (Peltier 1989).

Recognizing that problems will arise from applying data gathered on one

radar to an algorithm intended for a different radar, authors of the bird hazard algorithms took care to minimize incompatibilities. This was done by software massaging of data from each of the research radars to make the data resemble as much as possible WSR-88D data as described by the NEXRAD specifications (NEXRAD Joint System Project Office 1981), constituting a software emulation of the NEXRAD hardware. This effort succeeded largely because data from most research radars are available at higher spatial and temporal resolution than WSR-88D data, so that little or no information was usually lost in the emulation. This process, which we call "NEXRADizing", is accomplished by the computer code listed in Appendix IV.

A pair of before-vs-after color images (next page) illustrates NEXRADization on clumps of bird echo from migrating flocks of Canada Geese. Shown is the southeast one-quarter of a digital Plan Position Indicator display from 16 Dec 1987 at 1314 CST. The CHILL radar, located at Willard Airport in Champaign County, Illinois, is at the origin at the upper right and the radius of the image is 100 km. Echoes near the radar are ground clutter (no clutter suppression is being used); echoes beyond about 40 km are nearly all flocks of Canada Geese flying along approximately SSW paths and disappearing off the periphery of the image. In accordance with what has become a common convention on weather radar images, warmer colors represent higher reflectivity. The lowest reflectivity shown is 11 dBZ; 11-13 dBZ is blue; red includes all reflectivities > 32 dBZ. At the top are original CHILL data with 150-m range gates; at the bottom the same data after NEXRAD emulation. Smaller flocks of geese and miscellaneous unidentified small echoes are lost but the size, reflectivity, and echo topography of the medium- and large-size goose echoes remain after NEXRADization.



The WSR-88D system has point-clutter suppression ability, so that point targets will or will not be detected by the system depending on its mode of operation. The algorithms described here are conservative in that they assume that point-clutter suppression is active and that, therefore, bird echoes must be spatially-extensive to be detected. If point clutter suppression is inactivated, then intensely future interesting projects, such as recognizing migrating raptors, become possible.

The spectral width measure behaved more like a chimera than a Base Datum during this research. Spectral width is produced by the WSR-88D and by many research radars, but reliable spectral width data were available only very late in the present research. In particular, only negligible spectral width data were available on documented movements of migrating birds. Additionally, after dealing with spectral width data from five research radars, we learned not to assume that measures of spectral width are accurate and comparable based on engineering claims alone. Finally, spectral width data are gathered far more than they are used by radar meteorologists, so that a firm theoretical and empirical basis for interpreting spectral width data and for characterizing spectral width of clutter, weather, and other non-bird targets had been largely lacking. Although this situation is rapidly improving, partly due to the potential availability of plentiful, standardized spectral width data from the WSR-88D, recent developments have not helped the present research.

**II. Migrating birds**

---

Echo Components . . . . .	1
“Ground truth” . . . . .	4
Insects . . . . .	8
Spectral width . . . . .	11

---

The Migrating Birds Algorithm seeks to recognize and quantify widespread migratory movements of mixed species of birds, using the WSR-88D. Previously-described automated systems for real-time detection of animal migratory movements by radar (Beerwinkle, et al. 1993, Hunt 1975, Larkin and Eisenberg 1978) are more limited than the present effort in that they involve small, specialized, X-band radars that are aimed vertically rather than scanning a wide area.

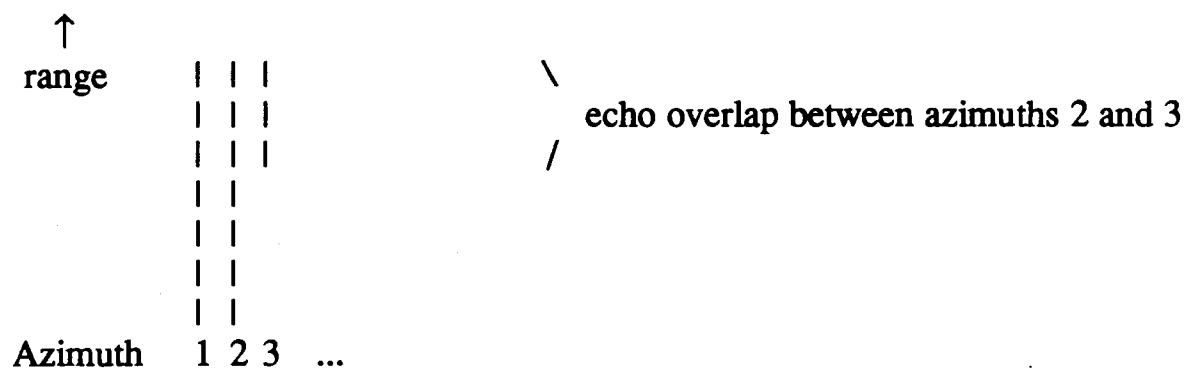
Largely because the Migrating Birds Algorithm was developed first, it is more fully described in earlier publications than the other bird hazard algorithms (Larkin 1990, Larkin and Quine 1987, Larkin and Quine 1989). Larkin (1982a) has color illustrations of the appearance of migrating birds on weather radar. However the Echo Components algorithm, which examines weather radar products and passes regions of contiguous echo to the Migrating Birds Algorithm, is not previously described and therefore is described here. The names of these algorithms were selected in parallel with WSR-88D algorithms that have similar function but which are less flexible and do not adequately handle echoes from animals.

The **Echo Components** algorithm operates at one elevation in the radar’s polar coordinates. It assembles at least NsegThL (see Appendix V) Echo

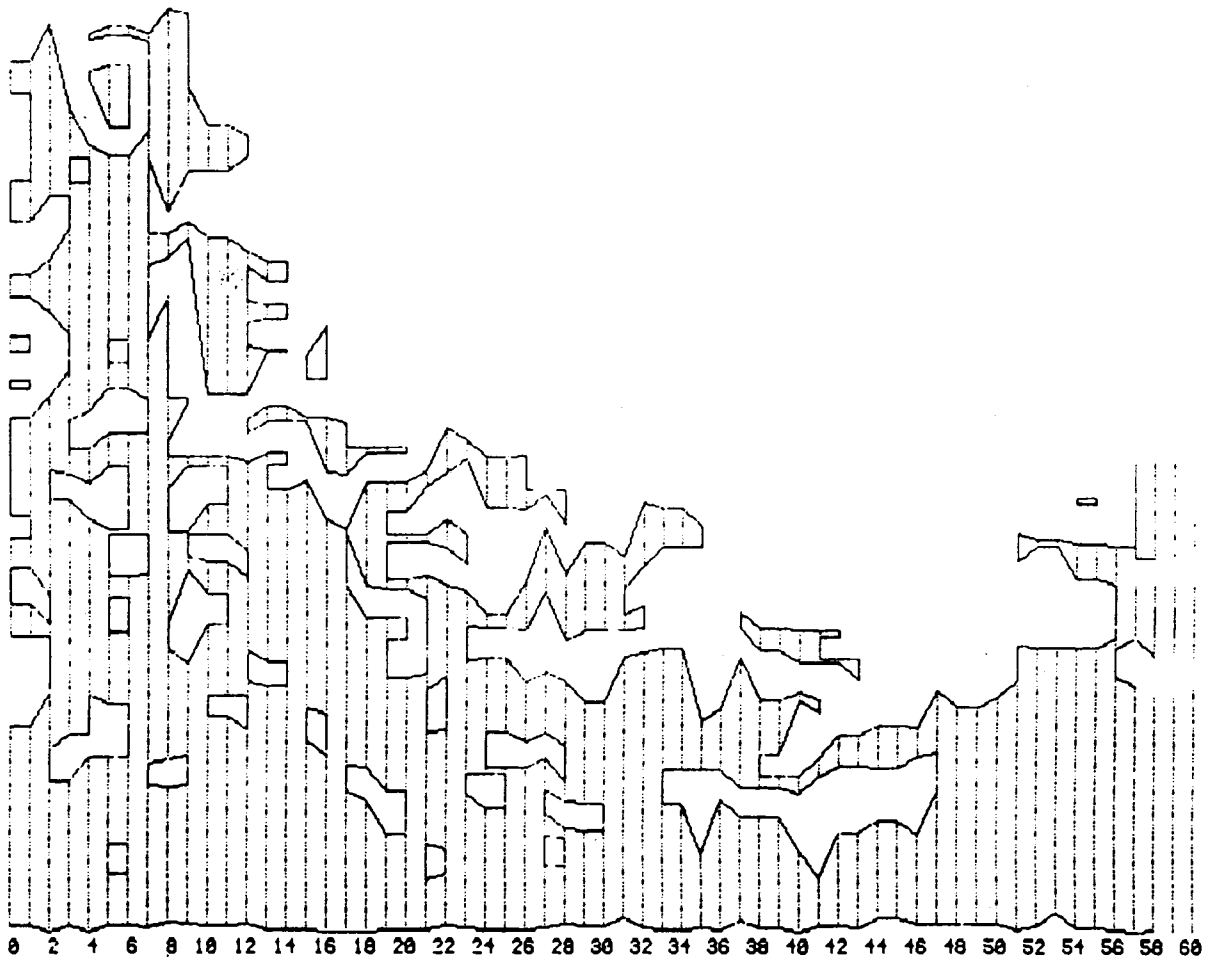


Segments of contiguous echo for processing by the Migrating Birds Algorithm. Its operation is preceded by collection of gates with reflectivity  $> \text{RefThL}$  into Echo Segments, consisting of at least  $\text{NgateThL}$  radially-contiguous gates with no gaps longer than  $\text{DropThU}$  gates. The Echo Components algorithm searches radially clockwise for echo segments that are not yet part of an echo component. Echo segments having gates with echo that overlap in range (see diagram below) and are within  $\text{DropThU}$  of each other in either azimuth are accumulated into the same Echo Component. For ease of later computations, small holes in echo components having gates with reflectivity  $< \text{RefThL}$  are flagged as artificial gates; they are not included in later analyses. (The process of filling small holes actually requires much more software logic than the functioning of the Echo Components algorithm proper.)

---



During its progress the Echo Components algorithm tallies the area of the echo component, to be used in later calculations.



The plot of range as a function of azimuth, above, illustrates the operation of the Echo Components algorithm on radials 1 through 60 ( $1^\circ$  through  $60^\circ$  azimuth) of a weather radar image of migrating birds. The dashed radial (vertical) lines represent supra-threshold echoes extending from close to the radar (bottom of figure, less than MinRange), where ground clutter has been filtered out, to the maximum range at which birds appear on the image (top of figure, determined by the maximum height of migrants on this night). All solid lines were drawn by the Echo Components algorithm and divide the echo region into regions of contiguous echo. There are one large echo region with many holes and incursions and several small islands of disconnected echo; five such small regions are shown in entirety in the plot. The algorithm's work on the

rightmost radials (57 through 60) is unfinished because of truncation of the figure, the entirety of which extends through 360°. All echoes in an Echo Component are submitted to the Migrating Birds Algorithm.

### **“Ground truth”**

Testing any method of recognizing and measuring bird migration with radar requires “ground truth”, or an independent means of determining what is producing a radar echo and quantifying the characteristics of the actual source of the echo, especially its quantity or density. Simplifying somewhat, widespread, moving echoes can consist of water (precipitation and dense cloud), insects, birds, or any mixture of the three. Although birds especially are less common in cloudy or rainy conditions than in clear conditions (Alerstam 1990, Richardson 1990), we feel that data to establish bird/nonbird boundaries should consist of independently-derived, numerical measures of the number of flying birds present as a function of height and, if possible, of space and time as well.

Before discussing such measures, polarization diversity in weather radar (Guli 1986, Seliga 1980) must be mentioned. Linearly-polarized radar waves may be oriented horizontally or vertically. Flying animals, which have bodies that are roughly horizontally aligned during cruising flight, give much stronger radar echoes from horizontally- than from vertically-polarized radar waves, provided that certain statistically-unlikely combinations of body orientation, body length, and radar wavelength do not pertain. In 1982, the CHILL radar could transmit and receive either horizontal or vertical polarization on a pulse-by-pulse (i.e. 1 ms) basis and generated differential reflectivity ( $Z_{DR}$ ) data, which consist of ratios expressed in decibels (Mueller and Larkin 1985). Valid  $Z_{DR}$  or similar polarization diversity data were not available on CHILL or on any other research radars used in this project after 1982. (Collaboration with CHILL ceased when it

moved to Colorado in early 1990.) Except during snow, it appears that polarization diversity can serve as a powerful tool to discriminate flying animals from weather and other echoes; however, the present project was not able to pursue this method further.

Because most bird migration and much insect migration occurs at night hundreds of meters or more above the ground, few methods are available for obtaining "ground truth" for flying birds. An auditory method, counting nocturnal flight calls of birds (Evans 1994, Graber and Cochran 1959, Graber and Cochran 1960) is very useful for establishing that certain species or species groups are in flight on a given night, but its usefulness as tools for counting nocturnal migrant birds is limited by several problems. These include the inability to detect quiet species and individuals and, in many cases high-flying birds; imperfect, if any, ability to determine height with available methods; and the present near-dearth of data cross-calibrating flight call counts with other methods. Visual methods of observing nocturnal migration include using beams of light and watching the moon. Observations with vertically-pointing narrow-beam lights (Able and Gauthreaux 1975, Gauthreaux 1969) generate useful quantitative data but are low-yield, generate only rough data on height and size of birds, probably fail to detect high-flying birds, and suffer from other difficulties (Larkin, in prep). Observing birds crossing the face of the moon through a telescope (Newman and Lowery 1964, Nisbet and Drury 1969) has similar positive points and problems. There are no published methods of automating the aforementioned techniques and the elements of subjectivity and observer skill and vigilance are poorly controlled in most studies.

An accurate tracking radar (GPG-1, X-band) was used in the present project to count and characterize bird and insect targets in nocturnal migration (Achtemeier, et al. 1987, Larkin and Thompson 1980, Larkin 1982a, Larkin

1982b, Larkin 1991a, Mueller and Larkin 1985). The tracker, although having only about one percent of the effective range of the CHILL radar, provided information on wing beats of individual migrants (thus discriminating birds from insects), their size (from calculation of radar cross section, Larkin and Quine 1987), their vertical distribution in the atmosphere (mainly via stationary, vertical-beam, automated operation; Larkin 1982b), and their flight speed and heading as well as their path across the ground. Flight speed and heading were calculated using accurate wind data from radar-tracked balloon-borne targets. As migrating birds and insects passed over and moved beyond the X-band radar, usually located near a research weather radar, the tracker sampled the flying fauna, which, no other indication to the contrary, was taken as representative of migratory fauna in other regions of the weather radar. In support of this and other projects in 1982-1988, the Illinois Natural History Survey tracking radar was operated until late 1988, when it could no longer be maintained.

Tracking radar data taken in cooperation with weather radars.

Date	Loc.	Begin	End	birds	in- sects	un- known	bal- loons	other	total
13MAY82	MRFS	2039	2142	0	0	21	1	0	22
14MAY82	MRFS	2229	2314	2	0	57	2	0	61
17MAY82	MRFS	2115	2358	0	0	68	2	0	70
19MAY82	MRFS	2226	0220	8	2	122	3	0	135
14JUN82	MRFS	2116	0007	3	0	49	2	0	54
29OCT84	AFGL	1758	0004	86	7	9	4	1	107
30OCT84	AFGL	1633	2058	71	13	4	3	0	91
02NOV84	AFGL	1800	2135	73	4	7	2	0	96
30SEP87	MRFS	1618	2240	33	28	15	2	0	78
07OCT87	MRFS	1818	2143	27	6	1	2	2	38
20OCT87	MRFS	1404	0021	58	7	17	2	0	84
27OCT87	MRFS	1614	0027	65	23	30	4	1	123
02NOV87	MRFS	1954	2133	8	9	0	1	1	19
04NOV87	MRFS	1214	2130	28	11	9	2	1	51
19NOV87	MRFS	1725	0355	46	6	11	3	3	69
20SEP88	MRFS	1848	2229	25	8	35	2	1	71
06OCT88	MRFS	0756	0554	49	13	7	6	2	77

Tracked radar targets. Identification of birds vs. insects is based on operator classification, which is concordant with several objective indications of target identity (Larkin, 1991a). "Balloons" were 15-cm spheres borne aloft by 100-g weather balloons, for local wind measurements. "Other" targets included aircraft. "Unknown" targets predominated in 1982, before the high proportion of insects in the population of tracked radar targets was known. "Begin" and "End" are times of tracking radar data collection.

MRFS = Monticello Road Field Site, about 10 km SW of Champaign, IL  
 AFGL = Air Force Geophysical Laboratory, Sudbury, MA

**Insects on radar are the subject of the subfield of radar entomology (Riley 1989, Vaughn 1985). Insects migrate at many times of the year, as indicated by X-band tracking radar observations of flying insects on 29-30 November 1984 at Sudbury, Massachusetts and beginning on March 1, 1985 near Champaign, Illinois. As indicated by tracking radar data from these two locations and from Wisconsin, Michigan, and New York, bird migration in Eastern North America usually occurs intermixed with insect migration. However, several important factors will usually separate bird from insect targets:**

- **Insects will seldom show the same distribution with height as birds show.**
- **Insects fly with lower air speeds than birds (Larkin 1991a). Birds will often cause discrepancies between independently-derived (e.g. Rawinsonde) winds and weather radar-derived winds, whereas insects alone will cause only small discrepancies, if any.**
- **Insects are smaller than birds, especially in relationship to the 10-cm wavelength of the WSR-88D and related radars. Therefore, in general, a disproportionately greater volumetric density of insects as opposed to birds aloft is required to generate a given level of 10-cm reflectivity. In addition, the common situation of a mixture of a certain density of birds and a certain density of insects aloft will result in echoes from birds dominating the radar return unless insects are a very large percentage of the animals aloft.**
- **Insects may show greater or lesser commonness of orientation at a given height than birds. Combined with differing distributions of body lengths between birds and insects and probably also influenced by different body shapes of bird and insect scatterers, different aspect effects of birds and insects can be anticipated sometimes. Such aspect effects show up as “dumbbell” or other patterns on scanning radars, including weather radars (see WSR-88D example, below).**

The following radar image was recorded from a single 0.5°-elevation sweep of the KOUN WSR-88 at Norman, Oklahoma at 2035 CDT on 10 Sept 1989 . KOUN was operating using circular polarization with Point Censor (clutter suppression) switched off. The middle of the State of Oklahoma nearly fills the image. The Base Reflectivity product of the WSR-88D shows echoes < 18 dBZ covering several counties; the corresponding Doppler image reveals that the region of echo is airborne, moving SSE downwind at slightly greater than the speed of the wind, as determined from the 1800 CDT N.W.WS. rawinsonde launched from the radar site. As determined from comparing sweeps at different elevations, the echoes appeared at low height around dusk (1934 CDT) and steadily grew in intensity and increased in height until plateauing and remaining roughly the same for several hours from about the time of this image. A later image from the same migration event is presented in monochrome in (Larkin 1991b).

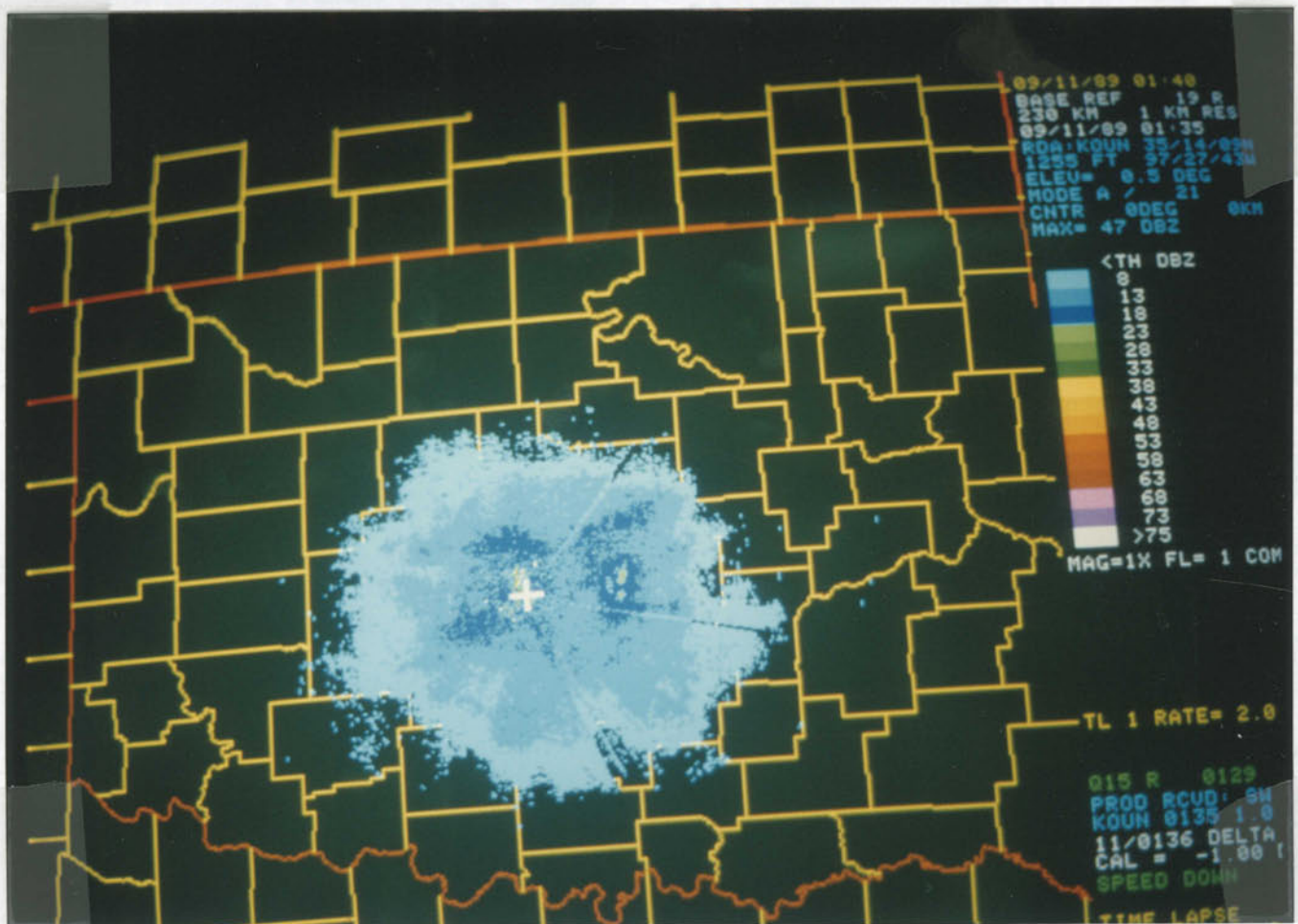
The source(s) of the extensive radar echo can be deduced from several lines of evidence:

- The echo was not ground clutter because it was moving.
- Skies were cloudless and reflectivities too high to be generated by refractive gradients.
- Decrease of reflectivity with range is consistent with a layer or truncated region of echo scatterers rather than meteorological volume-scatterers.
- The time and manner of appearance were typical, indeed nearly indicative, of the onset and ongoing progress of nocturnal migration as seen on radar.
- Wind was favorable for fall (roughly southward) migratory flight.



- Most of the echoes moved slowly (ca. 2 to 8 m·s<sup>-1</sup>) with respect to the wind.
- 10-cm reflectivity was characteristic of insect migration, with the highest values bordering on the lower values usually observed in nocturnal bird migration (Larkin 1982a, Mueller and Larkin 1985).
- Simultaneous visual observations at the radar site, using 8 x 40 binoculars coaxial with a stationary, vertically-pointed intense 1° light beam revealed a migration traffic rate of about 5 x 10<sup>4</sup> moths km<sup>-1</sup> of front hr<sup>-1</sup>. Some or many of these moths were undoubtedly flying too low to be detected by the WSR-88D, but others appeared to be higher, at heights corresponding to the limit of visibility. Migrating birds were also seen but their numbers were too few to quantify, certainly much less than is observed on favorable nights for fall migration in eastern North America.
- The region of more intense echo to the E of the radar is consistent with (1) higher reflectivity to the E than to the W of the radar and (2) an aspect-related reflectivity peak orthogonal to the direction of travel of flying animals, in this case roughly S or SSW (Mueller and Larkin 1985).

These WSR-88D echoes from 10-11 May 1989 represent a mixture of migrating insects and migrating birds. Although the proportion of insects vs. birds cannot be quantified with any certainty, the evidence suggests that insects were the principal source of the echoes. Our previous experience from eastern North America suggests that it is likely that the proportion of birds vs. insects varied with height.



The KOUN figure illustrates the difficulty of accurately discriminating birds from insects on large weather radars.

**Spectral width** is one of three base products of the WSR-88D (Larkin and Quine 1989, Sirmans 1988). Despite many unsuccessful attempts on several research weather radars, no completely satisfactory spectral width data were taken on known concentrations of migrating birds in connection with this project. This is especially unfortunate because some qualitatively-correct but quantitatively-suspect data that were gathered indicate that spectral width is one of the more powerful parameters with which to discriminate animal echoes from weather echoes.

### III. Roosting birds

---

Background .....	1
Methods .....	3
Ground truth .....	3
Single-sweep nature of the algorithm .....	5
Computation of civil sunrise .....	9
The running test algorithm .....	9
Overview of processing one sweep .....	10
The generalized Hough transform, coordinate transformation, and filtering .....	10
A modified Hough transform .....	14
Identification of roosts .....	17
Algorithm output .....	22
General characteristics of roosting birds on weather radars .....	23
Periods of data gathering .....	23
Times of peak departures of roosting birds .....	27
Reflectivity .....	28
Doppler velocity .....	29
Spectral width .....	33
Performance .....	35
Sample sizes .....	35
Tests with artificial data and special data .....	35
Echoes that are not roosting birds .....	36
Locations of roosts .....	39
Sizes of roosts .....	44
A test for extraneous targets using Doppler velocity .....	48
Computation time .....	52
Some foreseeable problems .....	52

---

#### Background

Roosts are places where aggregations of birds spend the night, typically in trees, human-built structures, or tall grass (Allen and Young 1982). The biological functions of such roosts are the subject of ongoing debate (Tye 1993). In fall and winter, roosts of  $10^5$  birds are common and roosts of  $10^7$  birds are

documented. Such concentrations of birds are an important hazard to aviation on takeoff and landing approach. Organized movements of birds flying to and from roosts are observable on radar. They were studied with meteorological radar as early as 1957 (Eastwood, et al. 1962, Harper 1959). These initial radar studies quickly established the seasonal nature of roost occupation, the low height of roosting flights, and the dramatic synchronization of morning departure vs. the more subtle patterning of evening return to the roost (Blokpoel 1970).

Work was begun in 1987 on a WSR-88D algorithm using image processing techniques to automatically locate and measure the size of roosts. Its rationale and method have been described in previous reports (Larkin 1990, Larkin and Quine 1989, Quine and Larkin 1987).

Several kinds of birds gather together in large communal roosts and are hazardous to aircraft, to varying extents. Some species are more amenable to observation with radar than others (Ansorge, et al. 1992). The most prominent roosting species in North America are collectively referred to as "blackbirds". Depending on time of year and other factors, they roost and often depart together and have similar behavior (Caccamise and Fischl 1985, Caccamise, et al. 1983). The European Starling is the most numerous member of the "blackbirds" in most of the roosts studied in this project. Its characteristic flight speed (ca.  $20 \text{ ms}^{-1}$ , Eastwood 1967) and roosting behavior are typical of those of other "blackbirds". The "blackbirds" are may be year-round residents in some parts of the USA but commonly they are migratory or partially migratory, becoming much more numerous in winter in the southern parts of their ranges.

Other important roosting species in North America are American Crow, American Robin, and several species of herons and egrets. These species, although not as ubiquitous as "blackbirds", are numerous and important hazards in their own right. For instance, traditional roosts estimated to comprise  $10^5$

American Crows (Black 1941:92) or  $3.5 \times 10^6$  American Robins (Graber, et al. 1971:10) are recorded in the Midwestern USA. A roost of  $7 \times 10^3$  American Crows at Danville, Illinois was visible on the CHILL radar in the studies reported here but the echoes from these crows were sometimes difficult to distinguish from those from nearby "blackbird" roosts.

Large cold-weather roosts used by "blackbirds" are traditional. The longest recorded winter European Starling roost in Britain was still in use in 1982 after 135 years and 70% of winter roosts in one study lasted >5 years in Europe (Feare 1984:49). Such long-lived roosts are probably more typical of Europe than the USA, where urban roosts are often harassed by their human neighbors and forced to relocate, but week-to-week stability in the location and approximate size of roosts is common even in urban areas.

At first, when we had data available on only one about species, this algorithm was called the Starling Detection Initiative. However, we noticed that the acronym for this name was already in use for a somewhat larger government project, so the broader name Roosting Birds Algorithm was adopted.

## **Methods**

"Ground truth" during the roosting birds research was supplied by field observers using binoculars and still cameras on foot or in vehicles. Thermal imaging (Marti and Heiniger 1987) to attempt to count "blackbirds" was tried unsuccessfully (Larkin 1990). Field observers sought to record the number of birds in roosts and their species composition. During morning departures they also sought to record for each flight of groups of birds the numbers, directions, times to the nearest second, and, when possible, paths leaving the roost. Some roosts could be observed by a single observer from a location such as a highway overpass, other roosts required more than one observer to document patterns of

departure.

Real-time communication between field observers and operators of the radar during the ca. 20-40 minutes of active morning departure was seldom necessary, but confirmation of the radar status before the observations benefitted morale and playback of the morning's data immediately after the departure was useful for comparing field with radar observations and planning for succeeding mornings' work.

The locations of active roosts were often known to the observers on a day-by-day or week-by-week basis. When this was the case, the principal challenges lay in scheduling radar observations and attempting to count the sizes and directions of departing groups of birds. However on the frequent occasions when season, bad weather, radar schedules or downtime, or other circumstances interrupted field work, it was necessary to determine where birds were currently roosting within the ca. 20,000 km<sup>2</sup> area in practical driving distance from the radar. It was almost immediately obvious to the field observers that they could locate roosts much easier by following groups of birds returning to the roost in late afternoon than by attempting to determine where birds observed flying in the morning had spent the night. What was not immediately obvious but soon became clear was that the field biologist's customary approach of finding the birds, then studying them on radar, was inefficient. Radar did a better job. A few minutes on a calm morning observing the real time color display of a weather radar usually revealed the locations (within a few km) of several or many roosts of varying sizes; the subsequent field work of documenting the exact location of the roosts then could be accomplished very quickly even by observers with minimal field skills.

Therefore, we scheduled the field work of locating and counting roosts around radar availability and weather. Roosts known to the observers were

studied prior to and on the morning of radar observations. Roosts found during a morning's radar observations were located and studied during the next 24-36 hours. Whenever possible, the numbers and times and directions of departure of birds were recorded on each morning when radar data were taken and were used in estimating the relationship of radar data such as reflectivity to number of birds. However, personnel were limited in number and sometimes unavailable for field sessions at 0430. Roosts that could not be observed simultaneously with radar observations were therefore sometimes counted beforehand (e.g. on the evening before radar observations were conducted) and recounted on subsequent mornings or evenings; stable counts indicated a traditional roost whose location and size was considered verified. Nevertheless, in spite of much field work, the yield of good-quality radar echoes and directly comparable, contemporaneous, complete field observations was low.

**Single-sweep nature of the algorithm.** When radar sweeps spaced at close intervals are available, the most distinctive feature of echoes of departing birds is their movement, radially outward like ripples from a stone thrown into a still pond. In fact, echoes even of large roosting birds are often indistinct from ground clutter unless they are spatially patterned (see figures on following three pages). However, present WSR-88D scan strategies include a lowest-elevation ( $0.5^\circ$ ) sweep only about every 10 min. Thus, in most cases, the relatively short distances travelled by roosting birds provide recording of echoes during only one or two sweeps from a given wave of departing birds. (However subsequent sweeps may record echoes from additional waves of birds from the same roost.) Therefore, the Roosting Birds Algorithm completely ignores information about the movement of echoes from roosting birds and relies entirely on (1) static spatial information from individual sweeps and (2) the traditional nature of roosts that change size and location only slowly on a week-to-week basis.

---

0629	0630
0631	0631
0632	0633
0634	0634

On the following pages are eight successive PPI images off CHILL, 0629 to 0634 12 Feb 89. The temporal arrangement of the images is shown in the figure at left. Elevation was constant at  $0.5^\circ$ , the square images are 160 km across, and principal roads make up a background map. CHILL echoes are not NEXRADized, to preserve their detail.

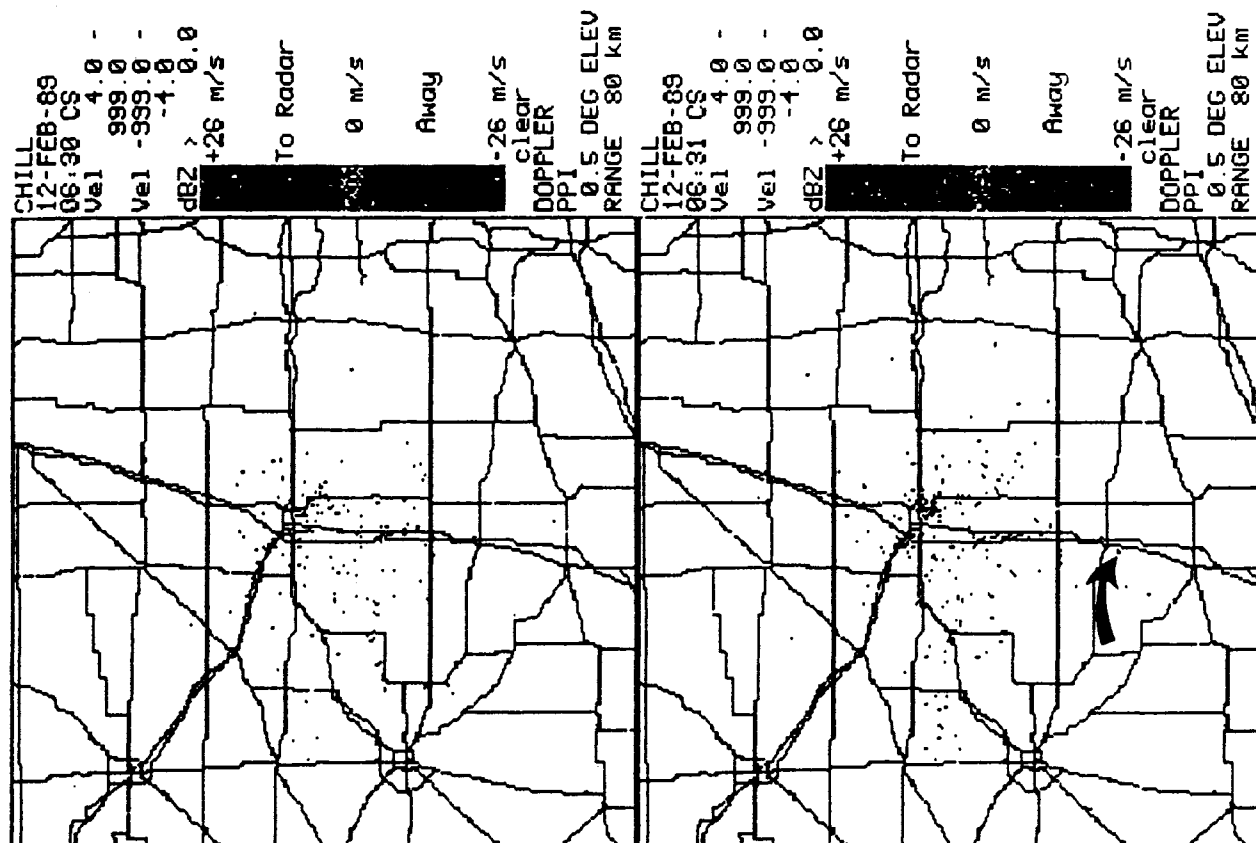
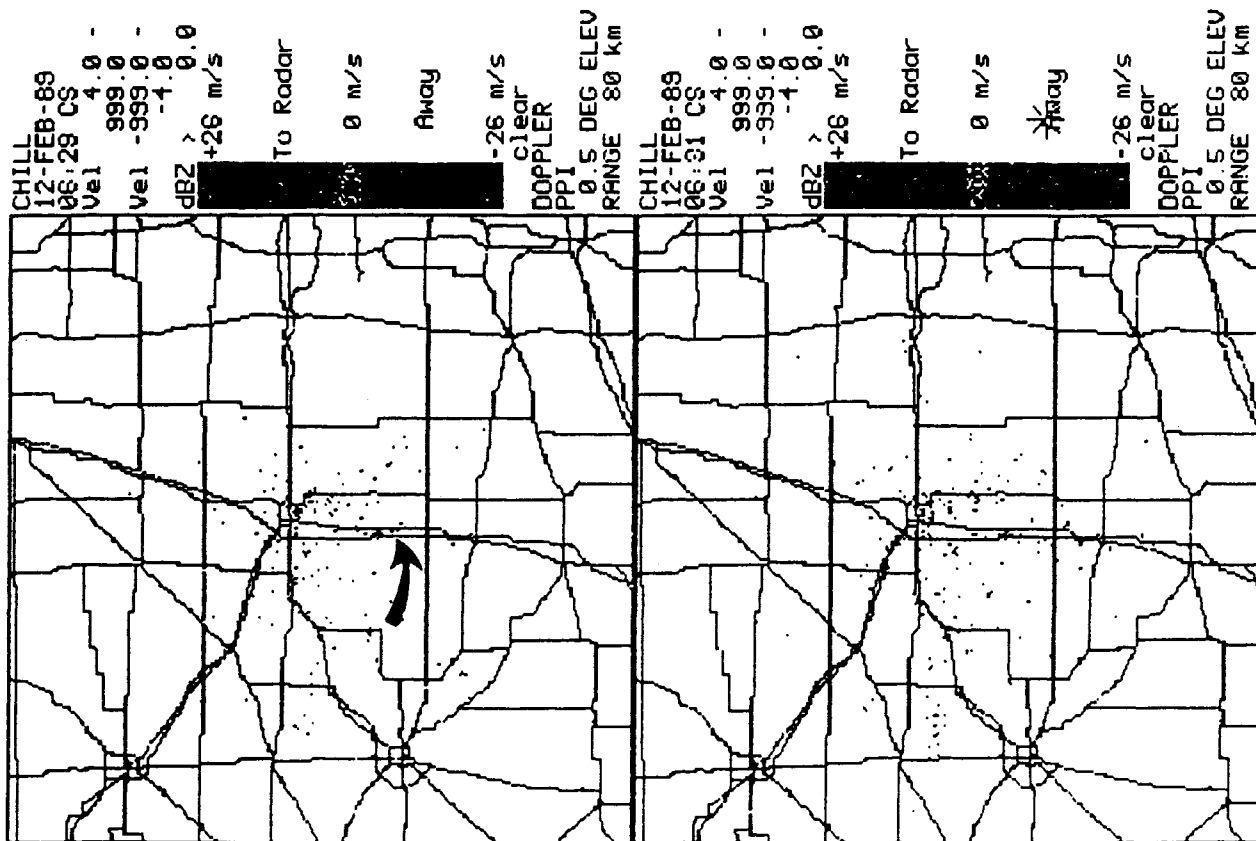
0629: The first arrow indicates several flocks of American Crows moving SW to SE out of Pesotum, IL. The movement was verified by observers on the ground.

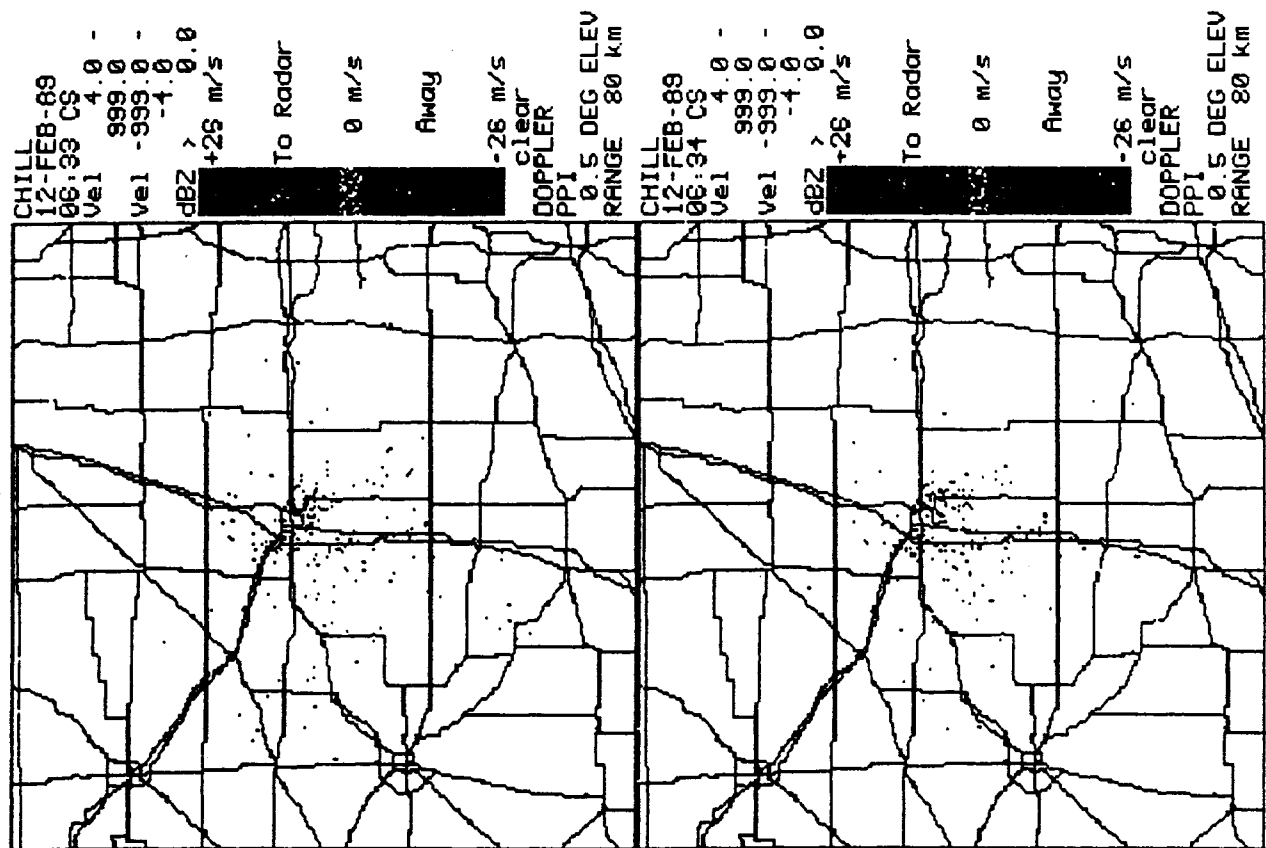
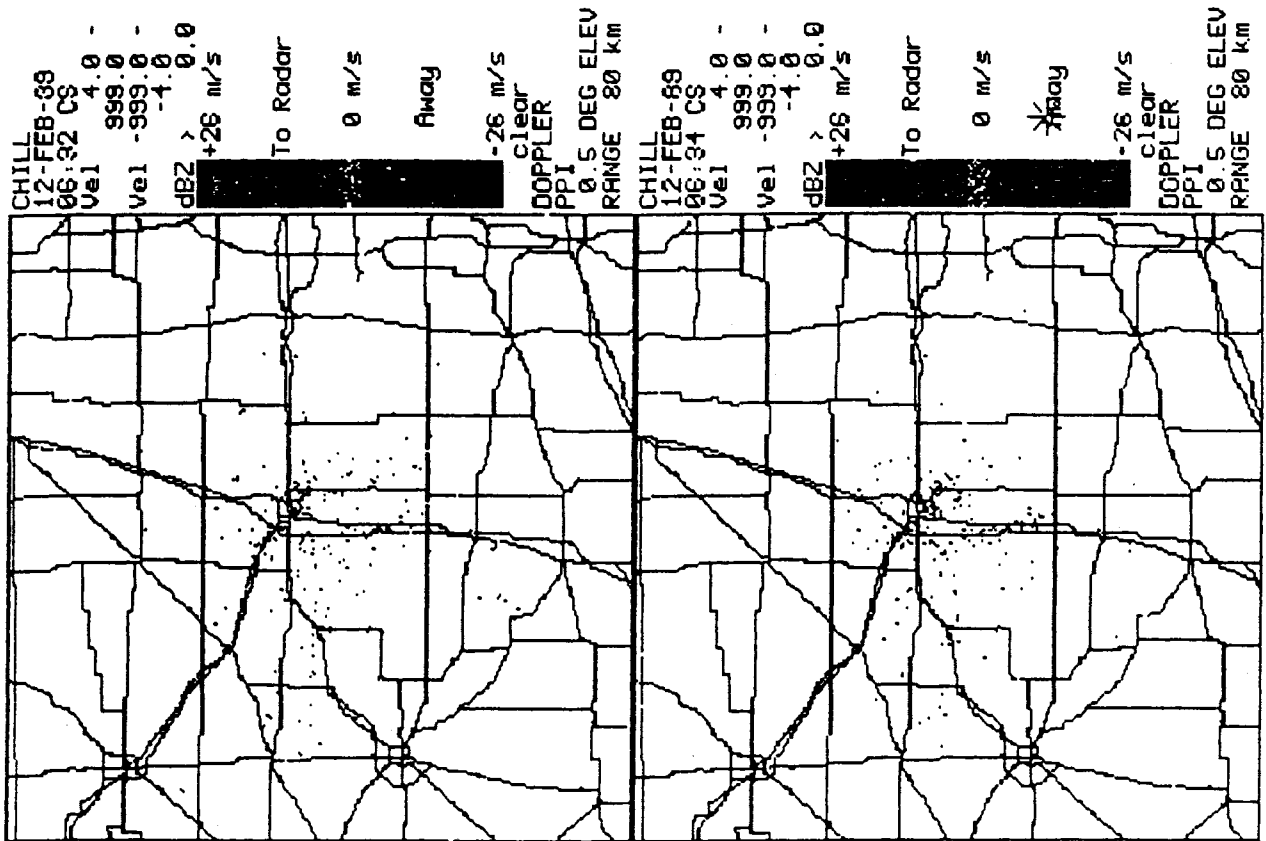
0631 (the latter 0631): The second arrow indicates the first of 5 images with one or two dot echoes moving S from Tuscola IL. These echoes are travelling about  $29 \text{ ms}^{-1}$  and are vehicles on Interstate Highway 57. Their distinct though small echoes can be seen progressing S, offset slightly to the W of I-57, until 0634. They are not distinguishable from the crow echoes in reflectivity or spectral width and are only about  $5 \text{ ms}^{-1}$  greater than the crow echoes in Doppler speed.

It is clear from spatially- and temporally-detailed images like these that roost departures moving bird targets are not discriminable from ground clutter without using information on the spatial characteristics of departing roosting birds.

---







**Computation of civil sunrise** is used to restrict the invocation of the algorithm to the time of day just before and just after dawn. This computation was obtained from a standard method (U. S. Naval Observatory 1987-1990) and coded in FORTRAN 77. Given latitude, longitude, and day of year (1-366), it estimates time of sunrise in decimal hours since 0000Z . Sunrise and other times were converted to local time. Even European Starlings enjoy the convenience of using US local time.

**The running test algorithm**, coded in VAX/VMS FORTRAN 77, requires only the name of a Universal Format (UF) input file and the name to be used for the Cartesian coordinate intermediate file; all other operation is automatic. Presently, the running algorithm expects the first sweep in the UF file to be the lowest elevation, typically nominal  $0.5^{\circ}$ , and it examines individual files without regard for morning-long or day-to-day history of the site. This test mode, necessary due to the intermittent nature of the data available from the research radars, will require enhancement to operate when continuous data are available as from WSR-88D's. Like the other bird algorithms being developed, the running algorithm reads most of its parameters, including most Adaptable Parameters (Appendix V), from an ASCII control file, so that adjustments to and experiments with different parameters may be performed to find appropriate values.

The running test algorithm outputs flat files of summary results and intermediate results. Both are suitable for later analysis, e.g. by statistical packages. In addition, it optionally shows its operation graphically on a color display screen by dynamically overlaying the double-triangular areas used for circle-searching over a map of the velocity data and, as roosts are found, drawing the center of the each roost over the data and the diameter of its circle under the data.

(The "center" of a roost will denote a single Cartesian location to be used for the geographic coordinates of the roost. In reality, any roost has some spatial extent and a large roost covers several hectares, but we require one characteristic location for the roost. In practice, on the scale of either weather radars or routes taken by aircraft, the distinction is not particularly important.)

**Overview of processing one sweep.** A sweep at  $0.5^\circ$  elevation is processed if it falls near dawn (see above) and if cloud, precipitation, bird migration, and insect migration can be ruled out as confounding factors at the lowest elevation. Positive results from the Storm Segments and (Migrating Birds) Echo Segments Algorithm in the  $1.5^\circ$  elevation are used to identify such confounding. This philosophy is similar to that used in the draft Microburst Algorithm.

Sweeps are first converted to Cartesian coordinates; see below. The Roosting Birds Algorithm then identifies up to MaxNRoost roosts in each sweep. This is done in an iterative process designed to locate the largest and most easily visible roost first and then locate successively smaller and less visible roosts. A modified Hough transform is performed and the largest roost is located. If or when a roost is located, the parameters of the roost are recorded and the echoes constituting the departure from that roost are removed from the input data. The Hough transform is then repeated on the data (minus any roosts already located) and this process is iterated until no more suitable roosts are found. The method is illustrated graphically from actual data in Figure 4 in Larkin and Quine (1989).

If this roost is too small (Total reflectivity < QuitThL) or too thin (Coverage < 2%), or MaxNroost roosts are found, the algorithm stops processing the sweep.

**The generalized Hough transform, coordinate transformation, and filtering.** The Hough transform is a generalized curve recognition technique

sometimes used in the field of computer vision. It is fundamentally statistical in nature as opposed to depending upon closed or other contiguous figures; this statistical quality is suited to the variable appearance of roosting birds on radar. A Hough transform relying on circles was selected to recognize echoes of birds departing roosts because in still air the pulsed departures of the birds describe arcs of concentric circles whose center is the location of the roost and whose maximum diameter is the distance to which the birds fly before alighting and beginning the day's feeding and other activities.

The equation for a circle,

$$r^2 = (x - a)^2 + (y - a)^2$$

is fundamental to the operation of the modified Hough transform.  $r$  is the radius of the circle, the points  $(x,y)$  are geographic locations on the circle, and  $(a,b)$  is the geographic location of the center of the circle (the roost). Notice that the circle is described in Cartesian coordinates. Except for the trivial and unlikely case of a roost located at the radar, description of a circle in the natural polar coordinates of weather radars is computationally unworkable. Therefore a polar-to-Cartesian transformation of the lowest radar sweep is necessary for the algorithm's operation. This is unsurprising because the birds, their food resources, and possibly their navigational mechanisms inhabit the (approximately) Cartesian coordinates of small portions of the earth's surface.

Polar-to-Cartesian conversion is performed on the reflectivity and Doppler velocity fields of the radar data. During coordinate transformation, both reflectivity and Doppler velocity fields are converted to square 0.25-km cells, corresponding to the resolution of WSR-88D Doppler velocity and spectral width fields. Presently the coordinate transform is performed on a 534 x 420 cell region centered on the radar. The 534 x 420 cell region is designed to include all roosts studied in 1987-1990 around the CHILL radar and to be configured into

different shapes of similar overall area if necessary. It was limited in total size (east x north) by the memory available in the computer. Coincidentally, this area was sufficient to contain the roosts studied from the Lincoln Laboratories FL-2 radar data as well. In a working WSR-88D RPG, the site-specific parameter MaxRange would determine the array size.

During coordinate conversion, Doppler velocities are unwrapped based on the nominal flight speed of birds (BirdFltSpd) and the surface winds. The scheme is essentially the same as that used in the Flocks of Waterfowl Algorithm and will not be described here.

The coordinate-converted data have been filtered to retain only gates with:

$$\begin{aligned} &\text{Noise Coherent Power} \geq 0.2 \\ &\text{RefThL} \leq \text{reflectivity} \leq \text{RefThU} \quad \text{and} \\ &\text{VelThL} \leq \text{Doppler velocity} \leq \text{VelThU}. \end{aligned}$$

These parameters will differ when used with a WSR-88D because of its different clutter filters. Considering the importance of close-in ground clutter to the functioning of the Roosting Birds Algorithm, making these parameters functions of slant range would be worth considering as a future improvement. No filtering on spectral width was performed, although

$$\text{spectral width} \leq \text{SWThU}$$

would probably improve the performance of the algorithm.

The next step in the algorithm is designed to avoid searching too much empty space for radar echoes. The Cartesian arrays are constrained by moving the edges of the 534 x 420 cell region inward toward the radar until the first row or column of interesting echo is found. This is done by a simple and rather conservative method: Running along the cells of an edge and treating sequences of continuous echo as one edge-echo, the number of edge-echoes are counted. If two or more edge-echoes are found, the present edge is fixed at the present

northward or eastward location and the next of the four edges is examined. But if no or only one edge-echo is found, the edge is moved one cell farther toward the radar and the process is repeated. The four edges are examined in the arbitrary order west, east, north, south. Note that counting edge-echoes on a given edge will be constrained by completed processing of preceding orthogonal edges.

Uninteresting zones around the periphery seldom include noticeable echoes from roosting birds except for isolated flocks of crows. Because the algorithm cannot locate isolated flocks regardless, the uninteresting zones beyond the constrained edges have proved to be indeed uninteresting.

We first consider the generalized, unmodified Hough transform, which is carried out by examining a Cartesian array. In the generalized Hough transform approach, each echo found, at  $(x,y)$ , would lie on one circle for each cell in the array. Each of these circles would have a center at  $(a,b)$ , the location of the other cell, and a radius of  $r$ , the distance from  $(x,y)$  to  $(a,b)$ . The generalized Hough transform would tally each of the circles. The circles for  $(a,b,r)$  combinations would be held in a large accumulator array, in this case, of dimension  $(534 \times 420 \times \sqrt{534^2 + 420^2})$ . It would search the constrained Cartesian array; the order in which the  $(x,y)$  are examined is inconsequential. For each  $(x,y)$  echo found, it would tally the  $(a,b,r)$  for all cells in the array, then proceed to the next echo.

Ideally, in this general case, after the transformation, the element of the accumulator array with the highest tally would point to the circle that contains the most echoes. The center of this circle  $(a,b)$  is likely to be the location of a roost. The radius  $(r)$  is likely to be the distance from the roost the birds presently located on the circle have flown since departing the roost. And a roost found in the same place on successive days is probably a traditional roost and can be reported as a hazard to aircraft in early morning and late afternoon.

**A modified Hough transform.** In practice this generalized Hough transform was modified by taking advantage of information that is available from Doppler radar images of roosting birds but is not available from abstract, isolated geometrical circles. Several aspects of the biology of roosting birds enable us to substantially increase the rate of success of the transform and enormously increase the efficiency of the algorithm. Increased efficiency results from the transform not wasting a lot of time finding circles that are biologically implausible. An early version of the modified Hough transform as the basis for the Roosting Birds Algorithm was briefly described in (Larkin and Quine 1989).

For the purpose of bringing the Hough transform to bear on the problem of recognizing roost departures, we consider birds departing from a roost as a process reduced to its essentials, disregarding the usual biological variability inherent in such a complicated event. A pulse of many birds departs from one point, the birds taking off simultaneously and flying straight away from the roost at speed BirdFltSpd (Appendix V). The birds in a pulse spread out and continue to fly straight, toward all points of the compass. A minute or two later another pulse departs in identical fashion. Each pulse flies a certain fixed distance and then the birds all descend and alight, becoming invisible to the radar. On calm mornings, the pattern is that of a bull's eye, but, when light winds are present, the circular pattern of departures is distorted by the addition of the wind to the birds' flight speed and heading. When food resources or perhaps visibility on the radar are not radially symmetrical about the roost, departing birds are not observed to depart in some directions; what would otherwise be complete circles become arcs of circles instead. This ideal is not realized in nature, although it is closely approximated when large roosts disperse on calm mornings.

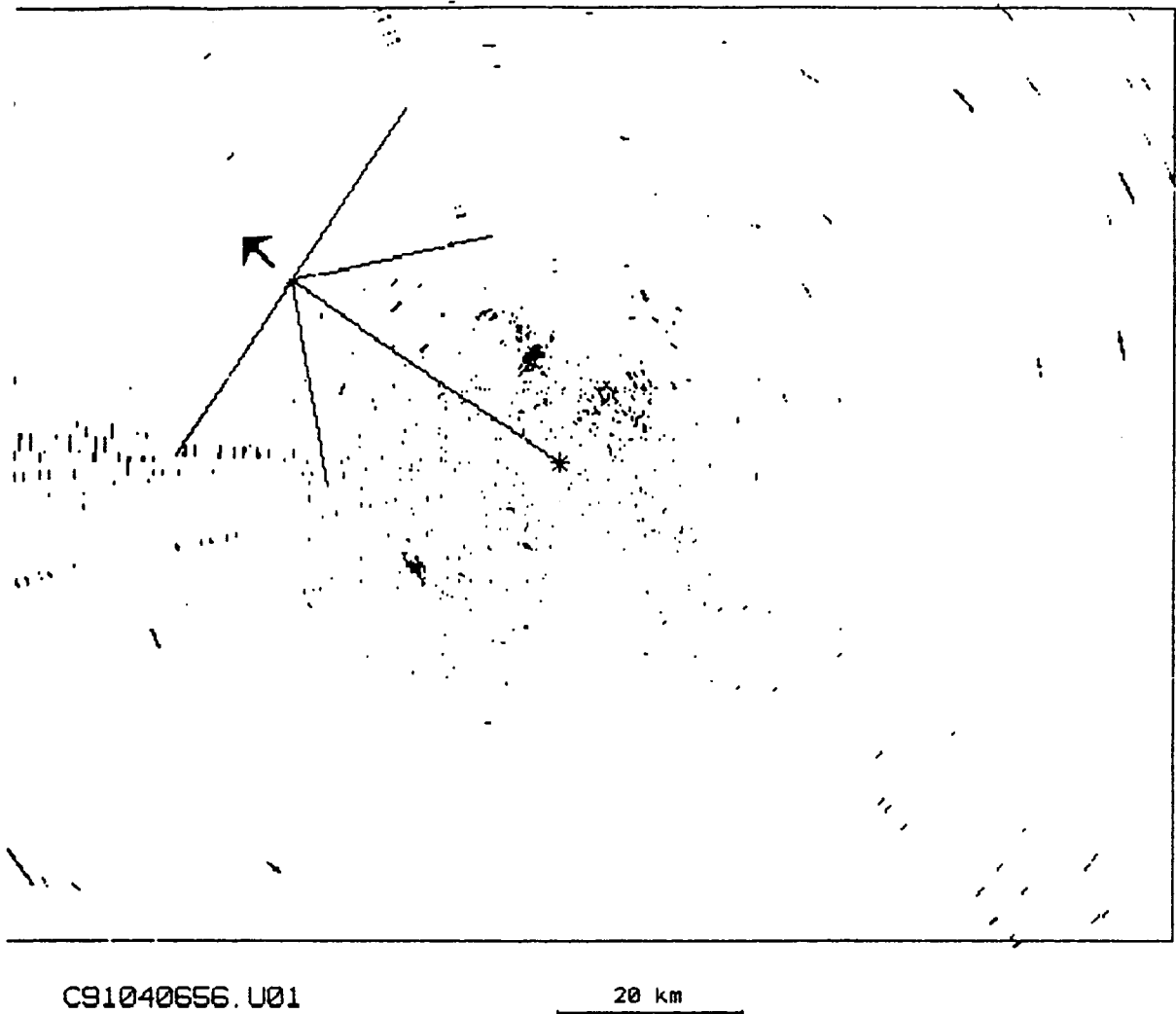
Because the algorithm examines only a single radar sweep at a time, it has no *direct* information about when the birds in an individual echo took off from the



roost, but other information is readily available. For instance, the birds fly only a certain maximum distance from the roost (in still air, MaxRad). This restricts the radius over which to increment the accumulator array, reducing the size of the array in the present algorithm to  $(534 \times 420 \times \text{MaxRad})$ , or almost a factor of 10 in the running implementation. A preliminary test of the algorithm using an alternative method, reduced resolution (increased cell size) in the accumulator array itself, rather than reduced dimension, decreased the performance of the algorithm. Therefore the idea of decreasing resolution was dropped in favor of using MaxRad.

Each bird is assumed to be flying in a known direction, namely along a line from the roost center to its present position, at the speed BirdFltSpd. Therefore its velocity vector is known and the approximate direction of the roost may be calculated because BirdFltSpd and measured Doppler velocity are known. This relationship restricts the directions in which to increment the accumulator array and greatly reduces the number of computations per echo. An ambiguity in direction remains because of the trigonometry: the roost lies to the right or to the left of a line connecting the echo to the radar, so that the accumulator array must be incremented in both these directions.

Two additional factors enter into these modifications of the Hough transform. First, any ambient wind will modify an echo's groundspeed in a known way, so that vector operations that include the surface wind are performed before each of the above modifications are performed. Second, because real birds do not always fly at BirdFltSpd, winds can be variable, and radar measurements will have error, the ground speed and therefore the measured Doppler velocity will vary. Variability in speed will expand the two lines describing the laterally-ambiguous possible directions into two laterally-ambiguous sectors. Variability in the winds is characterized by the parameter WindAdj.



These concepts are illustrated by a monochrome rendition of the display of the running Roosting Birds Algorithm (figure above). The box describes the edges of the Cartesian plane surrounding the radar. The small asterisk in the center locates the CHILL radar and the 20 km mark below the figure gives the scale. The particular echo being examined is at the intersection of the five lines. It is an outbound target with a rather low Doppler velocity, represented by the arrow. The low Doppler velocity ( $< [\text{BirdFltSpd} + \text{wind}]$ ) means that the echo could not have been flying at BirdFltSpd directly away from the radar, along the

radial line from the radar to the echo, but must have been flying roughly NE, within the wedge formed by the bottom pair of lines, or roughly SW or S, within the wedge formed by the top pair of lines. The length of the lines (MaxRad+wind) shows the maximum possible distance to the echo from the roost from which it originated. If the echo is a roosting bird, its roost lies within the two wedges.

Some details about the actual data in this figure: In fact, the particular echo illustrated is likely an isolated spot of clutter and did not arise from the nearest known roost on this day, which is located at a Kraft Foods plant in northwest Champaign, Illinois. Birds from the Kraft Foods plant are the dark spot about 11 km NNW of CHILL and nearby echoes. The moving echo about 30 km SW of CHILL is not departing a roost; it is a Norfolk and Western freight train. The Universal File name at lower left codes the site, date/time, and elevation of the radar volume. A schematic similar to this actual plot is Figure III-2 of (Larkin and Quine 1989).

A further modification of the Hough transform is made in the way tallies are built up in the accumulator array. Because the Hough transform takes place in a finite, bounded plane, the method will favor roost centers located near the middle of the plane (in this case, near the radar). The problem is stochastic and occurs even when working with completely random, ideal data on a bounded plane. It is overcome by a further modification of the Hough transform that, instead of using the Hough transform itself, uses instead the difference between accumulations of normal-velocity data and accumulations of reversed-velocity data. This modification to use "anti-birds" to remove the effect of the finite plane's boundary, is described in (Larkin 1990).

**Identification of roosts in (a,b,r).** After the modified Hough transform is calculated, the accumulator array consists of a three-dimensional matrix with regions of positive values where roost centers may be located and regions of

negative values where roost centers are highly unlikely. The Roosting Birds Algorithm examines the accumulator array and locates  $\leq 4,000$  elements of that array that have values over a threshold. The empirically-determined 4,000-element threshold is an adaptive one and its value is of importance only because it must be low enough that at least MinNcirc values exceed it and high enough that computational effort is not wasted accumulating  $\gg 4,000$  circles. It is initialized at AccInit and does not drop below AccThL. Because the algorithm adaptively raises and lowers the threshold by ReduceAcc, its value at any one time has an effect on the number of circles considered as roost centers but not much effect on which of these circles take part in the calculations, and therefore even less effect on the roosts located.

As the accumulator array is examined, the  $\leq 4,000$  circles in AccArray are kept indexed by their accumulated value, with the lowest values lost off the end of the list if  $> 4,000$  values above threshold are found. This sorted list of circles is the basis for finding the center of the largest roost in the accumulator array.

Before the departure radius is determined, the center of the roost is located. The rationale for giving priority to circle centers over the more global solution of looking for a maximum in all dimensions of the accumulator array at once is simple and powerful: Birds departing from roosts are often, and for large roosts usually, located on more than one concentric circle. These have more than one radius. Therefore, the algorithm again departs from the generalized Hough transform; it finds the most prominent center, then determines the radius of that center's outermost circle.

Location of the circle center takes place after lowering the resolution of the Cartesian array to  $(2 \cdot \text{SumDist}) = 0.5$  km cells. SumDist is included as a parameter in case it is desired to lower the output resolution further. This reduction in resolution lowers the resolution of the final product but allows for

imperfection in the circular shape of the echoes and in the positioning of the constituent echoes--the resolution of the radar data is retained in the earlier calculations. All of the circles up to 4,000 are summed across their radii and cast into the reduced-resolution array. The array is then examined and the position of its largest element is taken as the position of the center of the circle.

The final radius of a roost departure is determined by a several-step procedure. (The procedure could be simplified quite a lot, but probably at the expense of robustness.) First, the accumulator values within one cell of the computed center in (a,b) are summed, for each value of the accumulator array radius. This vector of accumulations  $f(\text{radius})$  is then examined to find the maximum value, which is the radius at which the maximum number of bird cells occurs. This is the peak of the most populous circle. Then the algorithm looks outward in radius to find the point at which the difference function of the accumulations  $f(\text{radius})$  becomes positive or hits 0 accumulations. This is the outward edge of the most populous circle. The final radius is then determined as the maximum of the outward edge of the most populous circle and the 98th percentile of the entire accumulations  $f(\text{radius})$  array. In summary, the final radius includes at least 98% of the accumulator values around (a,b) out to MaxRad, but is never less than the outward edge of the most populous circle and never greater than MaxRad.

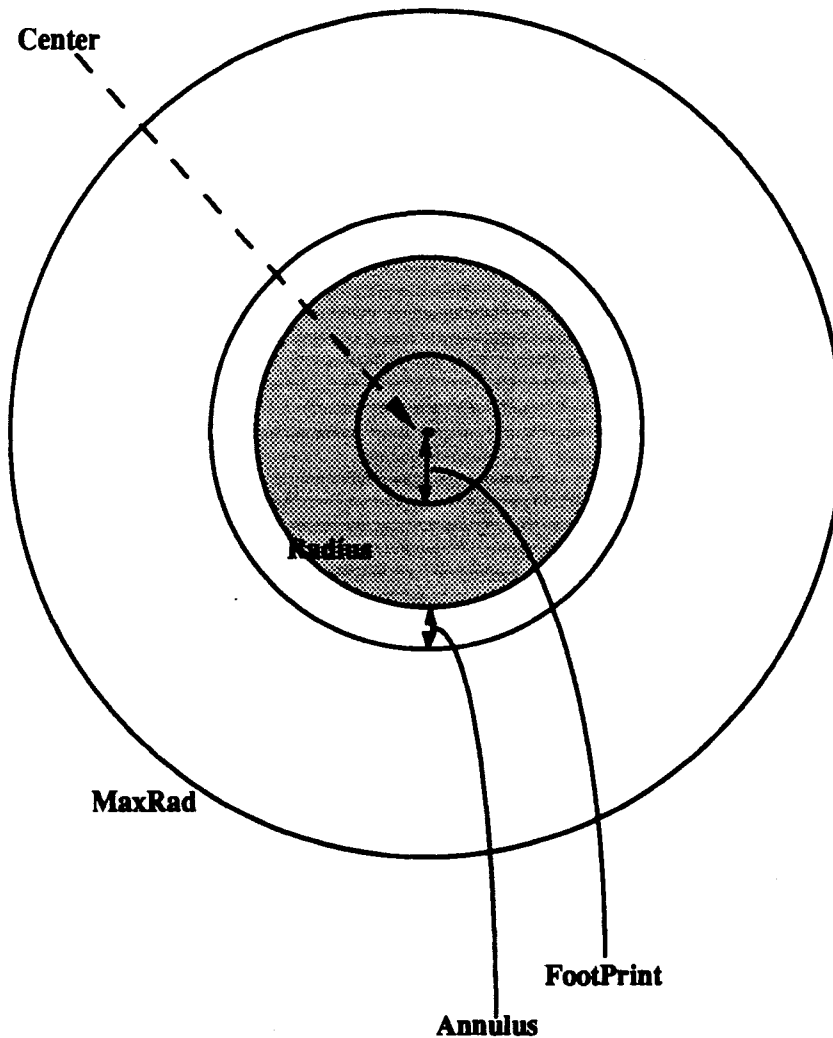
Total reflectivity of cells within a circle is computed in the normal fashion, by converting dBZ to ratios, totaling the ratios of each echo cell within the circle, and converting back to dB. When computing total reflectivity, it is desirable to discard infrequent but important echoes having high reflectivity but representing non-bird (or at least non-roosting-bird) echoes within the radius. Less important, there will usually be scattered low-reflectivity clutter mixed in with bird echoes. Therefore a certain proportion of the highest and lowest reflectivities, ChuckRef,

is recorded prior to computing total reflectivity. Notice that this scheme maintains Type I errors at a low level even when 100% of the echoes are roosting birds but avoids potentially large Type II errors when radar return includes infrequent large echoes as from traffic, railroad trains, or other moving objects.

One exception to this simple computation of total reflectivity arises from the case where circles from more than one roost overlap so that it is not obvious how echoes in the zone of overlap should be apportioned. Although this case was not common in the data examined for algorithm development and although completely accurate apportionment is not possible from static single images, this special case must be handled. We adopted the solution of assigning each individual Cartesian cell to only one roost, namely, to the roost most likely to have given rise to its birds. This is done using the Doppler velocity of each echo cell to allocate that cell's reflectivity to only one of the roosts that overlap. We assume that the echo is indeed composed of birds flying at BirdFltSpd, departing a roost. For each cell in the overlap zone, each of the overlapping roosts is examined in turn and the cell's reflectivity is given to the roost whose radial component of BirdFltSpd+wind along a straight line of travel from the roost center most closely matches the Doppler velocity of the cell. In this way even intermixed bird echoes from three or more roosts have a chance of being distributed among them in an appropriate fashion. In practice, the spatial patchiness of echoes from birds departing their roosts often enables the algorithm to distinguish intermixed bird echoes in a believable way because their Doppler velocities are unambiguously associated with only one of the overlapping roosts.

Coverage within a circle is defined as the area of a circle divided by the area of all cells in it that contain echoes, expressed as a percentage.

The following diagram summarizes the three roost-located quantities described thus far (center, radius, and MaxRad) and introduces two more. After



a roost is located and its radius determined, the cells within that circle are cleared so that their echoes cannot contribute to any further circles in subsequent passes of the algorithm on the current Cartesian array. Moreover, an annular area surrounding the circle is also cleared. This precaution was added because we found that scattered residual echoes around the periphery of a valid roost were sometimes

so numerous that they resulted in a subsequent and probably spurious roost being found close to the original roost but with a larger radius, its circle often enclosing the first circle entirely. The additional area is described by the Annulus parameter, which is expressed as a proportion of the original circle radius.

Echoes within Annulus but outside the radius of the circle probably result when birds from some large roosts travel farther than MaxRad from the roost, when more than one actual roost lie within a few km of one another in the field

and the algorithm encloses them in one large circle rather than more than one smaller circle, and, probably most commonly, when many bird echoes are still visible at the edge of a dispersing pulse of birds but are becoming fragmented and generally disorganized spatially, so that the algorithm does not treat them as a circle.

The parameter FootPrint prohibits any subsequent roost in the same sweep from lying too close to a roost that has already been located. Therefore the algorithm permits adjacent and overlapping roosts, but not too closely adjacent.

**Algorithm output**, a site-specific list of known roosts, would be maintained by a WSR-88D version of the algorithm. The biological basis for the list is the site tenacity of most roosting birds, which is even greater for larger and more hazardous roosts as opposed to small ones. The list would be the operational output of the algorithm; the algorithm's output would change slowly, over days or weeks, rather than in real time. Because the Roosting Birds Algorithm requires certain conditions to operate, especially low surface wind and absence of echo from clouds and migrating birds and insects in higher elevation scans, gaps of up to several days in availability of data are inevitable. The list of known roosts will serve to maintain the algorithm's output spanning such short-to-moderate periods of data drought.

As mentioned above, testing of this part of the algorithm depends on long, continuous runs of radar data, which have not been available from the research radars. Therefore the work done to this point enables us to set trial values for some parameters associated with the site-specific lists but not to advocate those values with any assurance.

For each roost in the list of zero or more roosts would be maintained both external variables, available to PUPs, and internal variables, used by the algorithm. The external variables, the products, would include especially the



location, size, and activity time frames observed for each roost. The internal variables would include the day-by-day history of each roost extending back for a period of some weeks.

On a once-per-day basis, the algorithm would compare the roosts, if any, found that day with the list of known roosts. The parameter RoostLife provides a maximum number of days a roost will be maintained on the list without being detected again by the algorithm. The parameter InterRoost establishes the spatial distance a newly-found roost may lie from a previously-known roost and nevertheless be considered the same roost over time. It is possible that InterRoost (or the certainty associated with it) should be a diminishing function of time since the known roost was last known to exist, to avoid roosts appearing to wander slowly over the landscape.

### **General characteristics of roosting birds on weather radars**

Mainly because of the importance of ground clutter in determining the appearance of roost departures on weather radar, no attempt was made to compute stipple for any of the radar base data (See Migrating Birds chapter). Stipple in reflectivity was determined to be not useful in brief studies in Florida with TDWR (Isaminger 1992).

**Periods of data gathering** using CHILL in central IL included two days in December 1982, and the much of the fall and winter seasons of September 1987-February 1990. The largest, most stable, and most dangerous roosts occur in cold weather. (The Boston, MSU, and PeachTree/Dekalb civilian aviation incidents all occurred during this time.) The technical quality of 1987 and early 1988 CHILL data did not quite permit including them in test runs of the algorithm; these early post-modernization CHILL data and associated field observations are not included in most summaries.

In addition, data from the Lincoln Laboratories FL-2 radar, including morning data from Huntsville AL and afternoon/evening data from Kansas City, were kindly made available to us by Dr. Ron Rinehart.

Because ringlike patterns of dispersing roosting birds are distorted by wind, the Roosting Birds Algorithm performs better in calm or low-wind conditions and the algorithm will not run unless surface winds are below a threshold (MaxWind). Therefore, radar and field observations were scheduled for low wind conditions, although incorrect or vague forecasts in fact provided inevitable opportunities for testing the algorithm in conditions of low to moderate wind.

Little effort was spent gathering quantitative data on birds returning to the roost in late afternoon. One reason is that artifact in the form of rush hour traffic is common in cold weather around dusk. A noteworthy instance of confusion between bird and vehicle echoes occurred at 1615 CST on 3 Nov 1989, when observers recorded a large flock of "blackbirds" of mixed species that flew directly above the center line of the northbound part of divided IL Highway 51 for a distance of at least 6 km, from Interstate 72 into and past the center of Decatur IL. From the birds' point of view, they were probably using the road as a convenient route among the city's structures and possibly as a leading line for navigation. From the point of view of weather radar, their echoes would have been mixed with or obscured by traffic. Vehicular traffic is present but generally much less common in the near-dawn time frame of departure from roosts.

Another, more general reason for concentrating on morning as opposed to evening roost movements is that evening return movements to a roost do not provide a clear spatio-temporal pattern (Clergeau 1990, Harper 1959, Tye 1993). Therefore the algorithm locates departing birds but ignores returning birds. (However, it is not unlikely that, once the algorithm locates a roost via morning

activity, the returning birds could subsequently be found and somehow exploited by the algorithm.)

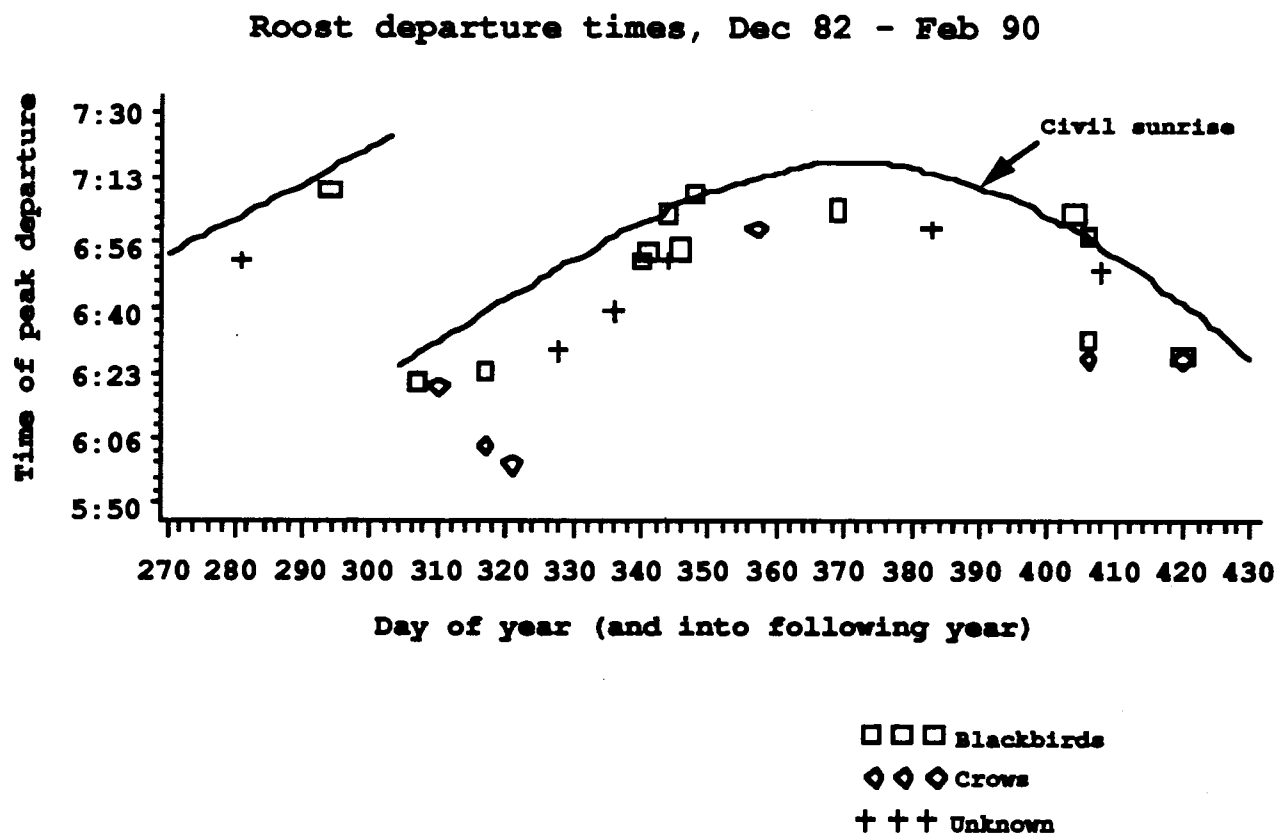
The following table lists times data were gathered and the locations of field observers. Locations are in east-central Illinois unless otherwise indicated.

Radar and visual observations of blackbirds and crows, 1982 through spring 1990. (Updated from Appendix I, Larkin 1990.)

	Times	Tape numbers		Surface wind*		Field observers
		CHILL	NHS	Speed	Dir	
18 Nov 82	0630-0650					S Urbana
	1600-1620					Windsor Rd
29 Nov 82	1630-1720					SHRC
30 Nov 82	1615-1630					S Champaign
1 Dec 82	0623-0700					Champaign
	1625-1640					NHS Annex, Kraft
2 Dec 82	0610-0652					Eisner warehouse
	1615					Eisner warehouse
6 Dec 82	0615-0704	2BRD007 (data bad)			W	Eisner warehouse
7 Dec 82	0615-0704	2BRD008	201	calm		Eisner warehouse
10 Dec 87	0635-0725	87IL033	209			Willard
12 Dec 87	0610-0729	87IL036-037	206	8 ms <sup>-1</sup>	W	Willard
	1600-1630					Tuscola
14 Dec 87	0643-0722	88IL038-039		LT	NE	Tuscola
8 Feb 88	0644-0748	88IL005-6 (CHILL down)		calm		Tuscola
10 Feb 88	0630-0725	88IL007-8	605-606	LT	NE	Tuscola
23 Sep 88	0615-0731	88IL126				none
7 Oct 88	2130-0800	88IL129-143				none
14 Oct 88		antenna failed				none
20 Oct 88	~0630-0740	88IL147-148		VLT	SE	Willard
24 Oct 88	0655-0720					North Champaign
25 Oct 88	1720-1810					Lake of the Woods
26 Oct 88		EL failed		LT	W	Lincoln & Windsor

23 Nov 88	0615-	88IL149	211			none
9 Dec 88	0636-0707	88IL158-159	(no VEL)	STR		none
22 Dec 88	0605-0705	88IL162	213	7 ms <sup>-1</sup>	SE	Rantoul
4 Jan 89	~0635-0724	88IL001		calm		Rantoul
	1652-1712			LT	S	Kraft
5 Jan 89	0635-0705			6 ms <sup>-1</sup>	S	Kraft
18 Jan 89	0614-0720	89IL010	214	LT	SW	Kraft
25 Jan 89		CHILL down				none
12 Feb 89	0600-0722	89IL042	624-626	LT	NW	Parkland College
	dusk			LT	SE	Big Ditch
13 Feb 89	1718-1747			LT	S	Pesotum
21 Feb 89	1650-1725					Pesotum
24 Feb 89	0600-0644	89IL066		calm		Rantoul, Pesotum
25 Feb 89	0555-0630			MOD	S	Big Ditch
29 Jul 89						Huntsville, AL
1 Nov 89	1635-1723			LT		N. Champaign
3 Nov 89	0600-0640	89IL165	661	LT	W	Parkland
	1611-1700			MOD	S	N. Urbana, Decatur
5 Nov 89	1634-1659			STR	S	Decatur
6 Nov 89	0610-0654			MOD	NNW	Pesotum, Tolono
	1608-1750			calm	--	Pesotum
7 Nov 89	1559-1700	89IL166		VLT	S	Philo, Tuscola
8 Nov 89	1607-1705			--	NW	Tuscola
9 Nov 89	1545-1615			4 ms <sup>-1</sup>	NW	Vermillion County
12 Nov 89	1622-1750			LT	E	Philo, Pesotum
13 Nov 89	0532-0642	89IL167		STR	SSW	Pesotum, Tuscola
	1634-1721			STR	S	N. Champaign
14 Nov 89	0545-0617			--	S	N. Champaign
	1604-1718			6 ms <sup>-1</sup>	S	Danville
17 Nov 89	0545-0635	89IL168		5 ms <sup>-1</sup>	SW	Danville
	1603-1700			5 ms <sup>-1</sup>	SW	Danville
19 Nov 89	0558-0646			LT	SW	Danville
20 Nov 89	1547-1700			MOD	WNW	Danville
21 Nov 89	1620-1707			LT	E	Danville
8 Jan 90	1625-1700			MOD	S	Champaign
9 Jan 90	1630-1742			VLT	NW	Pesotum
9 Feb 90	1710-1742			VLT	NNW	Pesotum
4 Feb 90	1716-1743			LT	NW	Pesotum
10 Feb 90	0540-0649	90IL022		calm	--	Pesotum

\* Wind directions are directions from which the wind is blowing. LT=light, MOD=moderate, STR=strong, VLT=very light



Time of peak rates of departures from roosts in east-central Illinois during cold weather. Times were recorded with binoculars (known species) or from inspection of radar displays (unknown species).

Times of peak departures of roosting birds are shown in the Figure, which is an update to Fig. 5 of (Larkin and Quine 1989). The "unknown" birds in this figure are almost entirely or entirely "blackbirds", but field observers

were not able to obtain accurate species counts. In the figure one sees a tendency for crows to depart earlier than "blackbirds"; such departures of crows in early morning were much more striking to field observers than is evident from the figure because observers often saw small flocks of crows flying in the predawn period many minutes before they saw any "blackbirds" flying. Times of first and last departures from roosts were extracted from the notes in addition to times of peak departures; they confirmed our rule of thumb for field work that the 30 min before civil sunrise is the time of maximum departure activity:

	Departure time (min) relative to civil sunrise		
	First	Peak	Last
N	23	25	17
mean	-27.0	-13.2	-2.2
S.D.	12.8	11.0	15.2

These data are appropriate for deciding for which early morning sweeps the Roosting Birds Algorithm should be invoked, but it is not immediately obvious that there is one best way to use the data. We suggest using as a working time window the period first departure - 1 S.D. to last departure + 1 S.D., or:

*40 min before civil sunrise to 13 min after civil sunrise.*

This window should be narrowed if numbers of false roosts or sweeps with no roosts found are generated disproportionately often at the edges of the working time window. The variation in the above data partly reflects delay of departures in fog or bad weather (Harper 1959:203). No way of detecting such conditions is presently available to the WSR-88D RPG. The time window may need to be modified as other species are studied for inclusion into the algorithm.

**Reflectivity** The basis for calculating a function relating radar reflectivity to numbers of birds is explained in the introduction and in the Flocks of Waterfowl Algorithm. Because species of birds vary in size, we choose to use the

blackbird-equivalent as a size unit, realizing that expressing the size of a roost in units of mass or in species-specific units may be more desirable eventually. A blackbird-equivalent will be defined as one European Starling, or the equivalent number of different-sized birds that would produce equivalent S-band radar cross-section to one European Starling. Variation in mass of birds across a season (Peach, et al. 1992) is not accounted for in this relationship. One American Crow is 2 blackbird-equivalents (Vaughn 1985, figure 5).

Masses of common roosting birds	
Male and female masses averaged, from Dunning (1992).	
American Crow	448 g
American Robin	77
European Starling	82
Red-winged Blackbird	53
Common Grackle	114
Brown-headed Cowbird	44

Relating observed  $\log(N)$  to total reflectivity expressed in dBZ (see chapter on Flocks of Waterfowl) and over a range of  $5.8 \times 10^2$  to  $1.0 \times 10^5$  blackbird-equivalents., we obtained:

$$\log_{10}N = 2.51 + 0.048 \cdot \text{Total Reflectivity}$$

, which is significant at  $p = 0.03$ .

**Doppler velocity** of roosting birds is discussed extensively under "a test for extraneous targets..." below. The predictable speed of birds spreading out near dawn is fundamental to the success of the algorithm, of course.

The power of Doppler is illustrated in the following color PPI image showing departures from roosts, at Champaign, Rantoul, and W of Tuscola, IL. Principal roads in Champaign County are drawn in white; CHILL is located just S of the city of Champaign, IL. Furthest echoes from the radar are 60 km distant.

CHILL 87  
23-NOV-88 05:29 CS

NEARAD GATES  
map  
-25

TO RADAR

0

AWAY

+25

clear  
meter/sec

DOPPLER

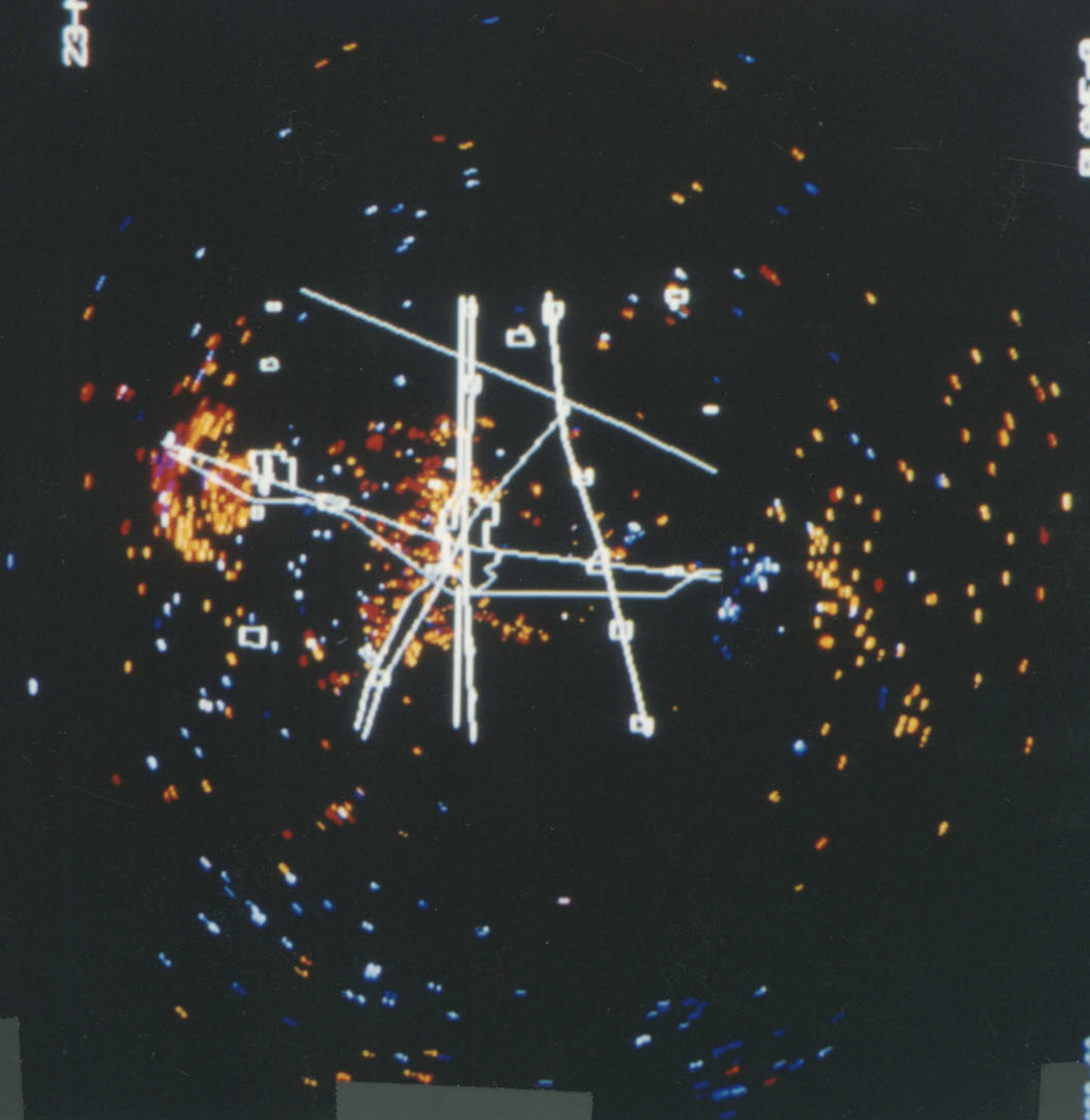
PPI

0.5 DEG

RA 60 km

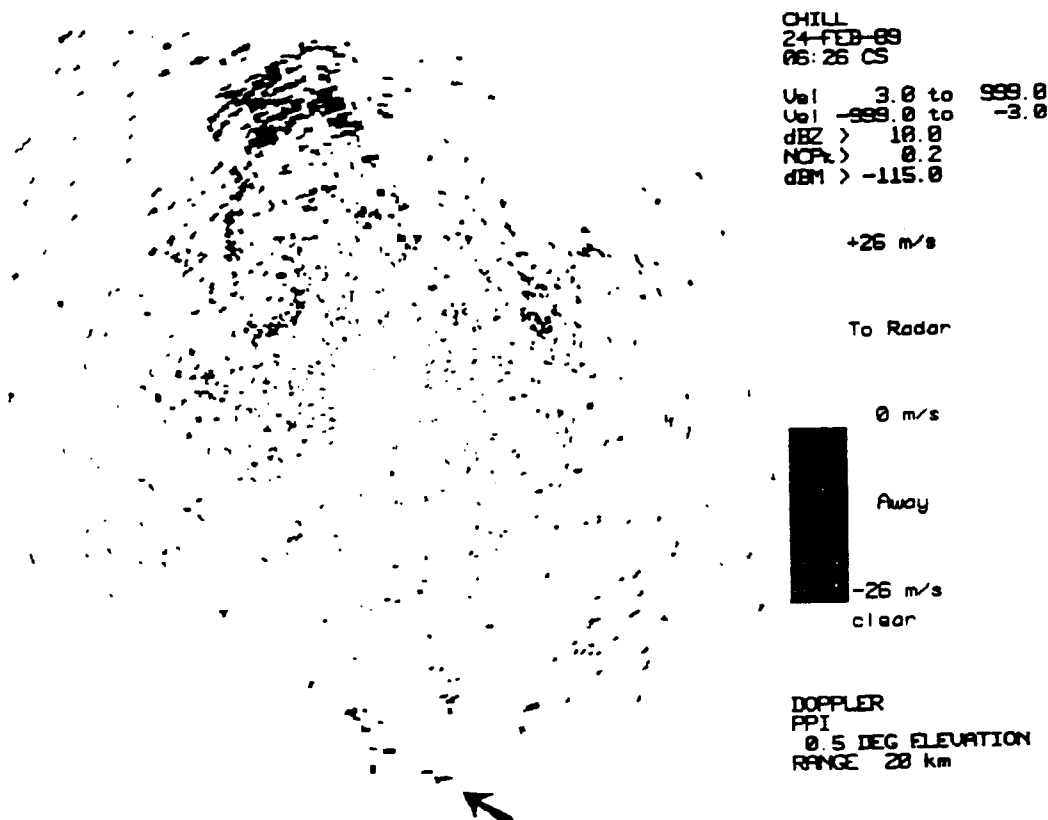
PLANE-0

DBZ> -1.



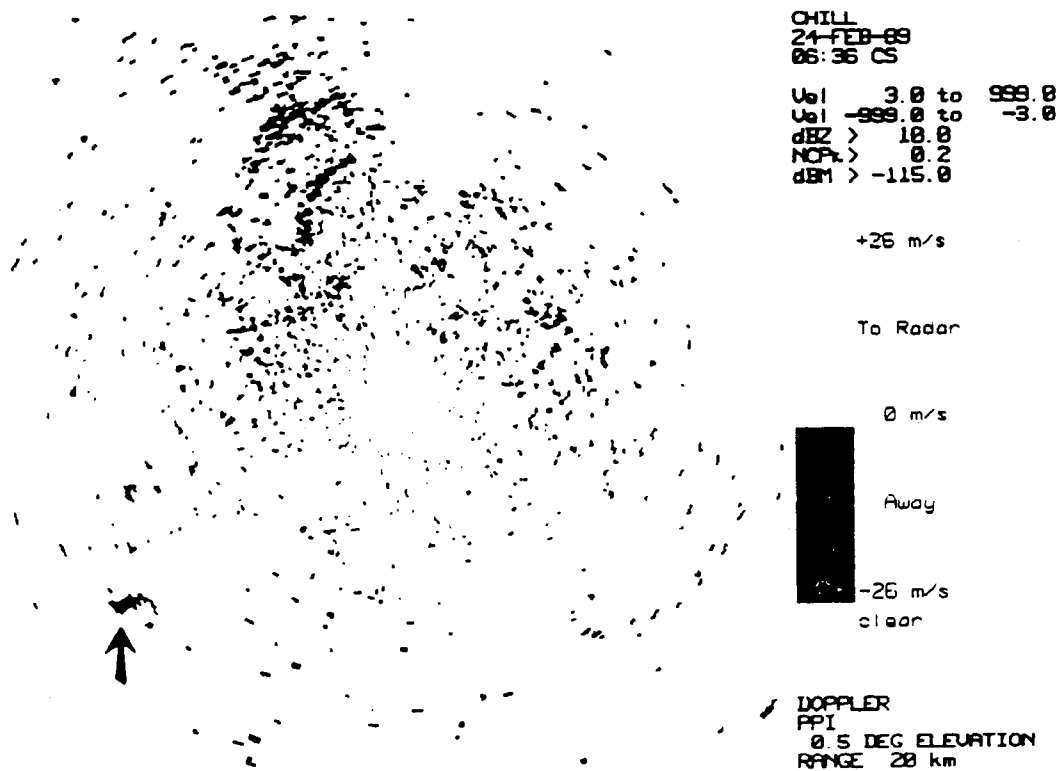


As an antidote, here follow two monochrome PPI's illustrating difficulties with interpreting images from Doppler information alone.



Outbound CHILL echoes at 0626 on 24 Feb 1989. Dense echoes (15-25 dBZ) in the NW quadrant are blackbirds departing roosts in W Champaign IL. A ring structure is visible in the echoes, which are travelling about  $21 \text{ ms}^{-1}$ . The echoes are above Yankee Ridge (15 m higher than CHILL altitude), which enhances their visibility on the radar.

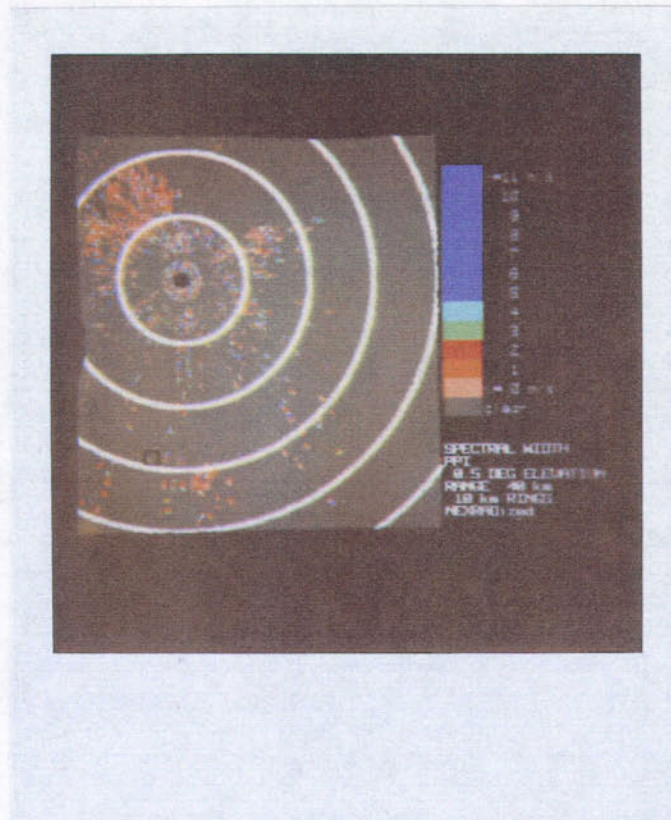
The arrow points to the SE-most end of a line of blackbird echoes departing a small roost at the USI Plant, Tuscola IL. The broken appearance of the line results from thresholding the display to remove echoes  $< 10 \text{ dBZ}$ . Positive Doppler speeds have been removed from this monochrome image.



Display identical to preceding figure except 10 min later. Although the blackbird echoes to the NW appear similar in some respects to the 0626 echoes, we know they are a later departure of different individuals, because the birds visible at 0626 would have travelled about 29 km by this time if they had continued flying.

The arrow indicates a long, high-reflectivity target, a railroad train, moving along the tracks of the Norfolk and Western railroad at about  $25 \text{ ms}^{-1}$ .

**Spectral width** of roosting birds is illustrated by the following PPI of a NEXRADized CHILL sweep at 0.5° elevation, 3 Nov 1989.



The displayed region (gray) is 80 km across, or 46% of the area used by the running test algorithm; range rings are at 10 km intervals. Spectral width is color coded so that orange ( $2 \text{ ms}^{-1}$ ) divides low spectral widths typical of roosting birds from high spectral widths typical of much clutter and precipitation. Echoes whose velocities have magnitudes  $< 3 \text{ ms}^{-1}$  or reflectivities  $< 3 \text{ dBZ}$  are removed from this display, to match the algorithm's working values of VelThL and RefThL. Echoes in the center of the display, within 3 km of CHILL, are ground clutter that has broken through CHILL's notch filter.

Two roosts were located by the Roosting Birds Algorithm in this sweep.

Birds spreading inside 20 km range at azimuths between north and west are about 6,600 "blackbirds" departing the Kraft Foods plant in western Champaign IL. They are flying into a light head wind from the NW, which reduces their Doppler velocities (not shown). Much sparser bird echoes near the bottom of the screen at range > 30 km are radiating southward from a USI Plant near Tuscola IL; a black square at range = 28.4 km shows the location of this roost. Regions of bird echo arising from both roosts are dominated by low spectral widths ( $< 2 \text{ ms}^{-1}$ ), whereas miscellaneous echoes such as highway traffic contain a greater number of gates with high values of spectral width.

Echoes 5 to 10 km north of CHILL appear to be clutter arising in Champaign IL, possibly mixed with some bird echoes. However, echoes between 10 and 20 km range centered on azimuth 65 degrees appear from their spectral widths to be birds. In fact, the algorithm included them in the large departure from the Kraft Foods plant. They are likely to be a moderate number of birds that roosted in NE Urbana IL; this situation of possible clusters of roosts is discussed below.

The patch of echo with uniformly low spectral width at 27 km range and 9 degrees azimuth has uniform Doppler velocities approaching CHILL at  $17 \text{ ms}^{-1}$ . Although no field observers were available to verify the identity of this patch of echo, later that winter American Crows regularly departed Rantoul IL in early-morning, moving in the same direction and, when they did, their echoes looked identical to this patch of echo in November.

Early morning departure from a starling roost observed from the KTLX and KOUN WSR-88D radars (linear polarization) on one morning in March 1993 was dominated by gates with nominal 4 kt ( $2.2 \text{ ms}^{-1}$ ) spectral width. This value is similar to but slightly higher than characteristic spectral widths observed on CHILL (as in the figure).

As with the other bird algorithms, spectral width certainly has promise in

applications to roosting birds, especially in thresholding to increase the bird/clutter ratio. We await actual WSR-88D data to make a decision.

## **Performance**

**Sample sizes** based upon independent observations should ideally be the basis for testing the performance of the algorithms. In the case of the Roosting Birds Algorithm, we were limited in having extensive data from only one radar site, the location of CHILL at Willard Airport in Champaign. Truly independent samples from such a geographically limited area are nearly impossible, for several reasons. We cannot expect factors such as the ground clutter situation and the nature of early morning non-roosting-bird echoes to be independent for a given roost from one morning to the next, or even from one season to the next. And a roost, especially a large roost, is traditional even from year to year, probably influences the locations of neighboring roosts, and, more subtly, reduces the motivation of field observers to diligently look for other theretofore-unobserved roosts in its vicinity.

Such considerations, applied strictly, would have resulted in only about 5 independent roosts in the sample, representing field work spread over four seasons. Therefore, as a compromise, the performance of the Roosting Birds Algorithm was based on  $N=39$  roost locations from four cold weather seasons that were as separate in space and time as possible and included multiple samples from the largest roosts, at Market Street and Kraft Plant.  $N=10$  additional roosts with thin Coverage were used to establish the value of the MinCoverage parameter (see below).

**Tests with artificial data and special data.** Artificial computer-produced "sweeps" with velocity values generated by vector algebra and arranged in single or concentric circles yielded correct behavior, namely centers correctly

located within the spatial resolution of the algorithm and radii equal to that of the artificial circle or of the largest artificial concentric circle. Fields of randomly-spaced echoes with randomly assigned velocities within the Nyquist limit yielded no roosts providing the anti-bird portion of the algorithm was employed in the computations. An interesting test sweep from FL-2 in North Dakota, composed of insects concentrated in distinct, dense rings around thunderstorm outflows, also resulted in no roosts being found.

A special situation pertained on a few mornings when sweeps at 1.5° elevation contained a few echoes of roost departures, presumably due to strong ducting of the radar beam. (In a neutral atmosphere, the radar beam lies above all but the closest low-flying blackbirds at 1.5° elevation.) Forced to run on the > 1° sweeps, and in some cases with QuitThL and other parameters temporarily reduced for this test, the algorithm located known roosts in two cases and a non-roost in one case. The known roosts were detected by the algorithm although they were nearly invisible to the human operator studying a thresholded PPI of the velocity data from the 1.5° sweep.

Similarly, testing of the algorithm purposely included roosts of a size that may or may not be large enough to be successfully detected and located in a WSR-88D environment (see figures below). Such small roosts are located less accurately than larger roosts, but several adaptable parameters can suppress them from algorithm output if desired (see below regarding all these points). One should keep in mind that smaller roosts, although biologically and numerically much less important than the many tens of thousands of birds in a large roost, are nevertheless hazardous to aircraft. For instance, the civilian incident at Peachtree-Dekalb in GA involved 3,000 European Starlings.

Echoes that are not roosting birds are widespread and rejection of such targets was a major design goal of the Roosting Birds Algorithm. Detection of

birds that normally fly at 50 m AGL necessitates dealing with many kinds of spurious echoes and clutter. In many cases, the algorithm was tested directly on data from the research radars, without NEXRADizing, to introduce dot echoes and other spurious echoes for test purposes. However many classes of clutter and spurious echo--including urban situations in large cities, sea echo, and mountainous areas--could not be tested due to lack of suitable data.

One series of images tested, from the FL-2 radar located at Huntsville AL in July 1986, was heavily dotted with echoes from migrating animals (see figure, following page). The dot echoes in this 0° elevation sweep cover the PPI uniformly from north to south but velocities away from the radar have been reduced to 20% ink density to better show the southward flow in the dot echoes. The dark spot at about 260° azimuth is the beginning of the departure from a "blackbird" roost on Finlay Island.

In these Huntsville data, reflectivity and other data were ambiguous, leaving us uncertain whether the spurious echoes were birds or insects. Their spotty coverage made it likely that these echoes would be filtered out of data from the NEXRAD RDA. However, because the UF versions of these data lacked the necessary parameters to permit NEXRADizing of the sweeps, this idea could not be checked. When a later sweep, at nominal elevation=0°, was submitted to the test algorithm it found a center for the large roost in the sweep but placed the center about 14 km from Finlay Island, probably because of the migrating animals. Such behavior is consistent with the design of the algorithm, not a programming error.

HUNT, AL  
29-JUL-86  
11:27 UD

Vel 1.0 to 999.0  
Vel -999.0 to -1.0  
dBZ > 1.0

+23 m/s

To Radar

0 m/s

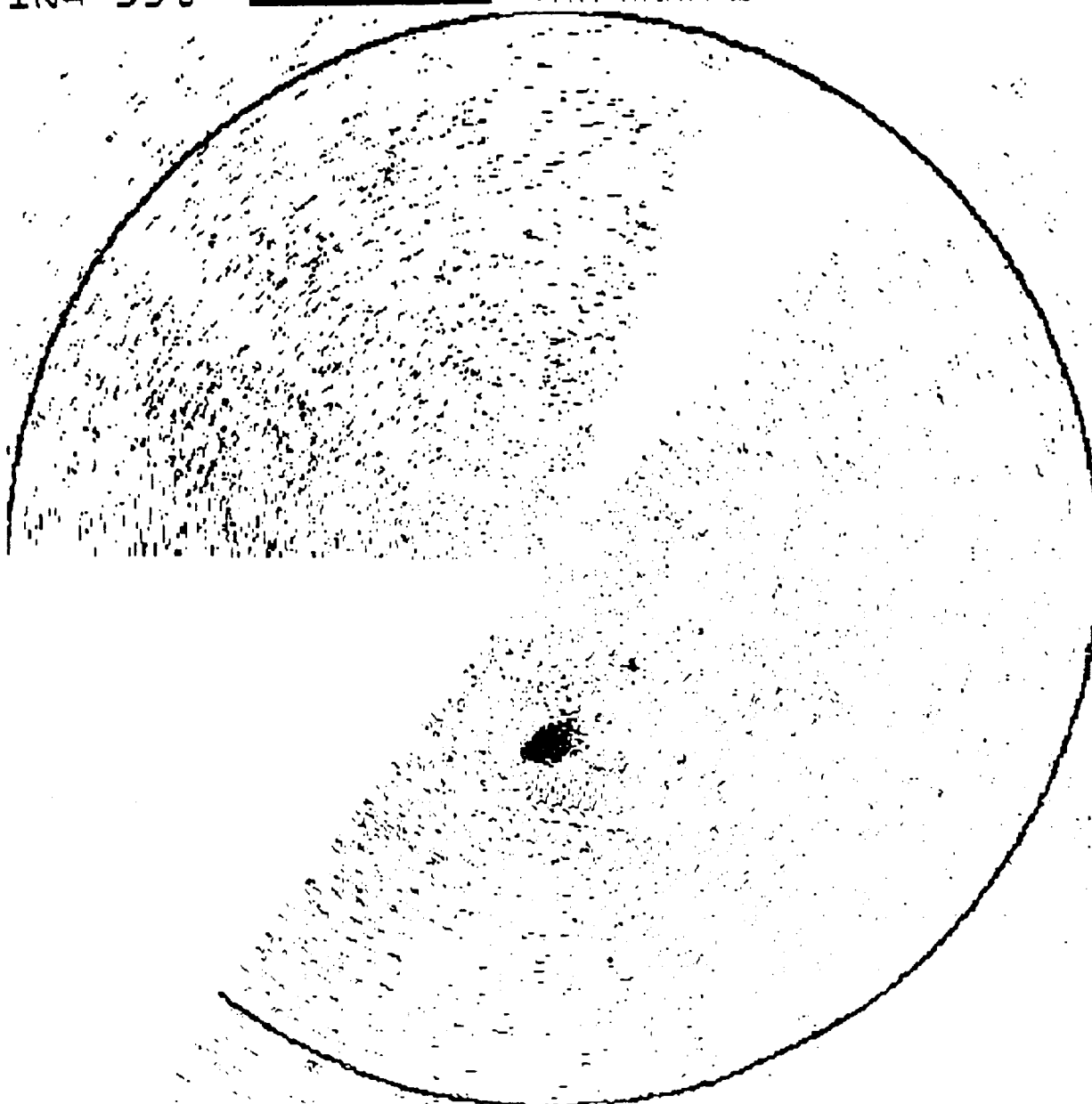
Away

-23 m/s

clear

DOPPLER  
PPI

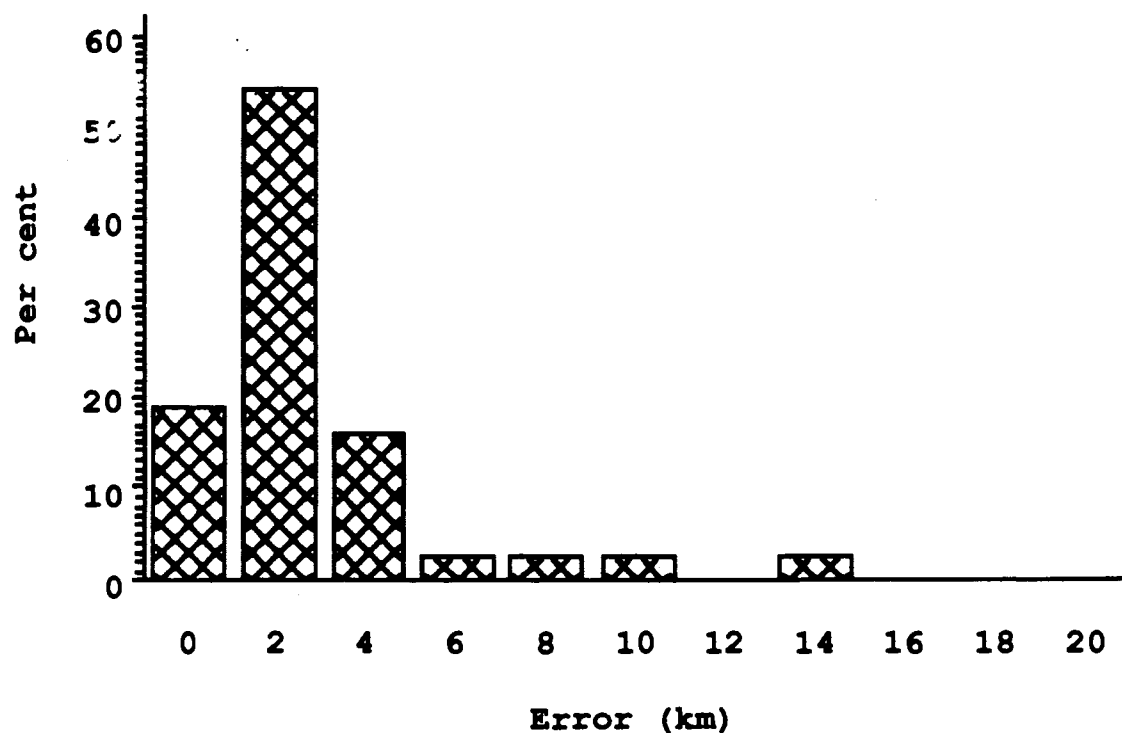
0.0 DEG ELEVATION  
RANGE 60 km  
60 km RINGS  
Univer





We expect that (1) restricting the algorithm to run only when significant echo is absent from sweeps at higher elevations ( $> 1^\circ$ ) and (2) suppression of dot echoes by the WSR-88D would prevent this mislocation of a roost from happening. However such measures will not suffice to prevent all such problems because other kinds of biologically interesting but heretofore infrequently-observed coincidental occurrences of different kinds of echoes in early morning will almost certainly arise at some sites in the future and cause other problems with this algorithm.

**Accuracy of roost localization**  
**5.1 % of circles corresponded to no roost at all.**



Locations of roosts, along with their sizes, are key items of information generated by this algorithm. In a single sweep, the Roosting Birds Algorithm is required to locate a roost sufficiently accurately to match it (within InterRoost km) to the same roost in previous sweeps. Furthermore, accurate location of a

roost is needed to properly position the radius of the circle describing the departing birds, so that their reflectivity and other characteristics may be accurately measured.

Accuracy of localization of roosts was measured as the linear geographical distance between the actual location of a roost as noted in field observations and the computed location of the roost center at (a,b). The preceding figure shows the frequency distribution of this measure of error, except for 5.1% of the circle centers that were located by the algorithm but that corresponded to no known roosts (false positives). The largest value, at error=13.1 km, is the Huntsville AL observation noted above as being corrupted by migrating birds or insects. Measured errors > 4 km were not frequent; this is the basis for setting the FootPrint parameter.

One may ask, "What is the likelihood of a false positive affecting the list of known roosts?" (This is the only way a false positive can impact the performance of the algorithm.) It could affect the list in two ways: by falling near enough to an actual roost to cause it to continue to exist after it had in fact moved or disappeared, or by becoming a known roost by a series of false positives falling near to one another (within InterRoost) on successive days.

The mean number of actual roosts per full sweep found by the algorithm was 2.1, in a 14,000 km<sup>2</sup> area. Assuming that, if two WSR-88D sweeps occur during roost departures, then the 2.1 roosts that would be located in each sweep would likely be the same roosts, totalling 2.1 roosts/day. Therefore, if the false positive rate of 5.1% is a reasonable estimate, we expect a false positive on about 1 of each 20 sweeps, or every ten days. Although this rate is unexpectedly and perhaps suspiciously low, we may conclude that, even if the actual rate is higher, there is but little chance of a false positive roost happening to be situated close enough to a known roost to have a long-term impact on its survival in the list of

known roosts and, equally importantly, there is a negligible chance of random false positive roost centers close to one another on successive days.

A note of caution: The above rough calculations, while appropriate in some respects, assume random occurrences of events that are probably not going to prove to be random in the real world of the WSR-88D. For instance, one might imagine a certain class of non-bird echoes that occur often or regularly in roughly the same geographical location on successive mornings. Such not-unimaginable but difficult cases will probably generate false positives in interesting and creative ways on the WSR-88D.

Two hypothetical situations might have influenced the measured errors. One is that the algorithm might generate a false positive roost that chanced to have its center located close enough to an actual roost that the investigators assumed the algorithm was functioning correctly and assigned the known roost to the output. If such a coincidence would occur, it would deflate the measured error rate. There is no indication this happened and the design of the algorithm makes it difficult but not impossible to imagine such a hypothetical situation. It might occur if perhaps diverging non-bird echoes surrounded an actual roost and if the bird echoes from the roost were somehow obscured from observation by the radar. This possibility is too bizarre to be worth being concerned about.

The other hypothetical situation is more likely and we can never be sure that it did not occur: the algorithm could locate an actual roost that was unknown to the field observers. This would inflate the measured error rate--a "false false positive". Unfortunately, field observations ceased before the completion and tuning of the algorithm were completed and thus the locations of the apparent false positives generated by the algorithm could not be known to field personnel. So we have no direct evidence that birds did not roost in these places. We must rely on several kinds of indirect arguments. The primary such argument is that

available roost sites for numbers of "blackbirds" are sparse in the study area and most of the false positive sites fell (as chance should dictate) in ornithologically barren agricultural land, not roosting habitat. East-central Illinois is some of the most productive farmland in the world and is so intensely farmed that possible roost sites are limited in number. For instance, in about 1987-1990 the land in counties in which the algorithm located apparent false positive roosts averaged 91% cropland, not including pasture land, towns, farmsteads, and roads (Clements 1989). Those roosts that exist are usually visible for many kilometers because nothing over 20 cm tall exists in the row crop fields during the cold months. Hedgerows, and even fences are few and far between after fall plowing; woodlots are a precious wildlife resource.

Another argument is that, in cold weather, rural roosts are overdispersed (in the spatial sense, not the statistical sense) in what roosting habitat there is available. Therefore the algorithm's success in finding a sizeable, stable roost in a certain location is to some extent itself an argument that other roosts do not exist nearby.

Finally, the research radar data allow one to follow the movements of birds nearly minute-to-minute and thus to be able to locate roosts based on more information that is available to the algorithm from individual sweeps isolated in time; the false positive roosts did not correspond to roosts we had observed in playbacks of radar data but rather seemed to result from combinations of echoes of roosting birds far dispersed from their roosts, railroad trains, and unidentified miscellaneous echoes that happened to be arranged with other echoes in roughly diverging patterns.

Admittedly, these are not entirely convincing arguments, but in any case the hypothetical existence of "false false positives" would merely artificially elevate the measured rate of 5.1% false positives and thus have a conservative effect on

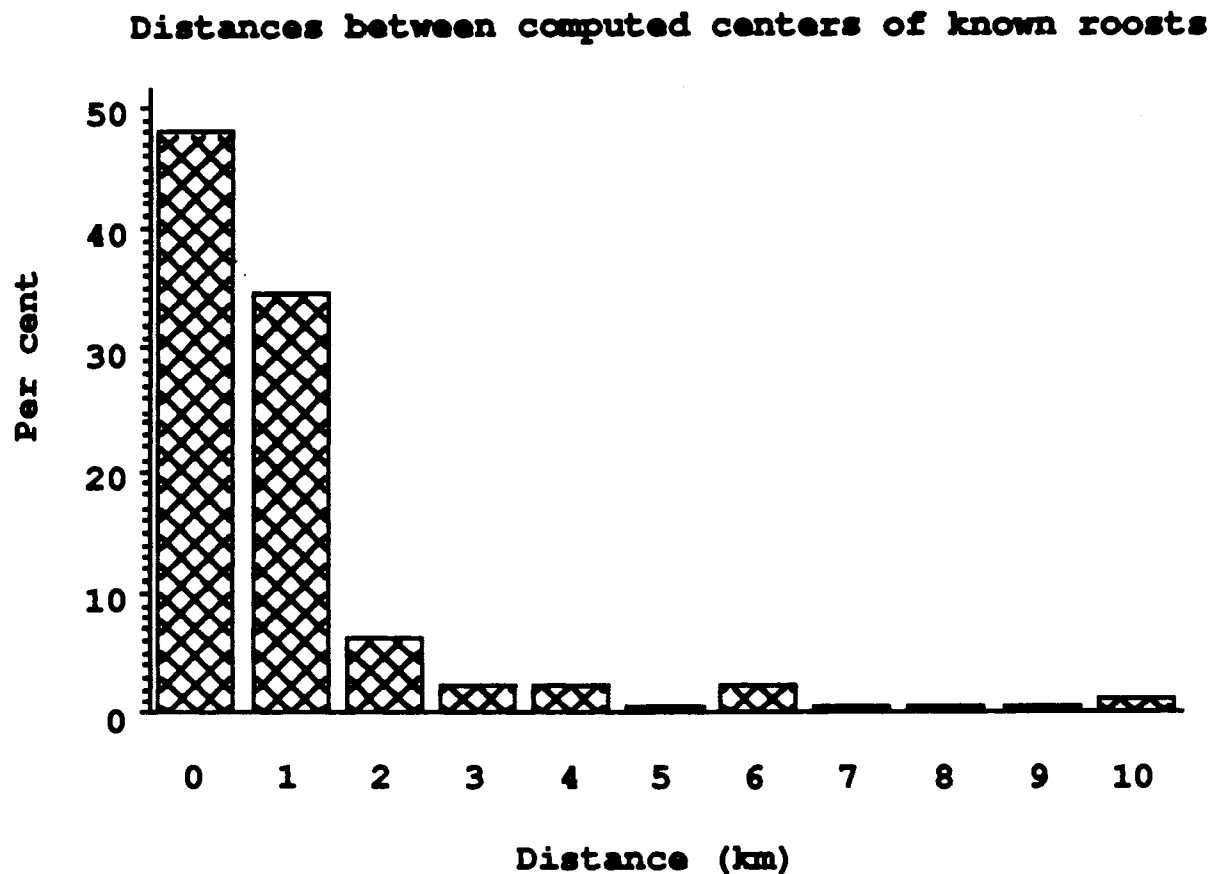
evaluating the algorithm's performance.

After conducting the field work and watching the algorithm identify roosts, we believe that the most frequent kind of "error" (note quotation marks) that the algorithm generates is not reflected in the above analysis. In some years, in roosting habitat that is spatially dispersed yet patchy (such as urban areas), and with poorly-understood and perplexing variation on a day-to-day or week-to-week basis, 2-3 roosts can coexist within a several km of one another yet be large and stable enough to be spatially distinct. The color figure of a PPI in the section on spectral width above illustrates how two such roosts can appear on weather radar. (The extent to which they are socially distinct, rather than merging with or interchanging member birds with each other is open to investigation. In fact, it is not obvious that it is inappropriate to regard such a cluster of roosts as ecologically one roost that is spread out because the habitat is patchy.)

The "error" the algorithm nearly always commits in such cases is to incorporate the several roosts into one large circle. The circle usually encompasses most departing echoes from each of the constituent neighboring roosts (thus counting most of the birds) and the roost center, coincidentally or not, often lies close to a large roost in the group of 2-3 (thus giving good results in the above figure on accuracy). At this point, it is clear neither whether this behavior is biologically an "error" on the part of the algorithm, nor, if it were, whether anything could be done computationally to correct the "error". The phenomenon of clusters of roosts or roosts in flux is an example of wild birds behaving as they wish; fortunately, when the algorithm encounters this situation it "fails" in such a graceful fashion as to function nearly normally. We cannot estimate how often such situations will occur in general.

A different linear measure helps to set the InterRoost criterion. Using series

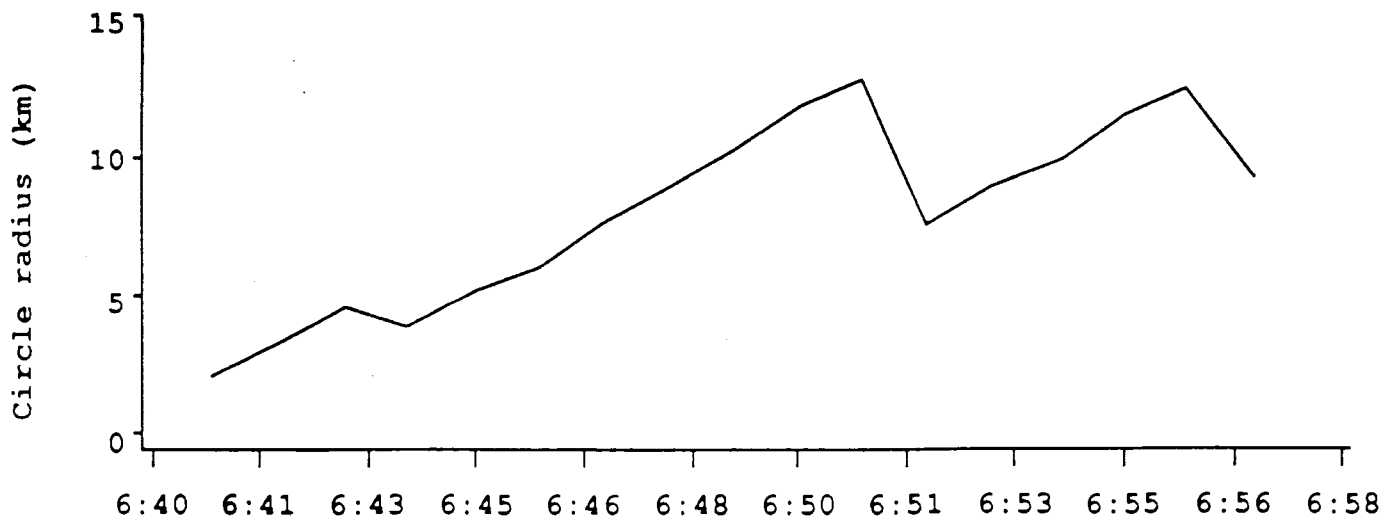
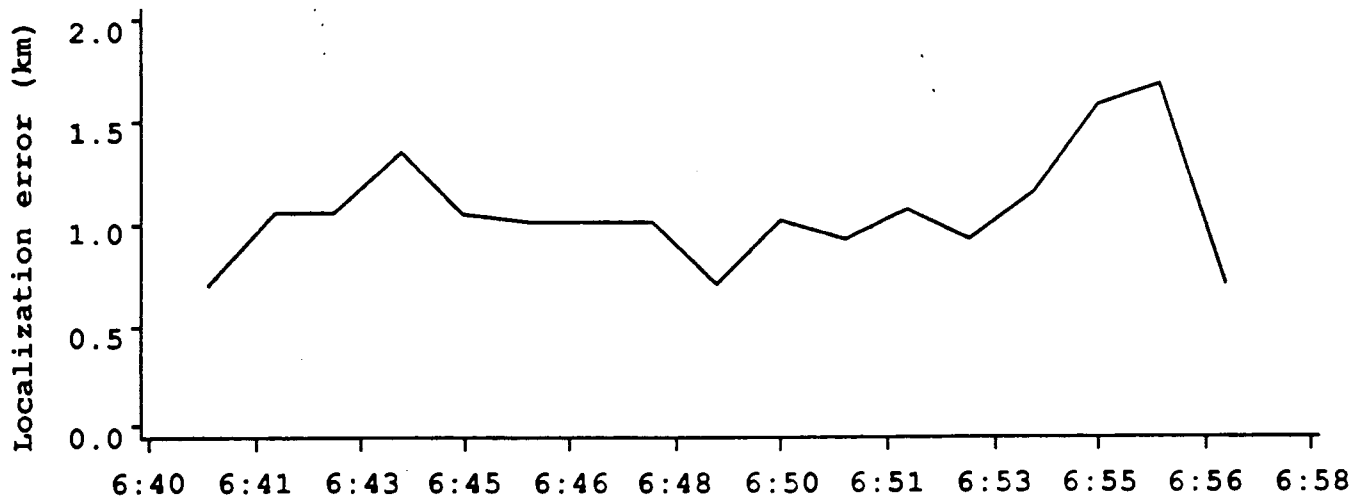
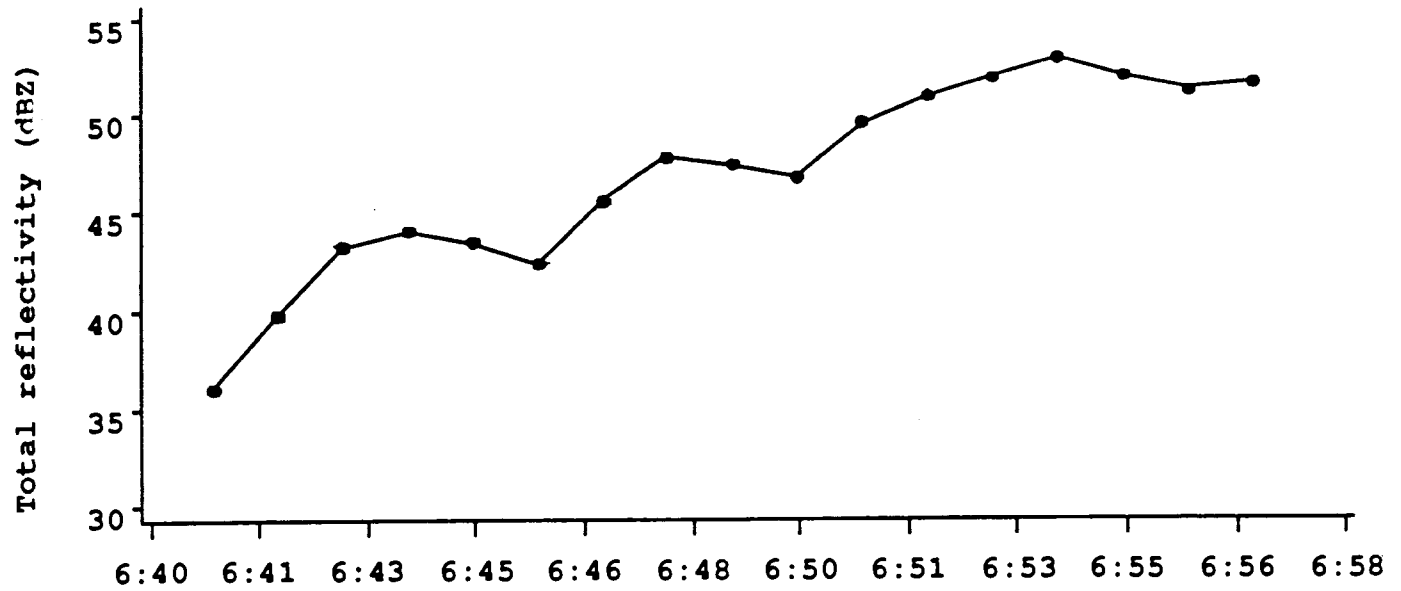
of locations of the same known roost by the algorithm, we measure the distance from each (a,b) roost center to each other center. The distribution of these distances (see figure below) gives an indication of the expected sweep-to-sweep or day-to-day differences in relocating the same roost, which is the algorithm's job. This is a measure of accuracy of the algorithm rather than resolution.



**Sizes of roosts** Aside from the highly significant correlation between total reflectivity and number of birds in a roost (see above), an additional indicator of algorithm skill in measuring roosts is the temporal change in roost parameters during the morning exodus. Birds depart from a large roost in pulses that place cumulatively more birds in the air surrounding the roost, spread steadily in

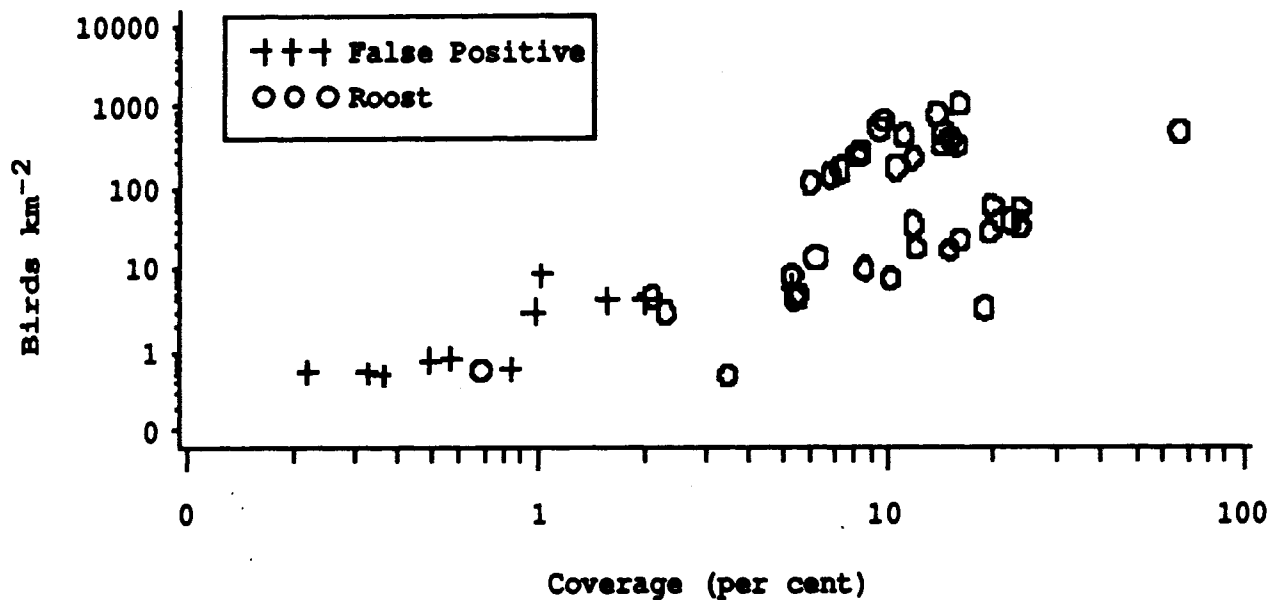
radius, and finally disappear as they reach a certain maximum radius. On 7 December 1982 the sector scan mode used by CHILL provided a time series of roost departure for European Starlings, closely spaced enough in time to examine the important algorithm outputs as a function of time during departure. The results from N=17 runs of the algorithm during the main departure period from this date are shown with the times of successive sweeps indicated by the dots on the top curve in the figure. Reflectivity climbs to an asymptote at about 105 birds, not steadily but as each of about three successive pulses departs the roost. The calculated roost center, on the other hand, remains steady very close to the actual stand of evergreens in which the birds roosted. It displays perhaps more variability near the end of the series as the birds vacate the vicinity of the roost itself. The radius of the outermost circle climbs smoothly except when the first pulse dissipates at about 0651 and the second pulse begins to dissipate at about 0656. The slope of the long smooth rise in radius from 0643 to 0650 is  $23 \text{ m s}^{-1}$ , close to the  $20.6 \text{ m s}^{-1}$  winter departure speeds previously reported by Eastwood (1967). These time series indicate the algorithm measures output values correctly for a large roost on a clam morning.

Time progression during sector scans, 7 Dec 1982





### Comparison of two measures of circle validity



Intuitively a circle that is sparsely filled with echoes should have fewer departing birds than a circle that is well filled and such a sparsely-filled circle should represent a roost with fewer birds or perhaps a dispersal movement just beginning or nearly completed. In testing the algorithm, it became apparent that sparse circles were apt to be false positive roosts. In evaluating this idea, two measures of "sparse" suggest themselves: blackbird-equivalents km<sup>-2</sup> and Coverage, or bird echo cells km<sup>-2</sup>. The figure plots these measures against each other for N=49 roost locations; it shows that (1) false positives are indeed much more common in sparse roosts, measured either way, but also that (2) Coverage is the better discriminator of false positives from actual roosts. This analysis is the basis for 2% as a working value for the MinCoverage parameter.

For the N=38 roost locations with Coverage > MinCoverage, which are therefore largely successful locations of actual roosts, we may ask the further question of whether the algorithm locates dense roosts more accurately than

Spearman Rank Correlation of localization error (km) with two measures of sparseness of circle filling.

	<i>r</i>	<i>p</i>
Blackbird-equivalents km <sup>-2</sup>	-0.54	0.0005
Coverage	-0.15	0.4

sparse roosts. Again we answer the question for both measures (see box). Circles containing stronger bird echoes are located more accurately.

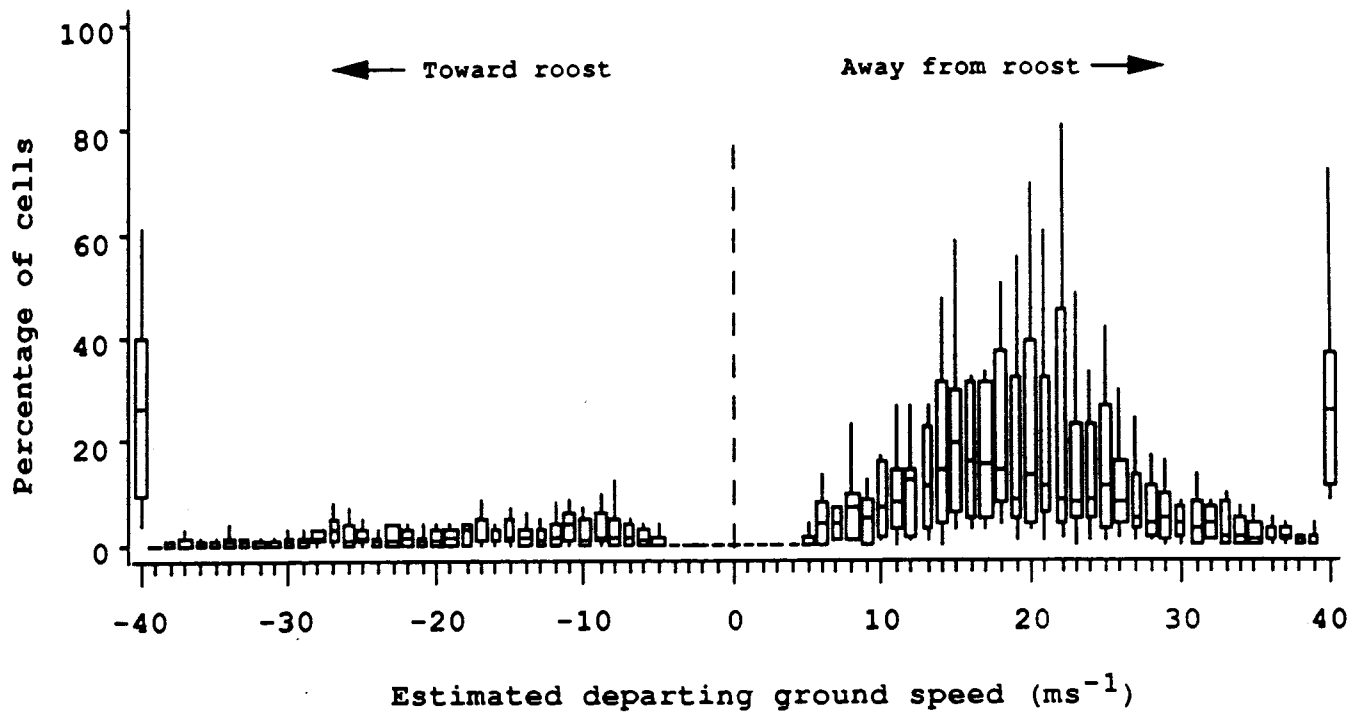
**A test for extraneous targets using Doppler velocity.** When the algorithm finds the location and radius of a circle delineating the putative departing birds from the roost, the circle will almost always include both roosting birds and other extraneous targets. This process of locating a roost is based on many factors. Among these is the nominal cruising flight speed of the birds in a roost, BirdFltSpd. The algorithm expects that the roosting birds take straight paths originating at the center of the circle and that they fly at BirdFltSpd. (In still air, BirdFltSpd equals ground speed.) Extraneous targets, in contrast, are expected neither to fly at BirdFltSpd nor to fly in any special direction (on average) relative to the roost center.

If a cell contains only departing roosting birds (and given other assumptions discussed below), Doppler velocities measured with radar will be determined by:

$$VEL = Speed \times \cos ( Track - \theta )$$

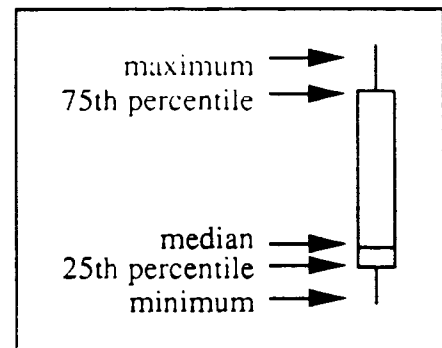
, where Track is the direction the birds in the cell are flying away from the roost,  $\theta$  is the azimuth of the cell, and Speed is BirdFltSpd.

# Estimated ground speeds inside roost circles



The estimated ground speed of all echoing cells within algorithm-determined circles, assuming each cell is composed entirely of objects moving directly away from (or toward) the algorithm-determined roost center. Speeds with magnitude over  $40 \text{ ms}^{-1}$  are set to  $\pm 40 \text{ ms}^{-1}$ .

Data are from all available ( $N=12$ ) circles with Coverage  $> 2\%$  on mornings with calm wind conditions at the surface. The ground speeds are thus equal to flight speeds.

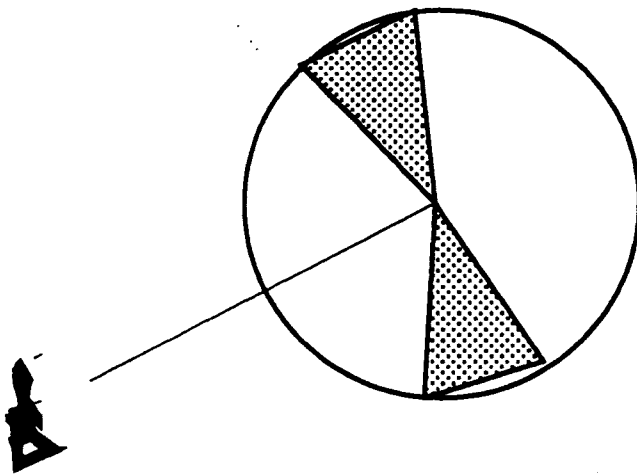


Box-and-whisker symbols

This relationship can be exploited to estimate what proportion of cells within roost circles may be attributed to roosting birds that behave according to expectation. Using only calm mornings, so that Speed=ground speed=flight speed, we solve for Speed and examine the proportion of Speeds that are centered around a value slightly below BirdFltSpd (for reasons explained below). Results of such a calculation are shown in the preceding figure as estimated ground speeds. The plot is constructed by generating a frequency distribution of Speed for each roost, then plotting, for each Speed, the median and other descriptive statistics across the N=12 roosts accepted into the calculation. The Speeds are not

weighted by reflectivity--weak and strong targets contribute equally.

The plot shows several noteworthy features. Low Doppler velocities ( $<V_{elThL}$ ,  $4 \text{ ms}^{-1}$  here) have been removed from the data prior to running the algorithm. Cells in regions tangential to the radar beam (see figure at left) but that nevertheless have moderate or



high Doppler velocities are clearly not departing the roost. Estimating their ground speeds as if they were departing the roost yields abnormally high speeds (pegged at  $\pm 40 \text{ ms}^{-1}$  in the figure). Together with cells approaching the roost, they represent targets that either are not departing the roost or at least are not departing in a straight line. Speeds in the general region of  $+20 \text{ ms}^{-1}$  (BirdFltSpd for starlings and "blackbirds") represent the plurality of the echoing cells; these are likely to be birds departing the roost.

Variation about the nominal  $20 \text{ ms}^{-1}$  flight speed of starlings (BirdFltSpd) is

attributable to several factors. Two common effects will reduce the measured Doppler velocity and thus produce modal estimated ground speeds  $< 20 \text{ ms}^{-1}$ : The birds fly low and ground clutter with zero Doppler velocity is averaged in, lowering the measured Doppler velocity. Second, as explained above, variation in the tracks of individual scatterers in the radar pulse volume, even if all fly at identical speed, will be likely to reduce the measured Doppler velocity.

Other factors will introduce variation both above and below BirdFltSpd. Inevitably, a certain number of echoing objects intermixed with the roosting birds are not roosting birds. The contribution of such objects (which include vehicles, railroad trains, and other birds such as pigeons) can be judged from the distribution between  $-5$  and  $-39 \text{ ms}^{-1}$  approaching the roost; such echoes are not roosting birds or at least largely free of contributions from roosting birds. Furthermore, not all the birds are starlings (although the majority are) and we have no evidence that even the starlings maintain perfect constancy in flight speed. Algorithm errors in location of roost centers will generate errors estimated ground speeds, as will multiple roosts lumped together by the algorithm. Finally, any undetected wind at the height and geographical position of the departing birds will appear as change in the mean flight speed. Examination of plots of the geographical distribution of the estimated ground speeds showed gradients along radials from the radar in one or two cases, suggesting light wind.

Nevertheless, in spite of the many sources of variation, the clear peak in the distribution just below  $20 \text{ ms}^{-1}$  is a strong validation of the algorithm's ability to selectively and accurately locate birds departing from roosts near dawn. 2493 of 5561 cells in this analysis, or 45%, lay within  $\pm 5 \text{ ms}^{-1}$  of  $19 \text{ ms}^{-1}$ . For future tinkering with the algorithm, is worth considering this estimated ground speed as a possible automated, day-to-day operational measure of the quality of a roost. For instance, it could be used along with InterRoost to decide when to accept a

new roost location as a known roost, providing that the seasonal species mix making up the roosts near a given WSR-88D can be predicted.

**Computation time** of the Roosting Birds Algorithm is not short. However it will run on only on 0-3 sweeps/day and 23-hr turnaround is acceptable for each day's calculations. Its running time on a 1987-vintage VAXstation 3200 (speed benchmark, about 3 SpecMarcs) varied greatly, mainly depending upon the number of gates containing bird echo, from about 5 min for a sweep nearly devoid of echo to about 80 min for the largest roost with 26,000 cells filled with bird echo. The runnable test program is optimized in some of the obvious ways (partial use of precomputed look-up-tables, etc.), but was designed for testing the algorithm rather than optimizing for speed. In particular, the algorithm repeats the entire Hough transform after each roost is found, recomputing circles even for echoes that lie distant from the roost that was found and could have had no interaction with it.

The longest running time of the algorithm can probably be reduced most profitably by short-cutting the Hough transform inside areas of continuous bird echo, so that the same lengthy calculations need not be performed for cells abutting one another. Several shemes come to mind for this sort of optimizing, which can probably speed the algorithm fourfold or so even on a slow workstation such as used in the test runs. In addition, the largest roosts, which are most time-costly, probably do not need updated information as often as daily, because they are almost always very stable seasonally and often year-to-year.

**Some foreseeable problems for the Roosting Birds Algorithm.**

The height AGL of "blackbirds" is commonly about 50 m but the flying height of other species is less well-known and all species may fly at much greater heights when there is ground fog (Harper 1959), as well as flying lower when

there are opposing winds. Therefore the 50 m figure should be regarded as provisional until other species and foggy conditions are better-studied. If and when fog sends massive bird echoes into higher elevation scans of the WSR-88D, both the Roosting Birds Algorithm and the microburst algorithms will probably malfunction.

MaxWind is currently set at 10 m/s, but we have few data from mornings with winds in exactly the right range of wind speeds for setting MaxWind. For instance, on 17 Nov 89 surface winds were about 8 m/s and flecks of apparent noise (ground targets waving in the wind?) covered the CHILL PPI. No combination of algorithm filter parameters (T\_CN, RefThL, MinNCP) reduced the noise but retained the (faint) roost echoes. Regardless, the algorithm gave much too large diameter circles. Three visible clumps of departing birds--N of Danville, Rantoul, and Decatur--were correctly located on the edges of the first 3 circles found, but (1) the algorithm continued to find more and more circles, because of noise of variable reflectivity all over the screen and (2) the departing birds were on the edges of circles with diameters nearly MaxRad in diameter, so that the centers were off position upwind from the clumps of birds. Resetting MaxWind to ca. 8 m/s would have obviated this particular image's problem, but at the expense of lowering the number of mornings on which the roosting birds algorithm is useful. Much more field work will be required to fully optimize the setting of weather-specific and probably site-specific parameters such as MaxWind.

More data are also needed on fall and early spring instances of overlap between nocturnal migration and roost departure. Only 2 such instances, both fortuitous, were available for this research.

More data are also needed on: other species, long series of consecutive mornings to test and tune the logic regarding known roosts, and of course actual

**WSR-88D data with operational settings of filter notch width and other critical values.**



## IV. Following flocks of waterfowl

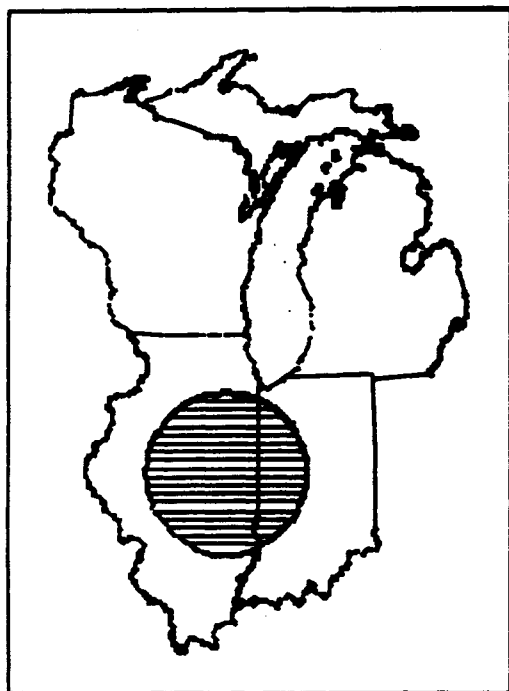
Background	1
Methods	6
List of variables	6
Filter criteria	8
Identification of echo segments	9
Constraining the problem of matching echo segments	12
Measures used to match echo segments	19
Linearity of paths	20
Parameters at AGE=1	20
Periods of data gathering	23
Echo segments per volume	23
Reflectivity	24
Doppler	25
Spectral width	26
Sensitivity analysis of measures used in matching echo segments	27
Maximum reflectivity	27
Spectral width	27
Tromboning the weightings	28
4-space vs. decision-sum	29
Choices	29
Performance	32
Comparing the algorithm's paths with hand-mapped paths	32
Length of paths	34
Speed and direction of echo segments	46
Following flocks appearing in different radar elevation angles	49
Identifying paths that correspond to flocks identified visually	52
Migration traffic rates	56

### Background

The Mississippi Valley Population (MVP) of Canada Geese (*Branta canadensis*) breeds in the Canadian arctic and winters in southern Illinois and parts of adjacent states (Samuel, et al. 1991). Most of the birds presently migrate southward in two stages, stopping in the region of south central Wisconsin. Although scattered southward migration occurs at various times in the fall, the

second stage of the southward migration often is concentrated in one or two brief periods of about 24 to 36 hours (Tacha, et al. 1991), massive goose movements that provide an opportunity to study the movements of large waterfowl on radar. The return migration to the breeding grounds is less well-organized and would be more difficult to study.

The coverage of the CHILL radar provided an excellent opportunity to study



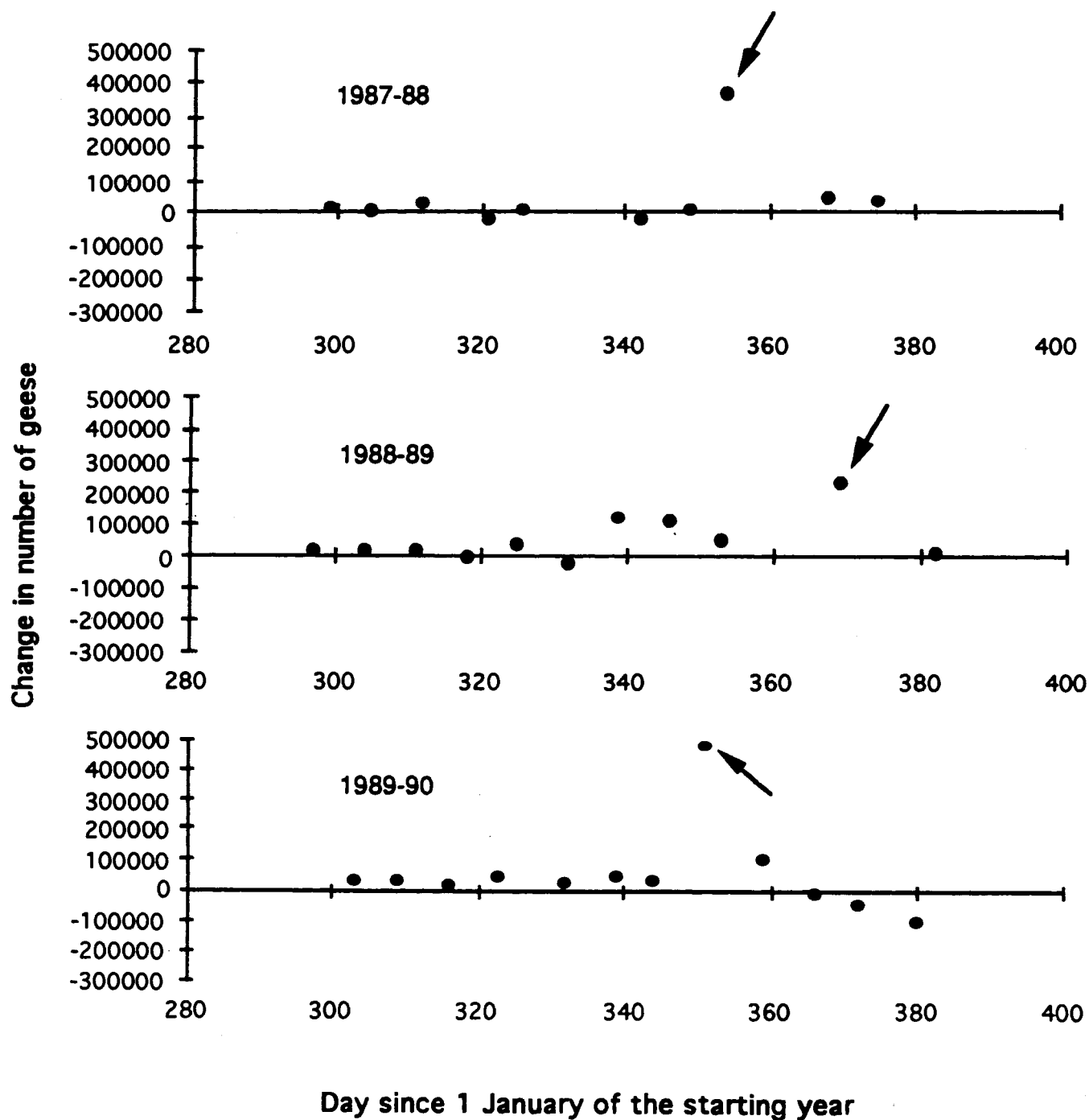
echoes from the MVP population (see figure).

Observation of the Canada Goose migration is documented in earlier reports and publications. Larkin (1982) reported on initial CHILL data on migrating birds and concludes that it is feasible to recognize birds on NEXRAD. Mueller and Larkin (1985) gave ZDR data on migrating insects observed with dual-polarization weather radar. Larkin and Quine (1987) presented data on the appearance of birds on Doppler weather radars and detailed the methods by which a small fire-control tracker is used to provide “ground truth” for weather radar data. Quine and Larkin

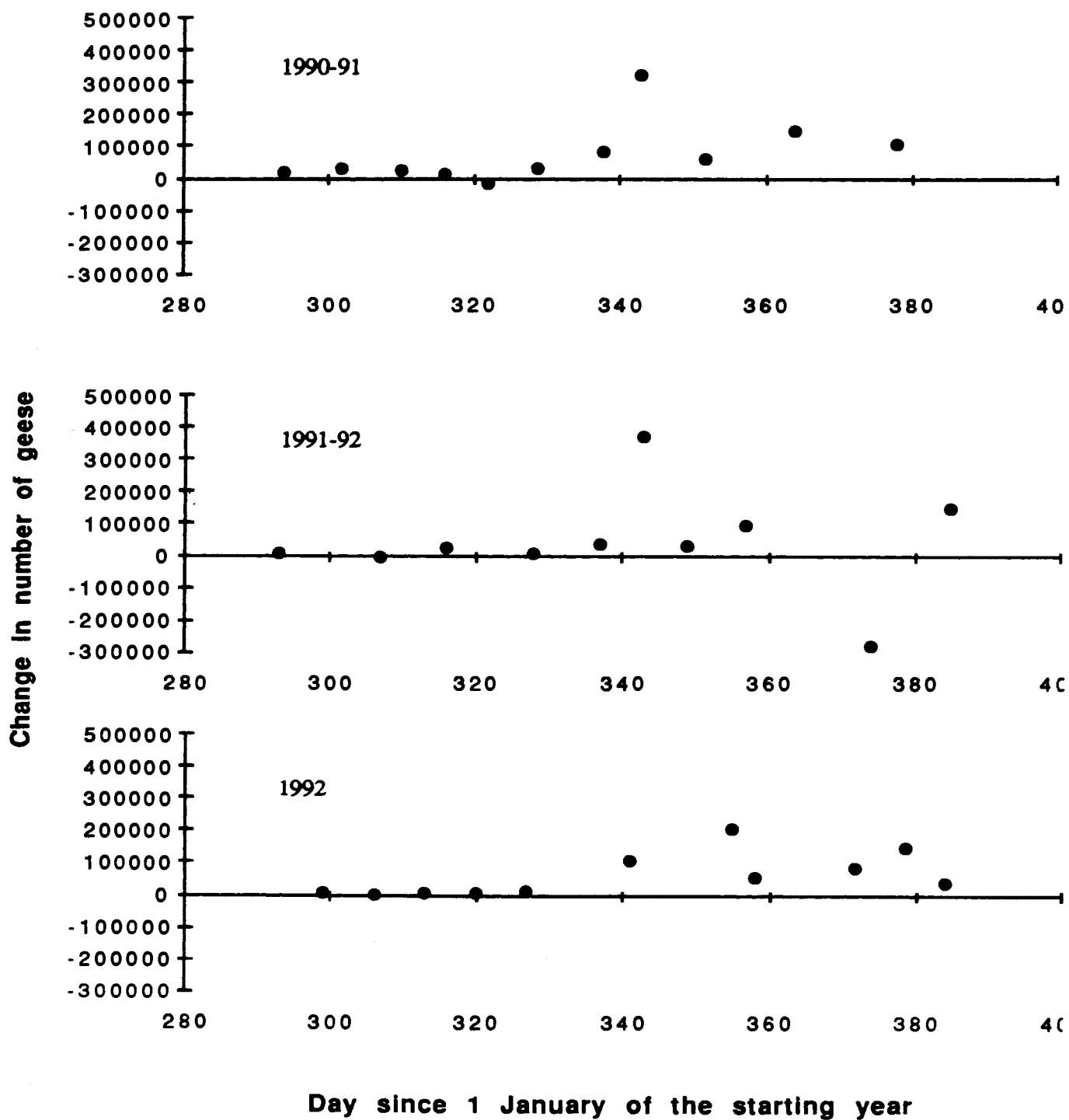
(1987) introduced the 1987 observations. Larkin and Quine (1989) discussed the biology of Canada and Snow Goose migrations over Illinois, puts them in the context of observations with the CHILL research weather radar, and describes general data-gathering methods. Larkin (1990) described progress in work on migrating birds and waterfowl, including massive migrations of geese, and introduced an algorithm for locating groups of birds departing morning roosts. Larkin (1991a) provided data discriminating migrating birds from migrating insects on radar based on their flight speed and other characteristics. Larkin

(1991b) illustrated the size of the Canada Goose flocks.

The CHILL radar became operational in 1987 after extensive modifications. It was moved to another state in Spring 1990. Therefore, data gathering on the MVP Canada Goose migration was limited to the fall seasons of 1987, 1988, and 1989. In each of these three seasons, the major Canada Goose movement of the season was recorded with CHILL (marked with arrows on figure) and simultaneous observations with tracking radar and visually were conducted. 1987 and 1988 CHILL observations were confined to daylight hours; in 1989 CHILL observations extended into darkness. In 1989 the population of MVP Canada Geese reached an all-time high (Babcock, et al. 1990).



Changes in counts of Canada Geese in Southern Illinois and adjacent areas, fall 1987-spring 1990, from data supplied by the Illinois Department of Conservation. Negative values in January (Day >365) often represent tentative northward spring movements. Arrows mark major movements recorded by the CHILL radar.



Changes in counts of Canada Geese in Southern Illinois and adjacent areas, fall 1990-fall 1992, from data supplied by the Illinois Department of Conservation. Negative values in January (Day >365) often represent tentative northward spring movements.

## Methods

**List of variables.** Reconstruction of the paths of goose flocks took place in three stages: first, filtering on a gate-by-gate basis, then, identification of echo segments from the gates in a volume and calculation of representative values, and finally matching of the echo segments with those of the previous volume. A listing of variables used in the algorithm follows; more detailed descriptions of some of the variables is given in the text where their function is described.

---

Variables used in path-following algorithm.

(ES = Echo Segment, distances are in km, reflectivities in dBZ, X is eastward, Y is northward)

---

Variable	Meaning
----------	---------

---

AGE	Volumes since path start; first volume is AGE=1
AREA_KM	Area of ES in km <sup>2</sup>
AX	X position of path at AGE=1, from fit, in km
AY	Y position of path at AGE=1, from fit, in km
AZIMUTH	Radar azimuth of ES, in degrees
BEARING	Measured XY track from VOL <sub>T-1</sub> to VOL <sub>T</sub> , in degrees
BEG_TIME	Time of ES at AGE=1
BS_FLTRD	BUNCHSIZ after trimming
BUNCHSIZ	Number of ESs in VOL <sub>T-1</sub> or VOL <sub>1</sub> included in matching
BX	X component of path velocity, from fit, in km hr <sup>-1</sup>
BY	Y component of path velocity, from fit, in km hr <sup>-1</sup>
CHOICE	Number of possible matches in VOL <sub>T</sub>
DELTA_D	XY distance, extrapolated-measured, in km

DELTA_X	X component of DELTA_D, in km
DELTA_Y	Y component of DELTA_D, in km
DOP	Weighted mean Doppler velocity of ES, in ms <sup>-1</sup>
DUPL_NUM	Number of elevations with duplicate echoes
EHR	Elapsed time (hr) since previous gap
ELEV	Elevation of the centroid of an ES, degrees
EMIN	Elapsed time (min) since previous gap
FLOCK	Identification number of a path
FLOCKSIZ	AGE at the last volume in a path, in volumes
INTERSTI	Distance to nearest other ES measuring between closest gates, in km
ISL_NUM	Identification number of an ES
KM_HR	Ground speed of a path from linear fit, in km hr <sup>-1</sup>
LINEAR	Categorical ranking of SE <sub>xy</sub>
MAXMATCH	Number of VOL <sub>I</sub> ESs to compare with ES in VOL <sub>I-1</sub>
MAX_REF	Maximum REF in an ESD, in dBZ
MAX_SRCE	Number of VOL <sub>I-1</sub> ESs that are compared with ES in VOL <sub>I</sub>
NULLED_M	Number of matches less likely than vanishing
N_GATES	Number of gates in an ES
N_LEFT	Volumes left until this path ends
PERIM	Measured perimeter of an ES, in km
POSTGAP	1 if the path began after a gap in data, else 0
PREGAP	1 if the path ended at a gap in data, else 0
RAD_ERR	Doppler-measured radial velocity  of ES, in m.s <sup>-1</sup>
RANGE	Slant range from radar of ES centroid, in km
SD_REF	S.D. of reflectivity in an ES
SEX	S.E. of X f(T) linear fit, in km
SE <sub>xy</sub>	Hypotenuse of (SEX, SEY), in km
SEY	S.E. of Y f(T) linear fit, in km
SPEEDXY	Measured ground speed from VOL <sub>I-1</sub> to VOL <sub>I</sub> , in km hr <sup>-1</sup>
SW_WGTD	Spectral width of ES weighted by REF, in ms <sup>-1</sup>
TIME	Time radar scanned past ES at best elevation

TOT_REF	REF for ES summed as voltage, in dBZ
TRACK	Ground track of path from linear fit, degrees
XRESID	Residuals from X f(T) fit, in km
XYRESID	Hypotenuse of (XRESID,YRESID), in km
X_COOR	Eastward coordinate re radar of ES centroid, in km
YRESID	Residuals from Y f(T) fit
Y_COOR	Northward coordinate re radar of ES centroid, in km
Z_COOR	Height of ES centroid, from elevation sin(range), km

---

**Filter criteria.** Gates were rejected as noise before being included in echo segments if they failed to meet any of the following criteria.

Reflectivity	$\geq 0.5$ dBZ
Noise-corrected power	$> 0.2$
Spectral width	$< 10.0$ ms <sup>-1</sup>
Doppler	$\geq 4.0$ ms <sup>-1</sup>
Height, corrected for Earth curvature	0.15 to 1.5 km AGL

In addition, echo segments were later discarded from the path-following section of the algorithm if they had high weighted average spectral widths, SW\_WGHTD  $> 7.0$ .

The |Doppler| criterion almost always resulted in false rejections of goose flocks travelling tangential to the radar, as discussed below; the other criteria resulted in few false rejections. The filter criteria were initially developed by examining PPI images of mixed geese and other echoes, including ground clutter, vehicles on highways, aircraft, and many unidentified echoes. Then filter criteria



were optimized during early runs of the algorithm to reduce the number of one-volume (unconnected) echo segments without reducing the duration or SE<sub>XY</sub> values of long paths (see below). With the exception of spectral width, valid data for which were not available before 1989, filter criteria developed for one or two years' goose movements could be used without modification for the other movements.

**Identification of echo segments** and calculation of radar product values for echo segments. Gates were considered to be part of the same echo segment if they lay within four gates in either direction along a radial or in this same region along adjacent radials. That is, the most distant gates considered part of the same echo segment have this configuration, or either of its mirror images:

Radial:	i	i+1	i+2
	x	.	.
	.	.	.
	.	.	.
	.	.	.
	.	x	.

The criterion of three gates' separation in range and one gate separation in azimuth was arrived at after construction of survivorship curves of nearest neighbor gates, in range and azimuth separately.

Four gates constituted the minimum number for an echo segment. Although some small flocks at long range were incorrectly discarded because of this range-independent criterion, the loss was not important biologically nor for determination of numbers of geese for bird hazard calculations.

As a noise-rejection measure, the maximum allowable length of the perimeter

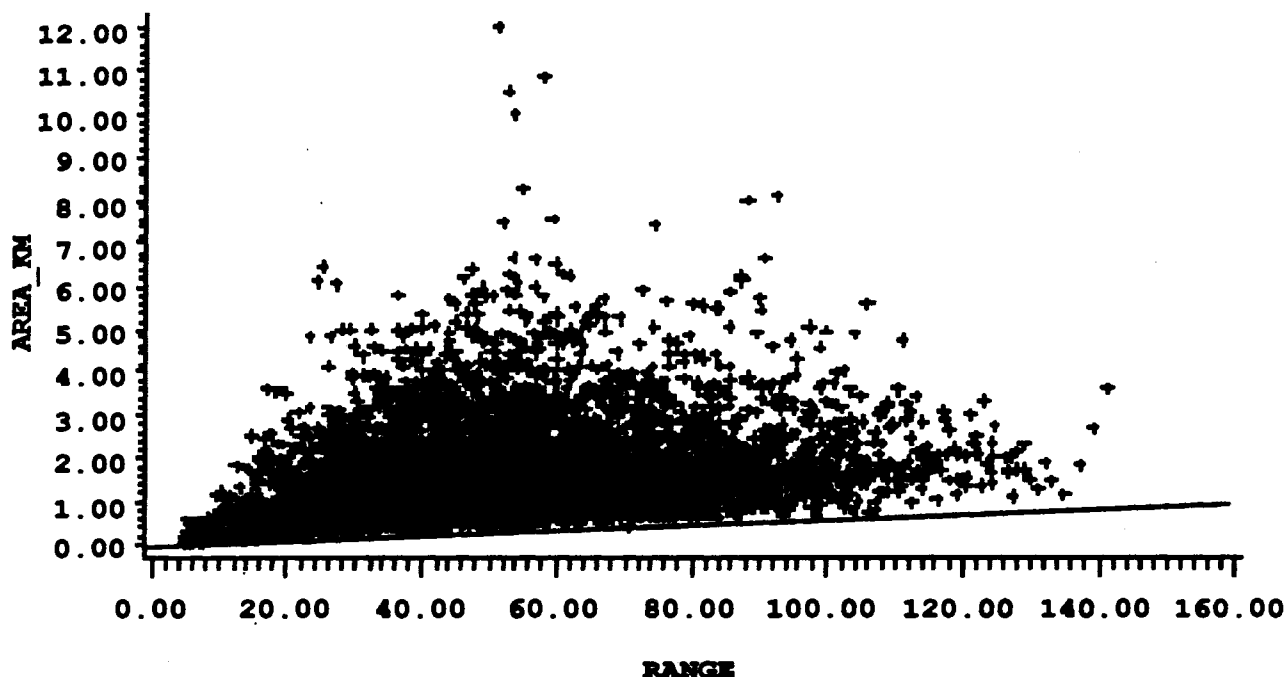
(PERIM) of an echo segment was set at 180 gates, a value larger than any observed goose flock. This criterion rejected occasional rays with continuous noise.

Characteristic values of Doppler (DOP) and spectral width (SW\_WGHTD) were computed for each echo segment by weighted averaging. A weight was computed for each gate in an echo segment by converting the gate's reflectivity from decibels to a ratio, then the weighted average of Doppler and spectral width was computed and used for the echo segment. Thus, gates with stronger echoes contributed more to the Doppler and spectral width values for the echo segment.

The area of echo segments (AREA\_KM) was computed by considering each Doppler values were corrected for aliasing before being used in the averaging. gate a rectangle of dimensions:

$$\text{range} \cdot \sin(\text{azimuth}) \times \text{gate spacing},$$

and summing the areas of all gates in an echo segment. Below-threshold or empty areas between gates were not included in measurements of area. The minimum area of flocks increased linearly with range, a result of beam spreading, as would be expected. An empirical correction, RANGE/160, was subtracted from the area of each echo segment to correct this artifact (see figure). After the correction was implemented, area was not seriously affected by range, as evidenced by the fact that approximately equal numbers of long flocks (FLOCKSIZ $\geq$ 15, 1988 data) decreased in area as increased in area as they approached the radar, from signs of least-squares linear fits of area f(range).



Area of echo segments in long paths, as a function of slant range.  
 $1 \text{ km}^2 \text{ 160 km}^{-1}$  (the line) was subtracted from echo segment areas to correct  
 for the radar's inability to resolve small targets at long range.

About 15% of the goose flocks generated echoes in two adjacent elevations in one volume scan (DUPL\_NUM=2). (The use of “echoes” here denotes a group of gates that otherwise qualified as an echo segment after the above computations were performed, but that might be discarded as a duplicate rather than qualifying as an echo segment.) Such duplicated echoes required special treatment. Echoes in the adjacent elevation duplicating a given echo in the current elevation were identified by the following process. First, a range overlap zone was defined as including the top half of the lower beam and the lower half of the upper beam. All range gates were identified that lay in the overlap zone. Echoes lying within the overlap zone in the current elevation were examined (“the given echo”).

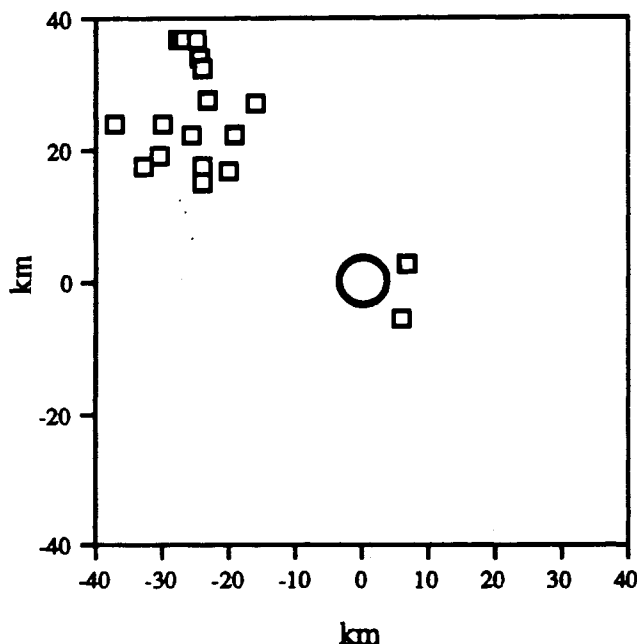
Next, all echoes lying in the overlap zone in the adjacent elevation and closest to the given echo were located by searching across the azimuth-range plane. The distance in XY from the given echo to the closest such echo was then divided by the time separating the two echoes. This time was usually the time taken by the radar to complete a sweep and slew upward in elevation to the next sweep, but could be greater if the radar passed over one of the echoes during slewing. The resultant value was the ground speed a flock of geese would have to maintain to be observed at their XY locations in both elevations. It was converted to estimated air speed by subtracting the wind vector. Estimated air speeds  $< 150 \text{ km hr}^{-1}$  between the two elevations were used as the criterion for considering the two echoes duplicates.

Only 0.6% of duplicate echoes consisted of instances of  $> 1$  echo in another elevation (0.09% of echo segments overall). In such cases, the stronger of the multiple duplicate echoes was used as "the" duplicate.

Causes of duplicated echoes included the antenna gain pattern, including side lobes, reflections of echoes off the ground, movement of flocks during the time between two scans, and probably other causes. The various possibilities and their effects on the echo's characteristics are complex. After investigating various methods for including the information from both elevations in the data in this condition, it was decided to use only data from the echo segment with the higher reflectivity, discarding the lower-reflectivity echo segment.

**Constraining the problem of matching echo segments.** The general problem of picking from  $\text{Vol}_i$  the most-likely continuation of each echo segment in  $\text{Vol}_{i-1}$  cannot be approached via straightforward brute-force calculation. One reason is the large number of echo-segments, on the order of 400/volume, seen in these data from Canada Geese. Another reason is that paths begin and end in each volume, so that each echo segment can end in a non-match as well as a match to

an echo segment in the other volume. But, most importantly, each different matching is a permutation; the number of calculations is governed by an expression of the kind  $\text{MAXMATCH}^N$ , where MAXMATCH is the average number of possible matches and N is the number of echo segments. Clearly the problem is intractable ( $\text{MAXMATCH}^{400}$  comparisons) unless the appearance on radar and flight behavior of the waterfowl are used to reduce the number of comparisons.



Geographical distribution of paths with BUNCHSIZ > 12, 1989 data. One echo segment of each of 18 paths that are part of large bunches is shown. The large bunches are concentrated ((N=2) very close to the E of the radar and (N=16) in an area NW of Champaign IL, congested with many geese, ground clutter from a low ridge (Yankee Ridge), and two interstate highways.

In seeking to eliminate unnecessary comparisons, care was taken to limit assumptions to the minimum. Care was also taken to allow any biologically reasonable flight behavior on the part of the waterfowl; that is, not to impose expectations upon the birds' orientation or other flight

behavior. These goals were met, except in certain extremely dense bunches of

echo segments that rarely (never in 1987, 0.5 hr<sup>-1</sup> in 1988 and 1989) appeared in the data. When these rare, extremely dense bunches occurred, a small number of echoes >10 ms<sup>-1</sup> different from the mean speed and direction of Canada Goose flocks were deleted from the data because the number of echo segments in a bunch was too large to be computed in a reasonable period of time. When this situation occurred, it was always caused by large numbers of flocks of geese flying into regions of CHILL coverage characterized by heavy ground clutter (see figure), so that bunch size (see below) artifactually exceeded 20.

In setting up assumptions to limit the problem,, the history of a flock of geese is defined as the extant duration (AGE), straightness and constancy of speed (SE<sub>XY</sub>), echo characteristics, direction, or other similar characteristics of a path. The probability of appearance or disappearance of a flock of geese (i.e. of beginning or ending of a path) should be independent of its past history, as should its current measured characteristics. Paths of migrating waterfowl should be unconstrained in their direction of travel, with the exception that going relatively straight should be favored over making acute turns. And flight speeds should be realistic. Migrating waterfowl, in this case Canada Geese, have species-characteristic flight speeds which can be termed a species' cruising speed.

However, the algorithm cannot rely on flocks of waterfowl always flying at their optimum flight speed, for several reasons. One reason is that maneuvers such as changing direction or milling about do occur and will reduce observed speed between two position samples (SPEED<sub>XY</sub>), so that the cruising speed should represent a maximum air speed, rather than an expected air speed. In addition, a radar's precision in locating echo segments, limited by the radar's 1° beam width and by distortions introduced by ground targets and other factors, introduces measurement error in estimations of the ground vector.

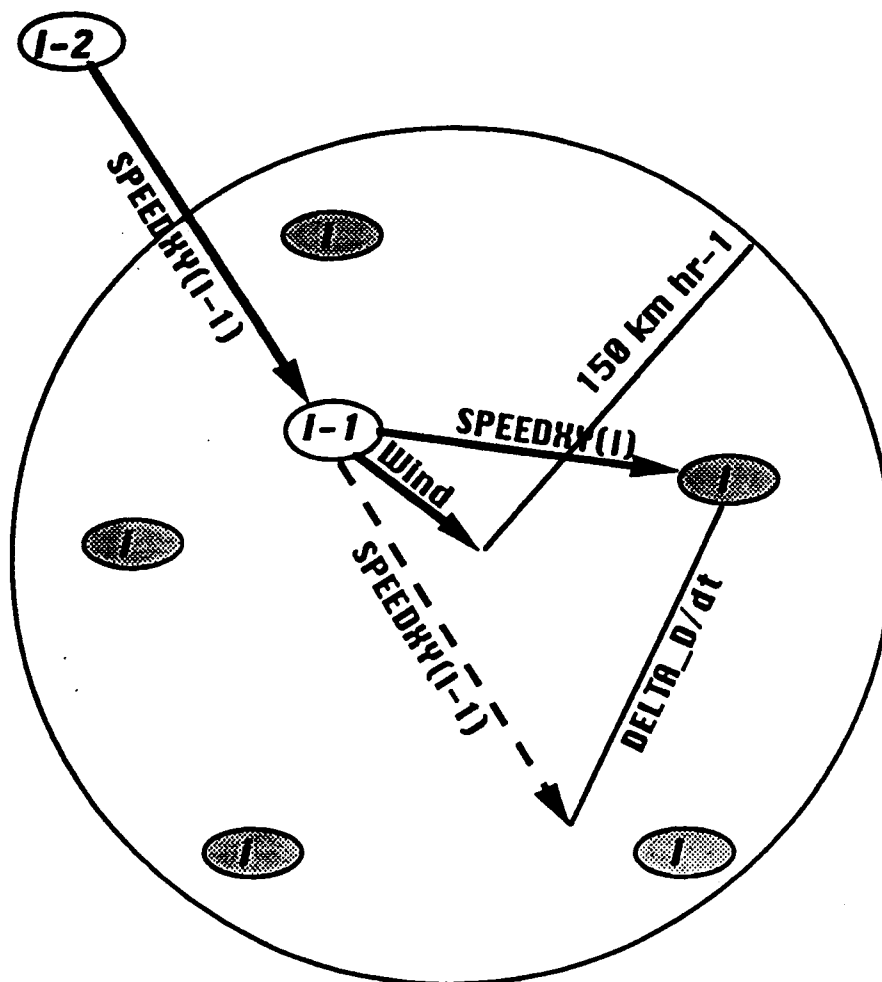
Simplification of the problem to make it tractable starts with recalling that

the observed vector of the flocks of waterfowl is  $V_g$ , the vector relative to the ground, which is the sum of the wind vector at the height the geese are flying and the birds' vector through the air. The equation is familiar to pilots:

$$V_g = V_w + V_a .$$

$V_g$  is measured by subtracting the centroid of an echo segment in  $VOL_{i-1}$  from the centroid of a possibly-matching echo segment in  $VOL_i$  and dividing by  $(Time_{i-1} - Time_i)$ . In the variable list  $|V_g|$  is SPEEDXY and the angle of  $V_g$ , also called track, is BEARING.  $|V_a|$  is air speed, the pilot's True Airspeed, called flight speed in (Larkin and Thompson 1980). The angle of  $V_a$  is heading, the direction the geese's bodies are pointing.  $|V_w|$  is the speed of the wind. The angle of  $V_w$  is the direction toward which the wind is blowing.

To constrain the search for matching echo segments while introducing the fewest assumptions about the birds' behavior, we set a maximum on  $V_a$  and use the known  $V_w$ . Setting a maximum  $V_a$  determines a maximum distance a target with a previous known location in  $VOL_{i-1}$  can find a matching target in  $VOL_i$ . Using the known  $V_w$  sets the best guess of the location of an echo segment at  $Time_i$  as its location at  $Time_{i-1}$  (known from  $VOL_{i-1}$ ) plus its displacement by the wind over the interval. The result is a circle of  $150 \text{ km} \cdot \text{hr}^{-1}$  radius with its center at:  $(XY_{i-1} + V_w \cdot [Time_i - Time_{i-1}])$ , as shown in the figure.



### Velocity vectors for flock paths.

One flock has flown from an observed position at time  $i-2$  to an observed position at time  $i-1$ . At time  $i$ , the present, there are five flocks that might match this flock (ellipses marked "1"). Labelled variables and constants are speeds (magnitudes of velocities), in km hr-1.

<b>SPEEDXY</b>	Speed from a position at one time to a position or possible position at the next time.
<b>Wind</b>	Speed of the ambient wind. All flying objects will be displaced to the end of the wind vector during a time increment.
<b>150 km hr-1</b>	How far out from the tip of the wind vector to look to find possible matches at time $i$ . This constant will correspond to the maximum cruising air speed of the species, estimated at 150 for Canada Geese. All flocks that are possible matches are within the 150 km hr-1 circle.
<b>DELTA_D</b>	At time $i$ , the error between the extrapolated position of the flock, assuming it flew straight and at constant air speed from $i-2$ to $i$ , and a given observed flock at time $i$ . DELTA_D is expressed as a speed.



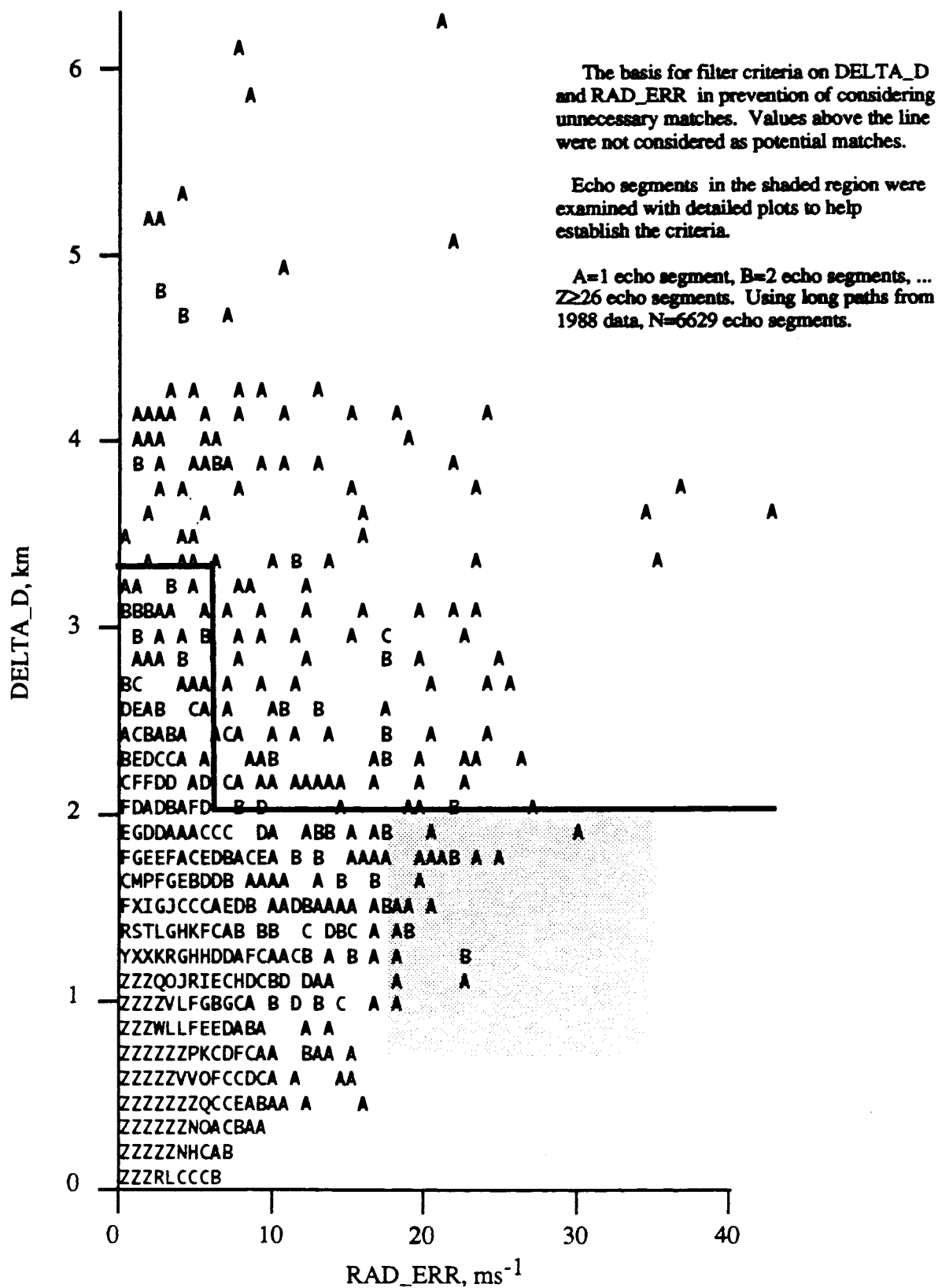
The approximate air speed of Canada Geese engaged in cruising flight plus two S.D.'s, or  $150 \text{ km hr}^{-1}$ , was used for the maximum air speed,  $\text{Max } |V_a|$ . All echo segments located within the circle constitute possible matches with the target at  $XY_1$ .

For each echo segment in  $\text{VOL}_{i-1}$ , a list of all echo segments in  $\text{VOL}_i$  that were possible matches was constructed; the list has duration  $\text{MAXMATCH}$ . Included in the possible matches were "null matches". Null matches provided a way of assessing an echo segment in  $\text{VOL}_{i-1}$  being unmatched in  $\text{VOL}_i$  (the end of a path) and an echo segment in  $\text{VOL}_i$  being unmatched in  $\text{VOL}_{i-1}$  (the beginning of a path). Only two of the measures used in comparing echo segments,  $\text{TOT\_REF}$  and  $\text{AREA\_KM}$ , were used to assess a null match.

Other criteria were invoked in the construction of lists to reduce the need to compute hopelessly poor matches. The criteria applied to the prospective matches were ( $\text{DELTA\_D}$  and  $\text{RAD\_ERR}$  are defined below):

- ◇ Same sign of Doppler velocity and
- ◇ (  $\text{DELTA\_D} < 2.0$  or
- ◇  $\text{DELTA\_D} < 3.3$  and  $\text{RAD\_ERR} < 5.0$  ).

See figure below for illustration of the latter two criteria. Because low Doppler



velocities were filtered out at the stage of identifying echo segments, there was no problem of rejecting near-zero Doppler velocities that are close to one another but have different signs.

When the lists were constructed, a bunch of echo segments from  $VOL_{i-1}$  that shared possible matches from  $VOL_i$  was assembled. These bunches were optimally matched by computing all the permutations, with two exceptions: first that an echo segment from  $VOL_{i-1}$  need not be tested against any echo segment from  $VOL_i$  that is less likely (a poorer match) than the disappearance of the echo segment from  $VOL_{i-1}$  (NULLED\_M counts these), and, second, the abovementioned criterion of  $10 \text{ ms}^{-1}$  from the average vector of the goose flocks in rare situations of very large bunches ( $BUNCHSIZ > 12$ ). The restricted bunches were of size BS\_FLTRD. Thus restricted, and performed on a 1989-vintage CISC minicomputer, the calculations took slightly under twice real time.

**Measures used to match echo segments.** Echo segments in one volume ( $VOL_{i-1}$ ) were matched with echo segments in the following volume ( $VOL_i$ ) on four measures. The position of an echo segment is the position of its echo centroid. The radar products of velocity and spectral width for an echo segment are calculated by averaging the product's values over the gates of the echo segment, weighted by reflectivity. The four measures were:

TOT_REF	Total reflectivity, dBZ	Difference in summed reflectivity
AREA_KM	Area, $\text{km}^2$	Difference in area of the echo segment
DELTA_D	Delta distance, km	Distance between extrapolated position of the flock at $VOL_i$ and its actual position
RAD_ERR	Radial error in velocity, $\text{ms}^{-1}$	Doppler velocity - radial component of measured XY velocity between position of echo segment at $VOL_{i-1}$ and its position at $VOL_i$

Each measure was normalized, after differencing in the case of TOT\_REF and AREA\_KM, and a decision sum constructed by applying weights to the four normalized measures and then summing them. Weights used were 1.0 except for sensitivity analysis (discussed below). Decision sums closer to 0 imply closer matches.

**Linearity of paths.** We examined graphs of algorithm-generated paths

Paths examined graphically by variable LINEAR		
	Number of paths	Mean SE <sub>XY</sub> (km)
Most linear paths	69	0.09
Paths with intermediate linearity	43	0.56
Least linear paths	92	1.77

from three categories of straightness in direction and constancy in speed (see box). These were used to fine-tune the parameters of the algorithm, with the primary objective of separating paths that represented apparently different flocks but that had been incorrectly joined into the same path, while retaining paths that actually turned or changed speed.

**Parameters at AGE=1.** The algorithm as described above uses the history of an echo segment to extrapolate its path to Time<sub>i</sub> and compute DELTA\_D. For AGE=1 echo segments, which have no history, an XY velocity was constructed by vector operations from an estimated radial velocity and an estimated ground speed. Doppler velocity was used as the estimated radial velocity. Estimated ground speed was calculated by subtracting wind speed from the average nominal air speed of Canada Geese (70 km hr<sup>-1</sup>). To determine if this approximation had

an effect on the ability of the algorithm to find realistic matchings from AGE=1 to AGE=2, distributions of DELTA\_D at AGE=2 were compared to distributions of DELTA\_D at AGE>2; the distributions were quite similar and thus the approximations at AGE=1 were determined to be benign.

## General characteristics of Canada Goose migration on CHILL

Data-gathering circumstances, Fall migrations of Mississippi Valley Canada Goose population

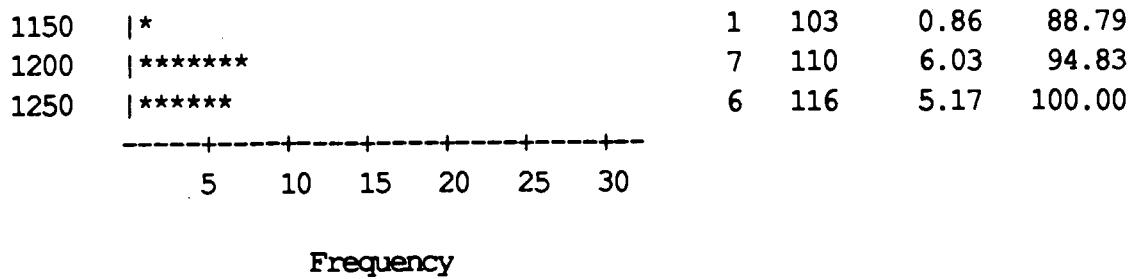
<u>1987</u>	<u>1988</u>	<u>1989</u>	
16 Dec	28 Dec	15 Dec	
0900	0948	0940	CHILL start operation
1453	1541	1957	CHILL cease operation
✓	✓		GPG tracking radar used at Monticello Road Field Site
✓	✓		GPG frozen/flooded/malfunctioning
✓	✓		Observers sited too near MTI wedge of CHILL
✓	✓		GPG flooded/frozen/malfunctioning
✓	✓		CHILL radar constant error, made REF 3 dB offset
		✓	CHILL has working clutter suppression
		✓	CHILL has ZDR capability
		✓	CHILL spectral width data accurate
		✓	Multiple-observer optical method, near Mansfield IL
		✓	Blizzard caused noise on CHILL and poor visibility in field
		✓	CHILL NCP thresholding available
5,950	8,700	4,450	Geese counted visually

Periods of data gathering, methods used, and operational problems are given in the preceding table. Although CHILL did not operate continuously, data sets up to 2.7 h long were acquired. 1989 data are emphasized below for the obvious reason of superior quality and consequent greater resemblance to WSR-88D data.

**Echo segments per volume.** Large numbers of echo segments were identified by the algorithm, as illustrated by the histogram below.

Number of echo segments per sweep for N=116 CHILL sweeps on 28 Dec 1988 and 15 Dec 1989. The largest dataset for each year was selected for this histogram.

Midpoint		Freq	Cum. Freq	Percent	Cum. Percent
0		0	0	0.00	0.00
50		0	0	0.00	0.00
100		0	0	0.00	0.00
150	*	1	1	0.86	0.86
200		0	1	0.00	0.86
250		0	1	0.00	0.86
300	*	1	2	0.86	1.72
350		0	2	0.00	1.72
400		0	2	0.00	1.72
450	*****	5	7	4.31	6.03
500	*****	5	12	4.31	10.34
550		0	12	0.00	10.34
600		0	12	0.00	10.34
650	*****	10	22	8.62	18.97
700	*****	13	35	11.21	30.17
750	*****	32	67	27.59	57.76
800	***	3	70	2.59	60.34
850	*****	10	80	8.62	68.97
900	*****	11	91	9.48	78.45
950	***	3	94	2.59	81.03
1000	***	3	97	2.59	83.62
1050	***	3	100	2.59	86.21
1100	**	2	102	1.72	87.93



**Reflectivity.** If flocks of geese were point targets, one would expect the relationship:

$$P_r \sim R^{-4}$$

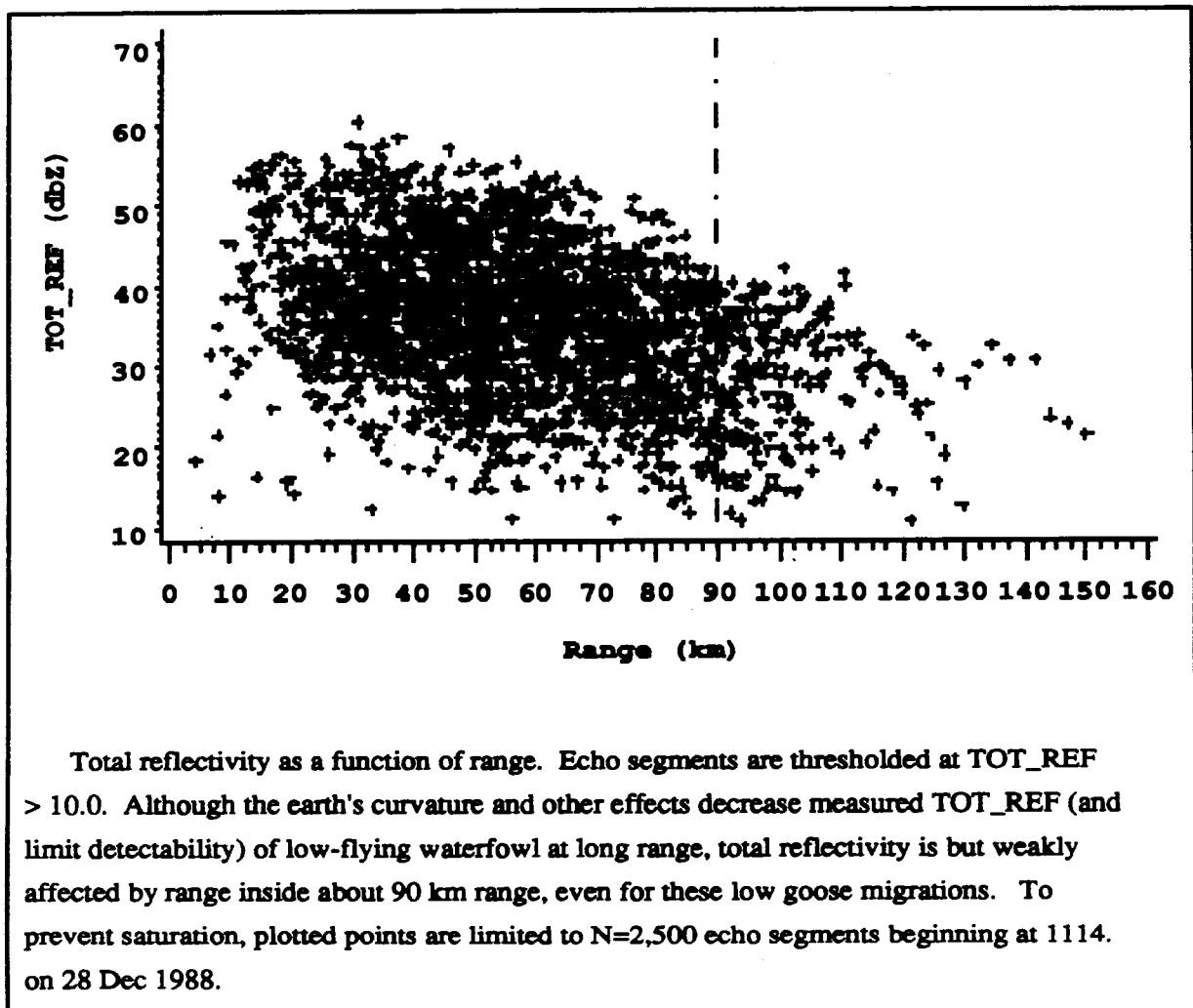
(See Appendix III on the radar equation.) If they act like volume scatterers, one would expect the relationship assumed by weather radar dBZ values, so that reflectivity will be independent of range:

$$P_r \sim R^{-2}$$

In practice, one expects that  $P_r$  of flocks of geese should fall off with range to an exponent between these values, because they do not occupy complete pulse volumes (e.g. in height) except at the closest ranges, yet they are spatially extensive, especially in XY.

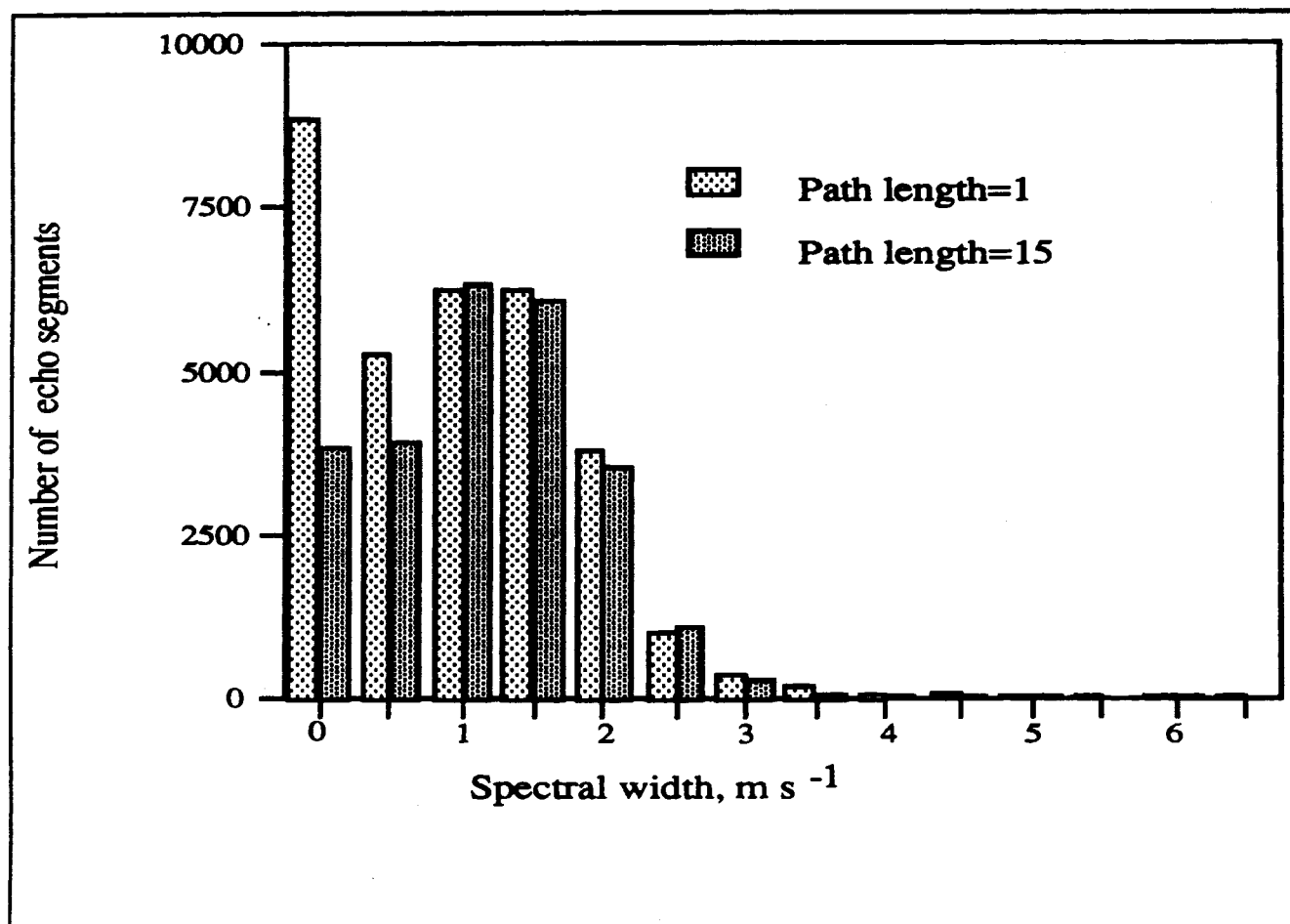
As shown in the figure below (scatter diagram of 2,500 echo segments), the majority of echo segments have reflectivity around 35 to 45 dBZ; however, beyond about 90 km the number of echo segments decreases and the reflectivity of those that appear is lower. Inside the region 20 to 90 km, corresponding to a range extent of 4.5-fold (~6.5 dB), very little effect of range upon reflectivity is evident. (No regression was performed, because, first, it would have little utility in bird hazard applications; second, the fit would be quite sensitive to whatever arbitrary windowing was performed on the independent variable, range; and, third, it is obvious the fit would be statistically significant yet explain little of the variance.) Flocks of migrating Canada Geese are not point targets, rather, they resemble volume scatterers on large weather radar.





**Doppler.** Because the goose flocks travelled straight, often passing near the CHILL radar, the Doppler velocity of course varied from the maximum SPEEDXY for flocks directly approaching or departing the radar to zero for flocks travelling tangentially. Low Doppler speeds were eliminated by CHILL clutter filters and by the algorithm's filter criteria, creating a classic "MTI wedge" along a line orthogonal to the flocks' track.

**Spectral width** of flocks of geese is low but does not peak at  $0 \text{ m}\cdot\text{s}^{-1}$ . As seen in the figure, from 1989 data (when the best spectral width were available from CHILL), spectral widths of goose flocks (at least 15 radar sweeps per path) lie almost entirely (99.2%) below or equal to  $3.0 \text{ m}\cdot\text{s}^{-1}$ . However the population



of, "paths" of duration 1 sweep (unconnected echo segments), which is comprised of a much higher proportion of ground clutter echoes, has more spectral widths near  $0 \text{ m}\cdot\text{s}^{-1}$  than long paths. Ground clutter has a higher proportion of very low spectral width than goose flocks.

## **Sensitivity analysis of measures used in matching echo segments**

The most critical of these are discussed in this section. The pioneering nature of this research mandated careful examination of the assumptions behind the algorithm, particularly which variables were used and how they were treated.

**Maximum reflectivity**, the maximum reflectivity of any gate in an echo segment, was investigated as an alternative measure to total reflectivity. It was compared with reflectivity for larger echo segments rather than small ones whose size distribution are apt to be influenced by lower limits of reflectivity in the filters. For such larger segments, it usually had a value about 5 dB below total reflectivity and behaved very similarly to total reflectivity according to several measures. For instance, one measure of the validity of a measure of reflectivity is the degree to which it remains constant from volume to volume for the same flock. One expects slow changes in reflectivity due to effects discussed below but correct functioning of the algorithm in following stable flocks of waterfowl should minimize large, sudden changes in reflectivity. Total vs. maximum reflectivity gave nearly identical results when the averaged differenced reflectivity was calculated for paths > 14 volumes in duration: 3.02 vs. 3.19 dBZ, a difference of 0.05 S.D.. However, total reflectivity was better-behaved for small echo segments and has an intuitive relationship to the total number of waterfowl or biomass in a flock. Thus total reflectivity was preferred over maximum reflectivity.

**Spectral width** was also considered as a potential measure on which to match echo segments but was rejected after comparing within-flock vs. across-flock variability of spectral width for long (at least 15 volumes) and fairly straight (SE of XY velocity <1.5) flock paths in 1989 data. The average magnitude of difference between spectral width of an echo segment of a flock in  $VOL_{i-1}$  and that of the next echo segment of the same flock in  $VOL_i$  was 73% of

what one would expect by comparing with another random point in some other flock (N=5,428 echo segments). Therefore, a given spectral width is only weakly characteristic of a given flock of geese and was not used to follow flocks over time.

**Tromboning the weightings.** Normally, each of the four above measures used to match echo segments is weighted equally in the decision sum when the measures are combined. To test the sensitivity of the algorithm to the four measures, a typical 0.71 h dataset of N=12,415 echo segments, including N=142 paths at least 15 volume scans in duration, was selected. For the sensitivity

Results of tromboning weights to 0.0 and 3.0	Baseline	With tromboning	
		Minimum	Maximum
Total number of paths	5442	5320	5597
Percentage of long paths (>14 volume scans)	2.6	2.5	2.6
Median straightness in km (S.E. of XY; Larkin and Thompson 1980)	0.67	0.65	0.67
Percent of paths of length 1 (i.e., unmatched echoes; many or most of these are junk)	73.0	70.5	75.3
Percent of long paths with sharp changes, evidenced by bimodal distributions with $F > 4.0$ (Larkin 1979) in:			
Total reflectivity of echo segments	30.1	24.4	30.8
Area of echo segments	29.4	29.4	34.1
Mean coefficient of variation for long flocks:			
Echo segment reflectivity	14.9	14.7	15.3
Echo segment area	39.7	39.3	40.9

test, these weightings were tromboned to extreme values. Each weighting was

first set to 0.0, removing the corresponding measure from the calculations, and then set to 3.0, trebling the measure's normal weighting in the decision sum. A series of statistics designed to examine the "quality" (duration, noisiness, variability) of paths was computed and the maximum swings from the baseline weighting (1.0) was examined:

The quality measures were largely insensitive to weightings, demonstrating robustness. None of the four measures that were used in matching echo segments had the ability to seriously affect the quality statistics; therefore, none was indispensable for proper operation of the algorithm.

**4-space vs. decision-sum.** The decision sum the algorithm uses to compare matches of echo segments in  $VOL_{i-1}$  with echo segments in  $VOL_i$  is computed as the weighted sum of normalized differences in the four measures. A decision sum approach, although conventional and useful, is merely one alternative way of selecting a single value to use in computing match quality. As a further test of the sensitivity of the algorithm to the calculation method, a test was run on a dataset with 26,810 islands using the distance between the flocks, computed in 4-space, instead of the decision sum. Again, the algorithm was robust. The only effects observed were decreases of 1% in the proportion of long paths and 2% in the within-path coefficient of variation of reflectivity for long paths (>14 volumes) with large (>2 km<sup>2</sup>) area. Although the decision sum approach was slightly superior, the specific calculation method for comparing echo segments was unimportant to the proper operation of the algorithm.

**Choices.** An echo segment in  $VOL_{i-1}$  may encounter zero, one, or several echo segments in  $VOL_i$  that are close enough in space to warrant attempting to compute match decision sums. This number of matchable echo segments in  $VOL_i$  is called the number of choices (variable CHOICE) available to the echo segment in  $VOL_{i-1}$ . Zero choices mandates that the path will end at  $VOL_{i-1}$ ; 1 choice

mandates that the path will match with the one possible (i.e., nearby) echo segment in  $VOL_i$ ; only in the case of 2 or more choices will the algorithm need to construct decision sums and compare matches to connect the echo segment across  $VOL_{i-1}$  and  $VOL_i$ . As seen in the table in the following table, the matching logic comes into play only about 2.4% of the time for paths long enough in duration to be meaningful goose flock flight paths as opposed to noise or fragmentary paths. 97.6% of the time, paths are inevitable.

---

Number of "choices" in  $VOL_i$  as a function of path duration, for paths >2 volumes, 1989 data.

Choices -->		0	1	2	3	4	5	Total
Path Duration     v	3	3226	6222	207	20	2	1	9678
	4	1947	5659	164	15	2	1	7788
	5	1333	5167	148	16	1	0	6665
	6	988	4805	125	10	0	0	5928
	7	804	4703	115	5	0	1	5628
	8	629	4294	107	1	1	0	5032
	9	654	5060	151	18	3	0	5886
	10	398	3464	106	10	2	0	3980
	11	324	3167	68	3	2	0	3564
	12	243	2603	64	6	0	0	2916
	13	216	2517	71	3	1	0	2808
	14	201	2542	66	5	0	0	2814
	15	177	2391	85	2	0	0	2655
	16	158	2304	61	5	0	0	2528
	17	140	2189	48	3	0	0	2380
	18	165	2742	60	3	0	0	2970
	19	112	1969	44	3	0	0	2128
	20	80	1488	31	0	0	1	1600
	21	68	1323	35	2	0	0	1428
	22	56	1157	19	0	0	0	1232
	23	52	1128	16	0	0	0	1196
	24	55	1234	31	0	0	0	1320
	25	41	963	19	2	0	0	1025
	26	30	733	17	0	0	0	780
	27	37	949	13	0	0	0	999

28	34	888	28	2	0	0	952
29	28	764	20	0	0	0	812
30	20	565	15	0	0	0	600
31	21	622	8	0	0	0	651
32	28	849	18	1	0	0	896
33	19	592	16	0	0	0	627
34	16	519	8	1	0	0	544
35	10	332	8	0	0	0	350
36	5	174	1	0	0	0	180
37	5	178	2	0	0	0	185
38	4	145	3	0	0	0	152
39	4	150	2	0	0	0	156
40	1	37	2	0	0	0	40
41	6	237	3	0	0	0	246
42	4	164	0	0	0	0	168
43	2	84	0	0	0	0	86
44	1	43	0	0	0	0	44
46	2	87	3	0	0	0	92
47	2	89	3	0	0	0	94
<u>50</u>	<u>2</u>	<u>97</u>	<u>1</u>	<u>0</u>	<u>0</u>	<u>0</u>	<u>100</u>
Total	12348	77389	2012	136	14	4	91903

---

However an alternative “lucky paths” hypothesis must also be entertained, namely that the long paths that persist are specifically those that were lucky because they encountered few situations where  $> 1$  choice existed and thus permitted the algorithm to malfunction. Hypothetically, under the lucky paths hypothesis, the algorithm frequently functions poorly when  $>1$  choice is possible and longer paths are lost or break up. The lucky paths hypothesis can be tested from the data. If it were correct, shorter, nearly-fragmentary paths (duration about 3 to 6) should be littered disproportionately with situations of  $> 1$  choice, because they were truncated by the algorithm. As seen in the table above, they are not. To the contrary, the short paths ended disproportionately often because they found no matches at all (0 choices). The lucky paths hypothesis is false.

In conclusion, the sensitivity analyses show that the rather remarkable insensitivity of the flock-following algorithm to some of the fundamental assumptions upon which it is based is due partly to the fact that these rather straight-flying flocks of geese over the agricultural Midwest are intrinsically easy to follow. A much simpler algorithm might suffice for following Canada Goose migration over nearly-level terrain. The simpler algorithm might merely extrapolate the path of a flock forward from  $VOL_{i-1}$  linearly into time and match with the echo segment in  $VOL_i$ , if any, closest in space to the extrapolated position. It is not clear, however, if a simpler algorithm would succeed in following smaller flocks, different species, or flocks over less ideal (flat) terrain.

### **Performance**

Verification of the correct functioning of the algorithm was carried out by comparing the algorithm's results with paths mapped by hand, by examining graphical and numeric data on the paths to see if they matched behavior of migrating geese, and by identifying paths that corresponded to flocks identified visually and with tracking radar in the field. These means of verification are discussed in the next sections. Data from 1988 and 1989 are used but data from 1987 were not used, because the CHILL radar's anti-clutter filter was inadequate in 1987.

**Comparing the algorithm's paths with hand-mapped paths.** Using 1987 data,  $N=37$  path segments of duration from 3 to 6 volumes were plotted by hand from projected PPI images of CHILL data. All paths that could be detected by eye in the northern half of the PPI were included. The centroids of the flock echoes were estimated graphically rather than calculated. These path segments, whose connections had been constructed by humans, were then compared with the paths generated by an early version of the algorithm:



Number of cases	
<b>Agree</b>	
14	Agree completely
8	Agree completely and algorithm follows flock farther
6	Agree except flock penetrates inside the minimum range used by the version of the algorithm
4	Agree except for one echo segment that was missing from algorithm because echoes too weak
32	Total agree
<b>Do not agree</b>	
2	Two paths merged into one echo, then re-appeared as two paths. The flocks appeared to cross over/under one another--the hand-drawn paths had the shape of an "X"
2	Paths composed of echo segments too faint to be used
1	Algorithm made apparently separate paths one
5	Total do not agree
37	Overall Total

Only three instances of clear malfunction of the algorithm were detected by the hand analysis. The cause of one of these (the last instance in the table) is now corrected in the present version of the algorithm. The two flocks appearing to cross over/under one another are more interesting. The algorithm has no memory of paths farther back than one volume (no analog of "momentum"); therefore, this is a known feature or weakness of the algorithm. It occurred in a situation that appears to be quite rare judging from our lack of success in finding any other apparent cases of flocks crossing in the data. (One instance of two

flocks merging was observed visually in the field.)

Therefore, the algorithm usually agreed with the hand analysis in a simple case. In more difficult cases such as congested areas with many flocks migrating together, the algorithm quickly exceeded our ability to follow the flocks by hand. We abandoned simple hand analysis as a technique for verifying the algorithm.

**Length of paths.** If flocks were followed perfectly by the radar, they would enter the approximately northern hemisphere of the CHILL's  $r=150$ -km coverage and travel roughly straight until they crossed the southern hemisphere. Flocks distributed evenly east-west would have path lengths averaging about  $\pi \cdot \frac{r}{2}$ , or 240 km. In 1987-1989, the hypothetical mean length would have exceeded this value because in all three years the migration was concentrated near the center of the CHILL radar's coverage. Although paths up to 111 km long appear in the data sets, the distribution of path lengths lies well beneath even half the 240 km ideal (data are given below).

Reasons for a path being interrupted and therefore ending are given in the following table. Paths may end for biological reasons (behavior of geese), for reasons involving limitations or exigencies of operating the CHILL radar, or because of limitations or mistakes in the algorithm. Of course, it is often impossible to isolate one and only one of these reasons when dealing with the etiology of fragmented paths in real data. The reasons in the Table are numbered and the more prominent or interesting ones are discussed below.

	Reason for a path being interrupted or ending	Occurrence
1	The behavior of waterfowl	

1a	"Apparent fission/fusion of flocks, including flocks passing over/under one another and temporarily or permanently joining together or splitting."	One observation of flocks crossing; one field observation of fusion of two flocks.
1b	Flocks landing or taking off.	None observed
2	<b>The CHILL radar</b>	
2a	"Malfunction such as missing ray, artifact."	"CHILL radar data showed several kinds of such problems, especially in earlier data. NEXRAD expected to perform much more reliably."
2b	"Gap in data collection due to radar off-line, power outage, change in scan strategy."	CHILL data have gaps for all these reasons. NEXRAD data projected to have >99% availability.
2c	Flock's range beneath radar's minimum range.	Inevitable problem with any radar; minimum range of CHILL effectively about 25 km for data in the lowest elevation scan.
2d	Flock's range exceeds radar's maximum range.	"CHILL maximum range 152 km, but NEXRAD's much greater, in general. Few Canada Goose flocks observed at CHILL maximum range, largely because of earth's curvature."
2e	Flock flies behind topographic or other obstruction.	CHILL site in central Illinois nearly free of topographic obstructions but cluttered with tall structures. This problem is critical for low-flying waterfowl but less important for high-flying waterfowl such as Snow Geese. A site-dependent factor.
2f	Flock flying below the lowest radar beam due to earth's curvature.	"Along with obstructions, the most important reason low-flying waterfowl are not detected on long-range radars." "

2g	Flock flying low above prominent ground clutter.	Frequently observed on CHILL. The importance of this factor depends largely on the details of anti-clutter programming in the radar signal processor.
2h	Flock Doppler velocity approaches zero because of flying tangential to the radar.	"Almost all flocks are tangential as they pass the radar. In 1989 data, only 2.1% of 1,208 paths of length > 14 volumes extended through the ca. 8 degree tangential sectors."
2i	One or more of the 4 measures used to match echo segments across time changes rapidly because of a sharp turn by a flock	"No positive instances found in algorithm's output. However, sharp turns were observed in the field on two occasions and failure to follow sharp turns would be nearly impossible to find in the algorithm's output."
3	<b>Limitations of the algorithm</b>	
3a	"Hypothetical bug resulting in omission, combining, or mismeasurement of an echo segment."	None are known to remain.
3b	Criteria used to identify separate echo segments is improper.	"This is a matter of definition, not a problem."
3c	Bunch size exceeds limit imposed to reduce computation time (BUNCHSIZ < 13).	"Observed infrequently (mean 0.04/volume) only at very close range to CHILL when the algorithm tries to track ground clutter along with waterfowl. In such cases, the clutter is much more of a problem than the arbitrary limit."
3d	Hypothetical bug resulting in non-optimum match.	None are known to remain.

3e	Initial XY velocity of a path very different from the SSE-ward value expected by the algorithm.	May result in FLOCKSIZ=1 errors for vagrant flocks; no instances observed in the data.
----	---	--

Reason 2a. Artifacts in research weather radars include missing radials, incorrect reported azimuths, bursts of noise, incorrect times, and scan rates differing from protocol. In CHILL data, a ca 3° sector at 269° azimuth was either missing or cluttered with artifacts.

Reason 2b. The CHILL radar, unlike NEXRAD, did not operate without interruption during the data-gathering sessions. CHILL was taken off line to take brief RHI scans, to change the data-collection protocol or scan strategy, or because of hardware or software malfunction. Our most complete data, in 1989, comprise 87,175 paths, of which 35,866, or 41%, began or ended at a gap in data collection. The distribution of durations for 1989 paths that did not begin or end on a gap are shown in the following table. Volume scans were taken at intervals averaging 1.55 minutes in these data. Note that fully 65% of the "paths" are only one volume (one echo segment) in AGE; that is, they are unconnected echoes. Most of these are artifacts or parts of continuing goose flocks that resulted from too-fine spatial splitting of goose flocks by the echo segment delimiting part of the algorithm. In this report, many statistics are taken from flocks at least 15 volumes in AGE; these comprise 2.5% of the data overall.

---

Distribution of durations (in volumes) of paths, 1989 data.

Path Duration	Frequency	Percent	Cumulative Frequency	Cumulative Percent
1	33344	65.0	33344	65.0
2	6635	12.9	39979	77.9

3	3056	6.0	43035	83.9
4	1819	3.5	44854	87.5
5	1233	2.4	46087	89.9
6	914	1.8	47001	91.6
7	730	1.4	47731	93.1
8	585	1.1	48316	94.2
9	432	0.8	48748	95.0
10	369	0.7	49117	95.8
11	302	0.6	49419	96.4
12	226	0.4	49645	96.8
13	192	0.4	49837	97.2
14	189	0.4	50026	97.5
15	162	0.3	50188	97.9
16	147	0.3	50335	98.1
17	129	0.3	50464	98.4
18	159	0.3	50623	98.7
19	81	0.2	50704	98.9
20	75	0.1	50779	99.0
21	64	0.1	50843	99.1
22	50	0.1	50893	99.2
23	46	0.1	50939	99.3
24	50	0.1	50989	99.4
25	38	0.1	51027	99.5
26	29	0.1	51056	99.5
27	34	0.1	51090	99.6
28	25	0.0	51115	99.7
29	27	0.1	51142	99.7
30	20	0.0	51162	99.8
31	19	0.0	51181	99.8
32	28	0.1	51209	99.8
33	19	0.0	51228	99.9
34	16	0.0	51244	99.9
35	8	0.0	51252	99.9
36	5	0.0	51257	99.9
37	5	0.0	51262	99.9
38	4	0.0	51266	100.0
39	4	0.0	51270	100.0
40	1	0.0	51271	100.0
41	6	0.0	51277	100.0
42	4	0.0	51281	100.0
43	2	0.0	51283	100.0
44	1	0.0	51284	100.0

46	1	0.0	51285	100.0
47	2	0.0	51287	100.0
50	2	0.0	51289	100.0

---

The table omits paths truncated by beginning or ending at a gap. Gaps due to interruptions in collection of data were important. For instance, the two paths of duration 50 volumes that appeared in the longest data collection interval were as long as or longer than the five other entire data-collection intervals on 15 December 1989.

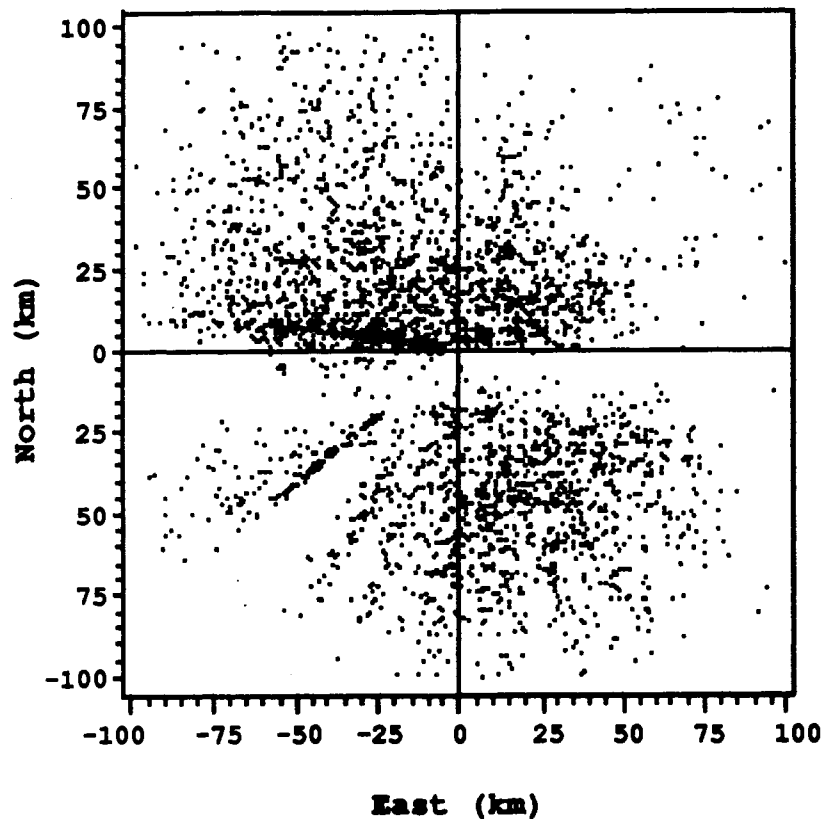
Reason 2c. CHILL, like most radars, can record data at closer ranges than are useful at low elevations such as used in work on birds, because of ground clutter. Nevertheless, at elevation 2.36 degrees, flocks were followed in to 3 km range. At the lowest elevation (ca. 0.5 degrees), the minimum useful range in 1987-1989 was about 25 km (see discussion of following flocks across elevations, below).

Reasons 2d and 2f. Flocks show apparent diminution of reflectivity at long ranges and, indeed, few strong echoes from Canada Geese were received at the maximum CHILL range of about 150 km. The curvature of the earth is more important than topography as a cause of obstruction of long-range targets in Central Illinois (Larkin and Quine 1989: Figure 11).

Reason 2e. This reason is often phenomenologically indistinguishable from 2g, below. For flocks flying at low height, these two reasons often result in intermittent attenuation of the return from the lowest-elevation scan but not from the higher-elevation scans, so that the paths do not end but appear to falsely pop up briefly in height, a phenomenon discussed below under "Following flocks across sweeps at different radar elevation angles". More direct evidence for the influence of obstructions and ground clutter obtains from the geographic distribution of locations of ends of paths (see following figure). CHILL was obstructed by the Willard Airport control tower at 270° azimuth and by other

obstructions to the SW. Many paths ended because they passed behind these obstructions (or flew tangential to the radar--see 2h below).





I

A 15.9-km long segment oriented along the modal direction of travel of paths. This is the median spatial length of paths at AGE=8; on average, paths must extend this distance for their ends points to be plotted at left.

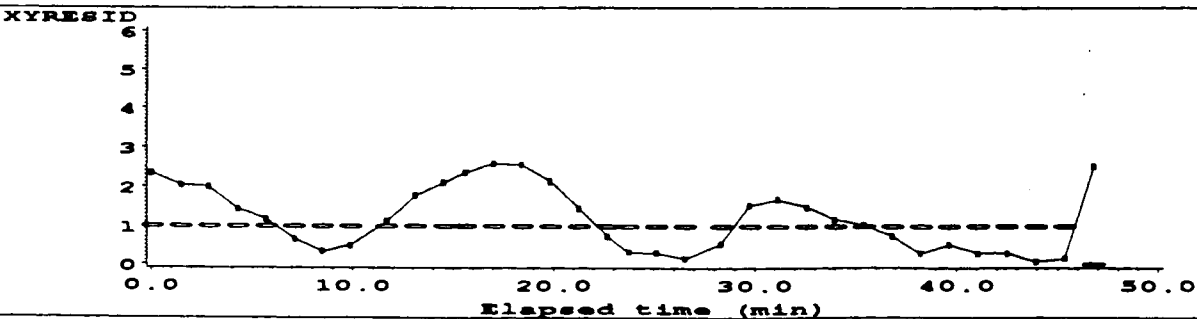
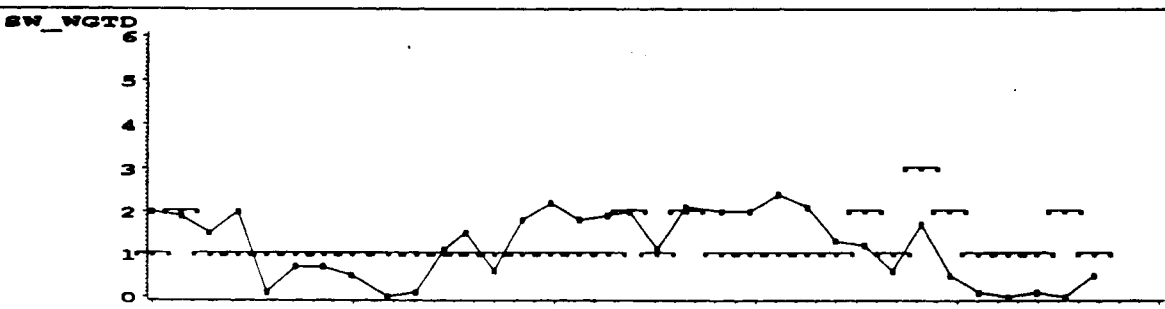
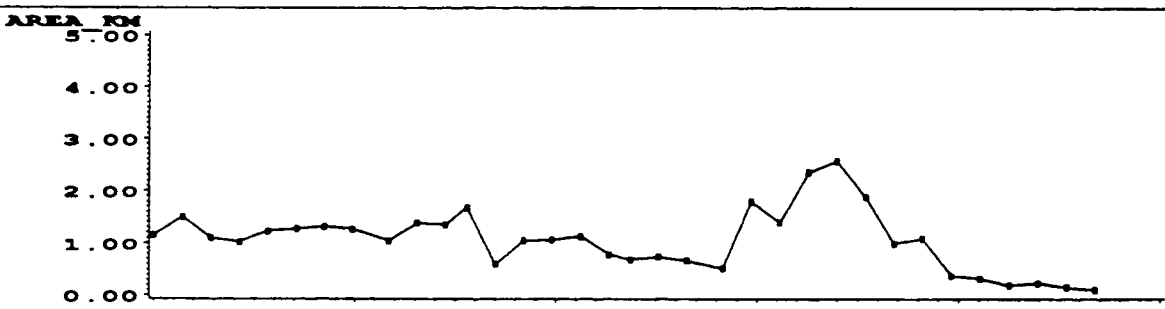
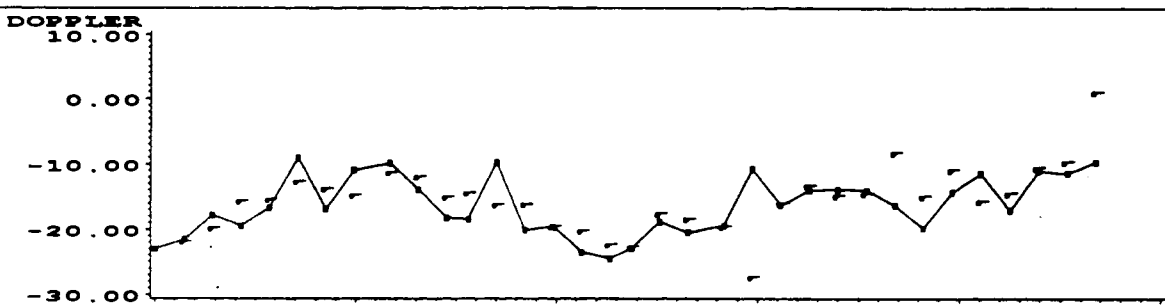
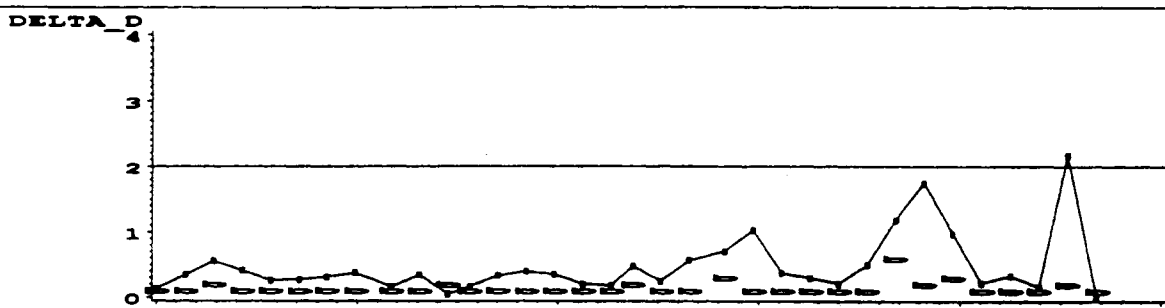
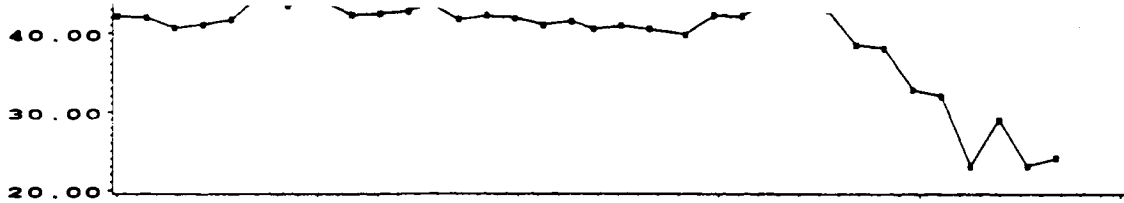
Spatial distribution of ends of paths. Included are all 1989 paths of duration > 7 volumes that do not end at gaps in data collection (N=3211), except for N=70 paths that ended outside the 100-km extent of the axes and had a diffuse and uninformative distribution. The CHILL radar is at the origin.

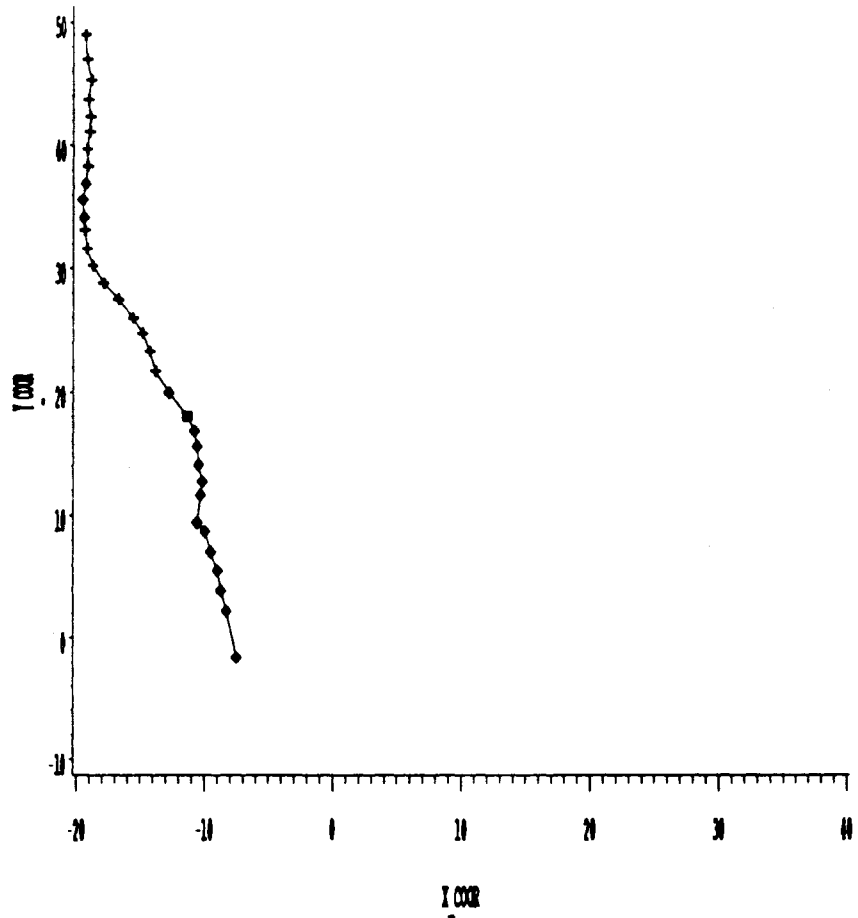
Note that the paucity of these medium to long paths to the SW is largely due to obstructions near the radar that prevent paths "surviving" for 8 volumes (15.9 km) in this region.

Reason 2g. Radar return from small moving echoes at low height is nearly always affected by added return from ground clutter.

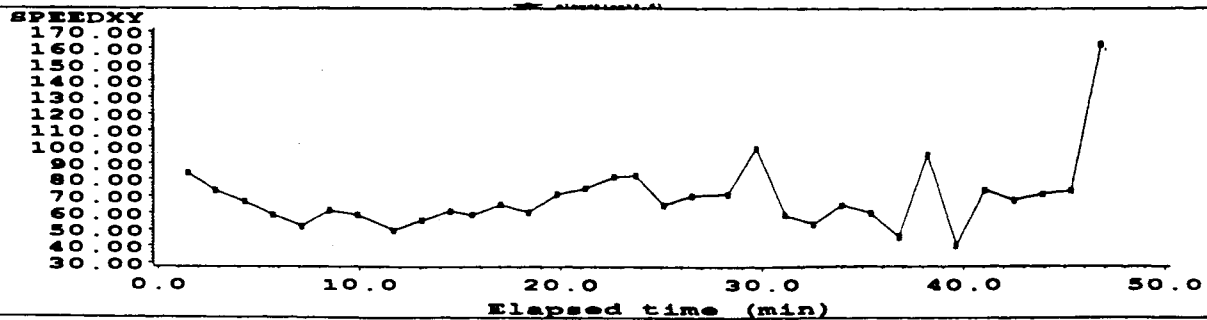
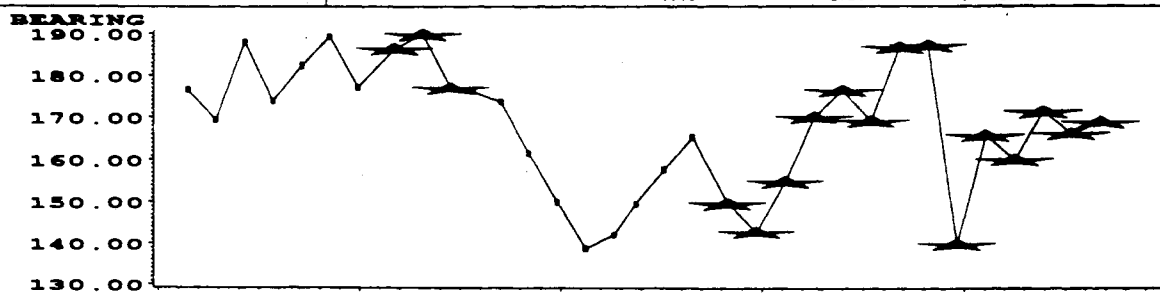
Reason 2h. One of the chief constraints on path durations is the Doppler velocity minimum imposed by the algorithm. Almost all paths that approach a tangent to the radar end when their velocity becomes too small; for instance, in 1989 only 25 of 1,385 paths with AGE > 14 echo segments crossed or partly crossed the region of zero velocity for paths travelling SSE. Paths that ended at about azimuth 85° and 265° usually ended because their Doppler velocity fell below the threshold (see figure).

Reason 2i. As explained in the table, turns that the algorithm fails to follow would be difficult to detect from the algorithm's data. However, turns and speed changes were often successfully followed by the algorithm, as illustrated by the following path, which began at 12:27:51 on 28 Dec 1988. The composite figure consists of eight panels showing plots of variables over time and a larger panel (second page of the figure) with a map (XY plot) of the flock's track over Illinois. The three symbols on the XY plot designate at which of the three elevation angles the strongest echo return from the echo segment occurred (or, in some cases, the only elevation angle at which echo return occurred). On the BEARING plot, elevation angles > 0.61° are marked with a (flattened) star. The CHILL is at (0,0) km on the XY plot. The smooth BEARING curve from a bearing of about 180° to a varying bearing around 160° is not accompanied by any sign that more than one flock of geese is represented in this path--note also the steady TOT\_REF, DELTA\_D, and DOPPLER during the first 70% of the path. The SE<sub>XY</sub> of this path is 1.43 km; the path was categorized as LINEAR=LEAST for this data collection interval. The flock appears to have been lost to the radar when it entered the low-Doppler, high ground clutter region roughly WSW of the CHILL radar.





+ 0.61    ■ 1.14    ◆ 1.41



Reasons 3... (limitations of the algorithm). The algorithm has no known bugs; its limitations appear to be those of (1) design and (2) tuning of parameters.

By design, the flock path algorithm compares echo segments from two and only two volumes at a time. Because the inevitable problems one has with radar data (Reasons 2...) will result in loss or diminution of the radar signal for a volume or two, paths are lost. They "wink out". If the flock path algorithm looked for best matches among echo segments across several volumes, it could in some cases tolerate brief interruptions in the data, span them, and generate longer paths. However, without the algorithm's being redesigned to look across several volumes, brief interruptions in the data were fatal to most paths: a 4-min gap in the 28 December 1988 data resulted in nearly no valid paths that crossed the gap. Insufficient locally available computational resources prevented this project from attempting to upgrade the algorithm to look across several volumes. The limitation appears to be practical rather than conceptual, although the intellectual task of generalizing the algorithm to  $n$  comparisons is nontrivial.

In engineering terms, classical TWS systems are designed so that the software considers deleting a tracked target if it is no longer observed for  $N$  scans or if its state space representation becomes decorrelated. This algorithm takes the simplest case of the former approach, where  $N=1$ . As discussed above, this simple scheme is shown to be appropriate empirically; it is also appropriate to the functional goals of the algorithm, which is to estimate the numbers, locations, and earth-frame velocities of flocks of waterfowl. Unlike, say, missile tracking, the consequences of losing one known target in a scan (probably temporarily) are small and, as discussed above, the long-term likelihood of a flock of birds becoming invisible to the radar at least temporarily is high.

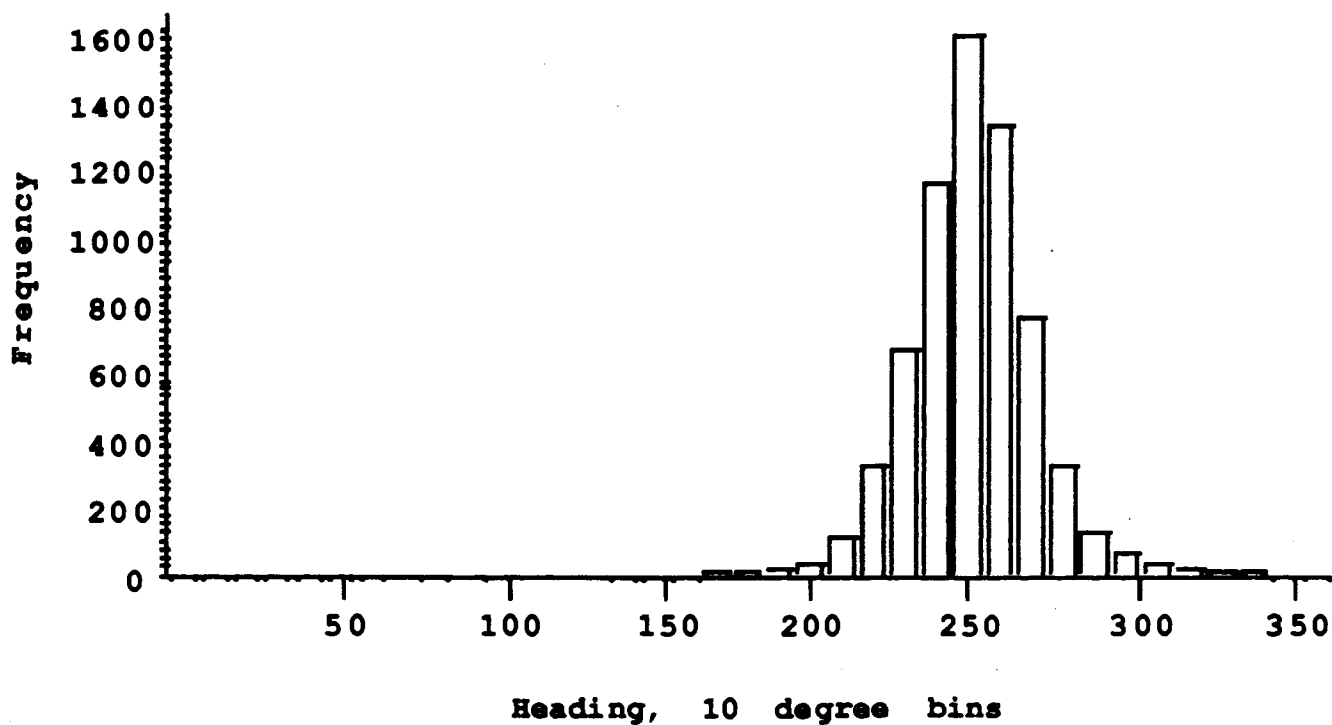
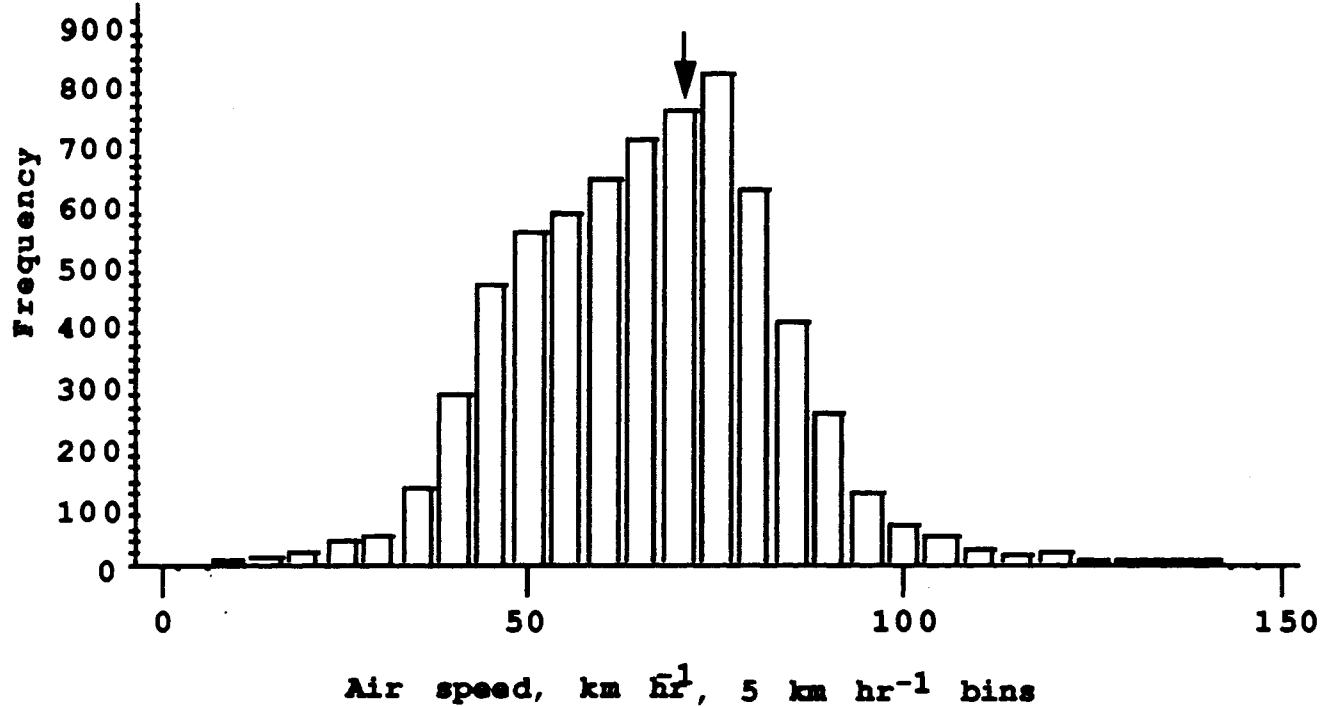
Tuning of the parameters of the algorithm has been performed to optimize following Canada Goose migrations in flat terrain. Further optimizing of some of the parameters probably would improve its performance following flocks of

Canada Geese. However, as demonstrated above, the algorithm is remarkably insensitive to variations in some of its critical parameters.

Further upgrading and tuning of this algorithm on these data sets has reached the point of diminishing returns. The effort would probably be better spent generalizing the algorithm to perform as well on other types of waterfowl movements and in other kinds of terrain.

**Speed and direction of echo segments.** The concentrated fall movement of the MVP involves nonstop flight from the latitude of Wisconsin to that of Southern Illinois. With the exception of occasional turns and speed changes, one expects that most radar echo segments from geese will move roughly southward at a steady air speed, and that the air speed most likely is the cruising speed of Canada Geese. In addition, lack of weather features and winds steady in direction on the days the mass movement took place in 1987-1989 provide further reason to believe that the geese would not change course, for instance, in response to encountering changes in wind.

These expectations were upheld in the data. 28 Dec 1988 wind profiles, gathered locally by tracking radar, are shown in Larkin and Quine (1989:42). Subtracting these wind vectors from XY position changes over time of the echo segments of a goose flock allows computation of air speed and heading from the radar data. The figures below show air speed and heading for N=6437 echo segments, all taken from paths at least 15 volumes in AGE and having SE<sub>XY</sub> values under 2.0 ms<sup>-1</sup>. Thus these criteria for air speed analysis eliminate paths whose echo segments are not overwhelmingly derived from flocks of geese but permit the analysis to include short doglegs in paths, jumps sideways from one flock to an adjacent one, and paths that travel in any direction.



The figures show the geese flying at a median air speed of  $66.4 \text{ km hr}^{-1}$ , which is near the measured air speed of Canada Geese of  $68.0 \text{ km hr}^{-1}$  reported by Bellrose and Crompton (1981) and marked by an arrow on the air speed histogram. The geese are compensating strongly for the NW wind this day, heading toward a median direction of  $251^\circ$ .

Apparent variability in air speed and heading includes, first, actual biological variability over time and among flocks of geese, second, error in tracking the flocks and, third, possible error due to algorithm malfunction. Considering that goose flocks are often a kilometer or more across and the XY position measures are separated by only about 1.2 km average distance and 1.41 minutes, small changes in calculating their centroids will introduce errors in tracking. Furthermore, documented changes in wind velocity over the 1.7 hr represented in the figures must directly affect the calculated air speed. Therefore, one would expect that biological variability added to errors in tracking would produce much more variability than is evident in the figures. The surprising accuracy indicates that the algorithm produces well-directed paths. The paths correspond closely to what one expects of the flight speeds and directions of Canada Geese over central Illinois in fall.

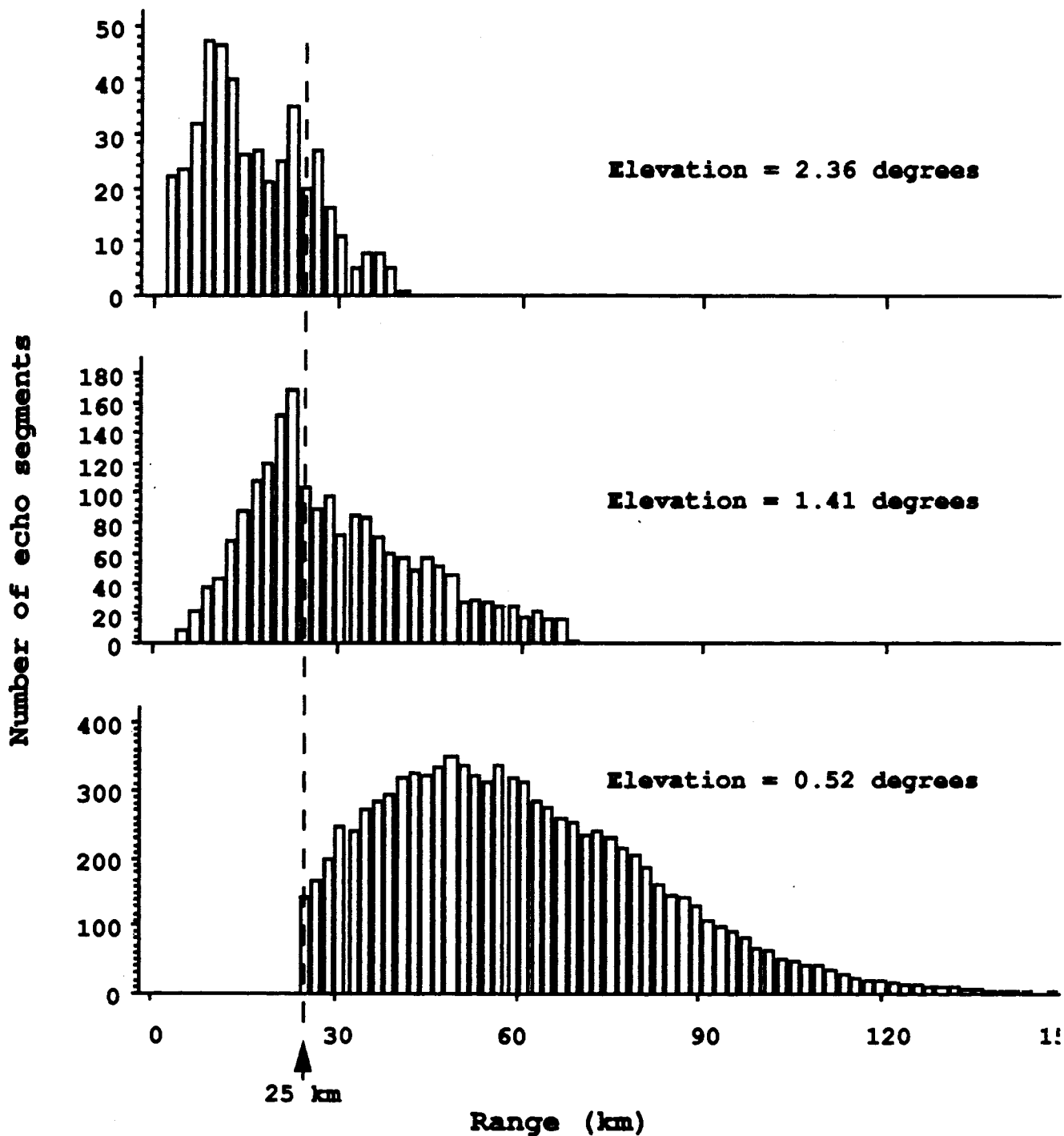
The absolute difference between the Doppler-measured and algorithm-estimated radial component of velocity, given by the RAD\_ERR variable, provides a separate check on the speed estimates of goose flocks. Low values of RAD\_ERR indicate that these two independent measures of the flocks' velocities agree, at least in one dimension. (Of course, because RAD\_ERR is also one of the measures on which paths are based, the algorithm output is biased toward providing low values of RAD\_ERR when CHOICE is not 1.) The median RAD\_ERR for long paths in each data-collection period on 15 December 1989 ranged from 1.03 to  $1.14 \text{ m}\cdot\text{s}^{-1}$ , or about 4% of the median groundspeed of the



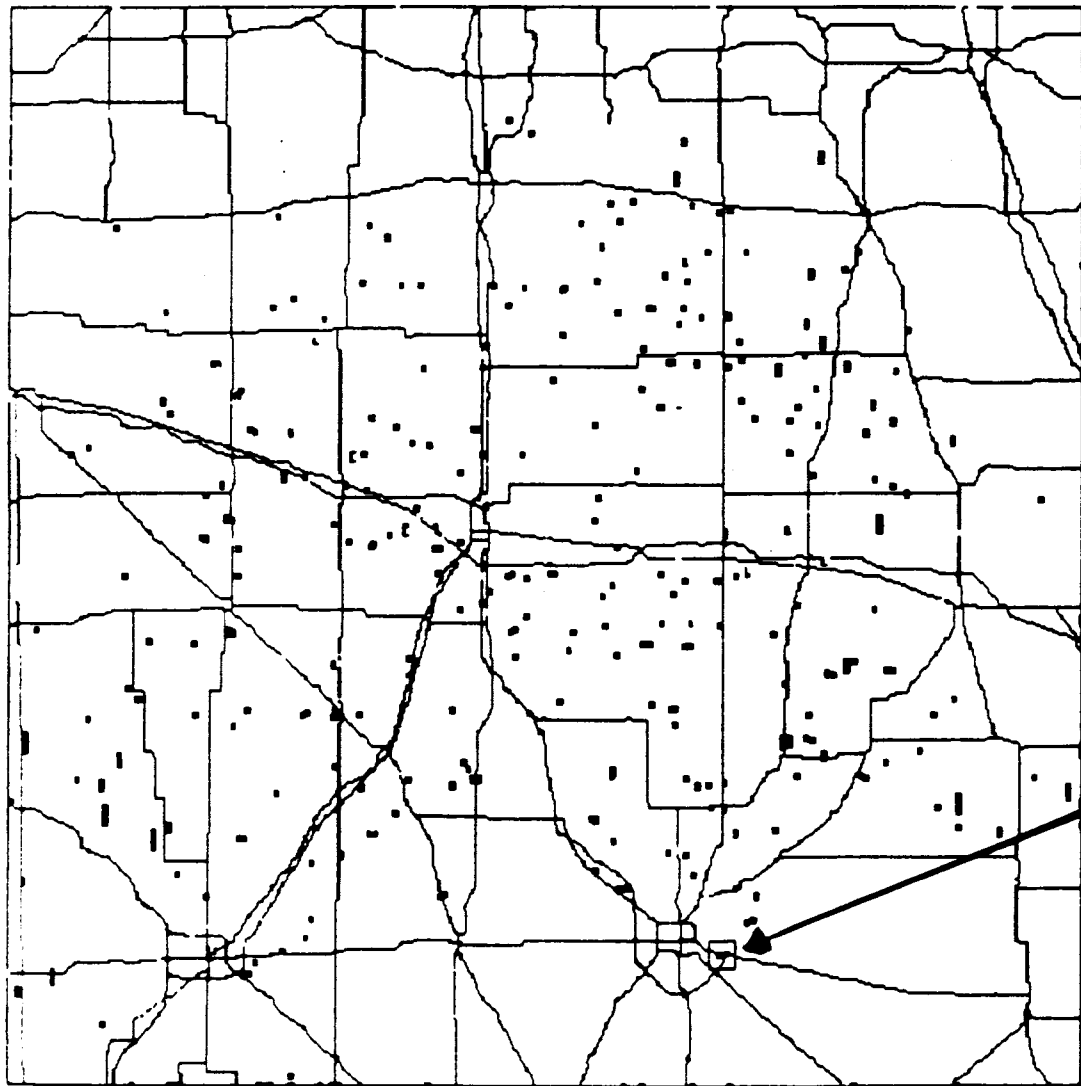
geese. Doppler-measured and algorithm-estimated speeds agree.

**Following flocks appearing in different radar elevation angles.**

On a statistical basis, the height of waterfowl is related to the elevation angle giving the strongest echo by ( $\text{height} = \text{range} \sin[\text{elevation}]$ ). As one would expect from radar targets maintaining a fairly constant height as they fly, echo segments from Canada Geese appear in higher-elevation scans when at closer range to the radar (see following figure). The median height of the migrating geese can be estimated roughly using these data. In 1989 at about 8 km range equal numbers of echo segments from long flocks appear at elevation angles of  $1.41^\circ$  and at  $2.36^\circ$ . Therefore the midpoint between these two elevation angles,  $1.89^\circ$ , is roughly the angle that bisects the height distribution of the goose flocks.  $8 \text{ km} \sin(1.89^\circ)$  gives 296 m estimated median height of goose flocks, which is in the same ballpark as the visually observed median height (Larkin and Quine 1990:13-14) of 210 m, considering that visual observations during the blizzard of 15 Dec 1989 were biased toward low-flying flocks that could in fact be seen.



Distribution of long paths of length > 14 volumes among the three elevation angles. Counts of echo segments are shown; note that the vertical axis scales differ. The lowest elevation is ignored by the algorithm at ranges under 25 km (dashed line).



15-DEC-89 16:43:11

map  
> 45  
38 TO 41  
32 TO 35  
25 TO 29  
19 TO 22  
13 TO 16  
< 10  
clear

TOT\_REF  
0.5 DEG  
RANGE 80 km  
(17-DEC-82, PLANE=0)

Elevation:

0.61° 0.61° 0.61° 0.61°

A flock is receding from CHILL, with the strongest echo from the lowest elevation angle, 0.61°. Directly over a railroad overpass at Elwin, IL (small square), the higher elevation receives the stronger echo, due to contamination of the 0.61° elevation by the overpass.

The same calculation theoretically could be performed for the bisection of the  $0.52^\circ$  and  $1.41^\circ$  radar elevation angles; however, in practice, the  $0.52^\circ$  elevation is not valid to use at the ranges of interest because of clutter problems and the range cutoff at 25 km.

Several factors conspire to diminish the ability of 10-cm weather radars to measure accurately the height of echoes near the ground. Contamination of the lowest elevation angle by obstructions and ground clutter often attenuates the return so that a duplicate echo in a higher angle is stronger, the algorithm selects the higher elevation, and the path falsely appears to "pop up" briefly (see figure of flock over Elwin, IL, preceding page). The curvature of the earth further obscures the lowest elevations at long range. Reflection off water or level ground and refraction (in some weather conditions) give steady or intermittent false height indications. And finally the beamwidth of the radars limits their angular resolution--a  $1^\circ$  beam is about 1 km wide at 60 km range.

**Identifying paths that correspond to flocks identified visually.** In 1989 N=14 flocks were counted by field observers during breaks or partial breaks in the blizzard. N=9 of these had both complete data including X, Y, time and number of geese, and clear correspondence to a path of duration at least N=3 in the algorithm output. The other N=5 flocks passed the observers between CHILL data gathering periods or could not be matched unambiguously with CHILL paths.

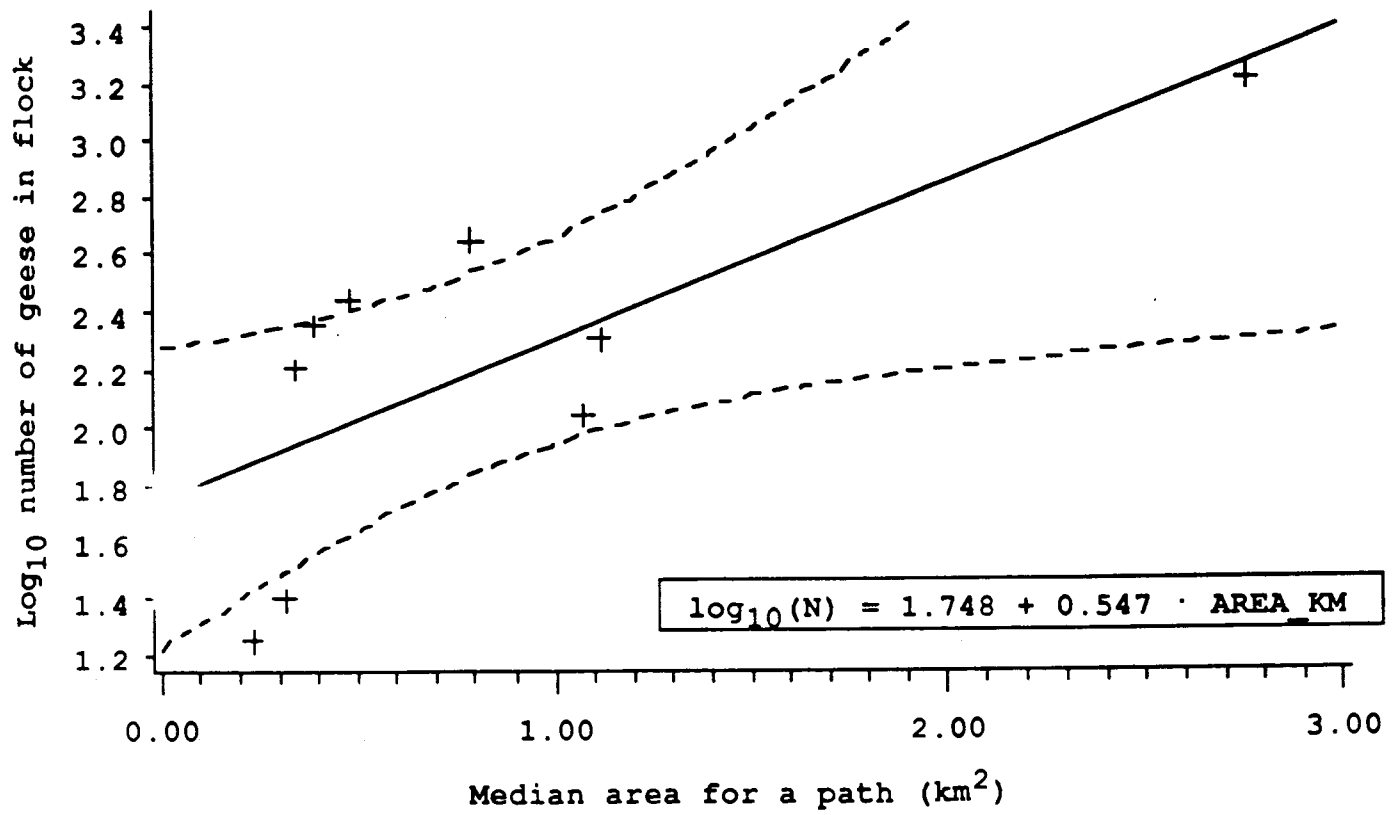
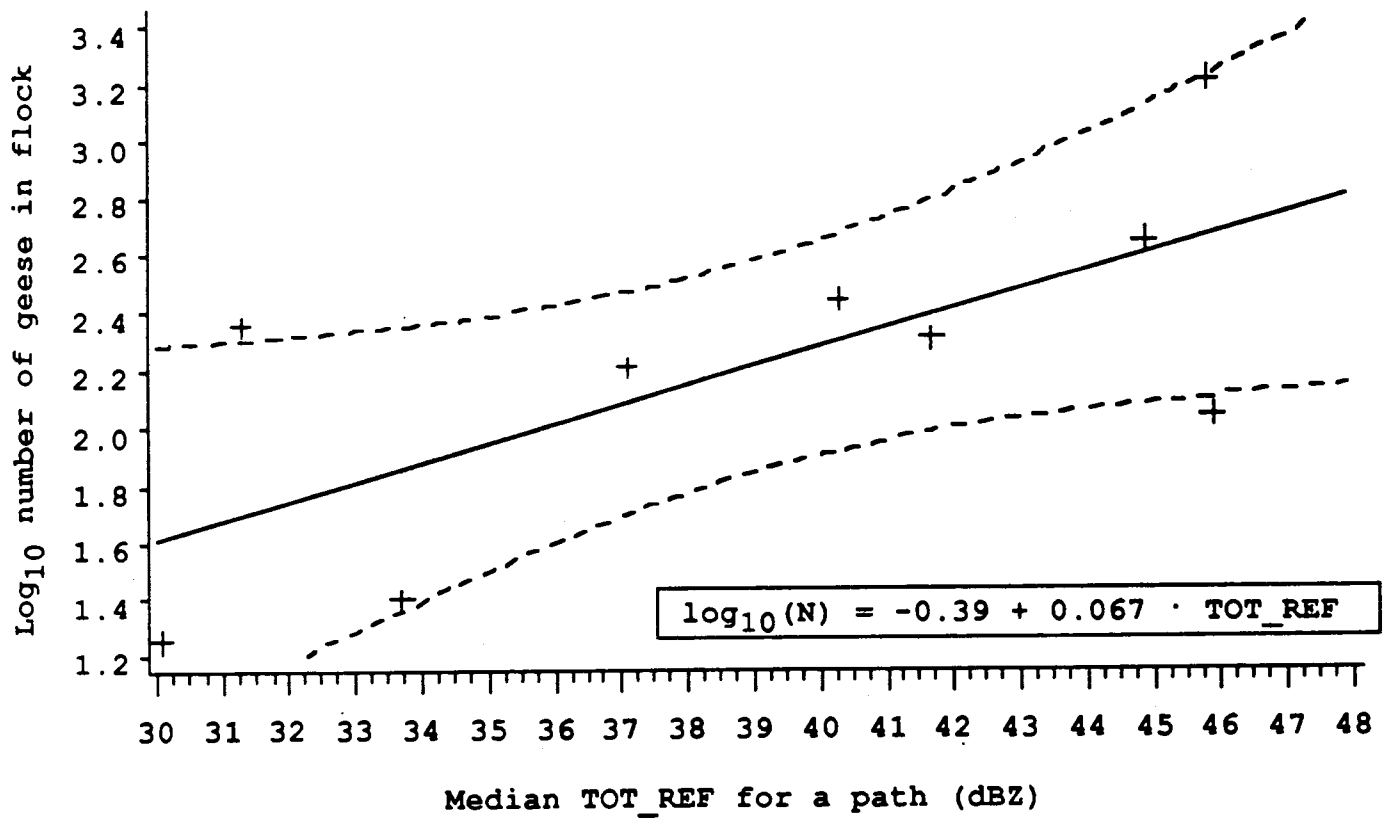
The common logarithm of the number of geese in a flock was plotted and regressed against the principal predictor of number of geese, reflectivity TOT\_REF, with the expectation that it would show a loglinear relationship, reflectivity in dBZ itself being a logarithm. Three other variables were also studied: AREA\_KM, MAX\_REF, and the "diameter" of the flock with the simplifying (and doubtless incorrect) assumption that the shape of the flock on weather radar is circular. The latter two variables proved to be so similar in

their behavior to TOT\_REF and AREA\_KM that they are omitted from this presentation. (For instance, MAX\_REF was consistently about 5 dB below TOT\_REF, with similar slope and confidence intervals.)

Careful inspection of the paths revealed that, like most paths of flocks approaching close to CHILL, TOT\_REF varied both slowly, e.g. due to coming over the horizon, and volume-by-volume, e.g. due to ground clutter. Therefore, the median TOT\_REF for the entire path was used as the central tendency of TOT\_REF in the calculations below. Implied in this decision is that the number of geese in a flock varies little relative to the aforementioned artifactual and stochastic variation of TOT\_REF. Indeed, fission or fusion of flocks was observed only once in the field.

Plots of median TOT\_REF and AREA\_KM, fitted linear regressions, and 95% confidence limits are shown in the following figure. Both relationships are significant: TOT\_REF  $p=0.04$ ,  $R^2=0.47$ ; AREA\_KM  $p=0.028$ ,  $R^2=0.52$ . Incorporating both TOT\_REF and AREA\_KM in the model produced a modest increase in proportion of variance explained, to  $R^2=0.59$ , but at the expense of increased likelihood of the null hypothesis at  $p=0.07$  ( $df=2$ ).

Low-flying flocks are suspected to contribute to much of the unexplained variance in the relationship. CHILL data permitted the algorithm to recognize Canada Goose flocks to the maximum range of 150 km in some cases and provided consistent measures of reflectivity and other products out to about 90 km; nonetheless, low-flying goose flocks were subject to underrepresentation and diminished measured values for reflectivity, especially at longer ranges. For this reason, the observers stationed themselves fairly close to CHILL at 25 km range in 1989. In spite of this, some flocks are suspected of flying so low that their measured reflectivity was continually diminished by obstructions and other



problems. (In neutral atmospheric conditions, line-of-sight from CHILL obscures part of the beam below nominal 51 m at the 25 km range, even without any topographic or other obstructions--Larkin and Quine 1989.) For instance, the flock with median TOT\_REF only 31.3 also has median AREA\_KM only 0.4 km<sup>2</sup>, but is a moderate-sized flock, N=225. CHILL followed this flock through the region near the observers with difficulty (path duration in this region=3) because it was approaching on the azimuth of Mansfield, IL and flying at an estimated height of only 93 m AGL. In repeating this work, which is highly desirable, it may be wise to use only flocks flying above some threshold height to eliminate such outliers in reflectivity.

Interpolating/extrapolating the Log<sub>10</sub>(N) / TOT\_REF relationship at 25 km. (mass estimates are calculated below in this section):

dBz	estimated N geese	estimated mass (kg)
5.8	1	4
20.7	10	40
35.7	100	400
50.6	1000	4000

The slope of the relationship is about 15 dBZ per 10 dB (tenfold) increase in number of geese, which implies either a nonlinearity or other error in the estimator or in some other factor entering into the relationship. One is tempted to suspect that small flocks of geese fly lower than larger flocks and thus have their reflectivities underestimated. In any case, the above relationship is determined empirically with an actual migration of Canada Geese and may therefore be used to calculate the number and mass of such geese in the air regardless of the slope of the relationship.

TOT\_REF is an especially interesting measure because it permits calculation of radar cross-section,  $\sigma$  (see Appendix III), for a Canada Goose on weather radar. In this case,  $\sigma$  is calculated for 10-cm wavelength. Note, however, that

the calculation must be interpreted with some circumspection, because  $\sigma$  assumes a dot-echo target whereas Z, the basis of reflectivity, assumes a volume scatterer. Therefore, a value of  $\sigma$  wildly inconsistent with published values from other birds may be dismissed because of gross violations of assumptions. A consistent value may be valid or may be due to coincidence.

Converting to dBm and 25 km range for  $N=1$  Canada Goose,  $\sigma = 0.153 \text{ m}^2$ , or  $1.53 \times 10^3 \text{ cm}^2$ . The mean mass of a *B. canadensis interior* male is 4.2 kg, a female 3.5 kg (Raveling ref. in Dunning 1984); or roughly 4 kg/goose. Reported 10-cm  $\sigma$  values for birds of mass roughly 2 kg are in the range  $1.6 \text{ cm}^2$  to  $17 \times 10^3 \text{ cm}^2$  (Vaughn 1985). Therefore, and perhaps somewhat surprisingly considering the several assumptions and limitations entering into the calculation, these results for 4 kg birds from a weather radar fall at the top of the previously-published range reported for 2-kg birds and are thus in rather close agreement.

The hazard to aircraft should be most closely proportional to either numbers or (numbers  $\times$  mass) of birds. On the basis of these calculations, the median Canada Goose flock would be about  $N=160$  birds and the total mass of the median flock about 600 kg.

To summarize these results from coordinated visual and radar observations of Canada Geese, a characteristic total reflectivity for a path may be computed and this total reflectivity may be used to estimate the number (or mass) of geese in the air.

**Migration traffic rates.** In 1989 data were collected over a ca. 10-hr period, sampling a large but undetermined fraction of the MVP goose population. Using the relationship of the number of geese as a function of TOT\_REF, the Migration Traffic Rate (MTR) may be estimated, along with the total number of geese flying in range of the radar. MTR is a flux, defined as the number of birds per unit time crossing a line of specified length perpendicular to the track of the geese. MTR is usually estimated by integrating over all heights. Although MTR

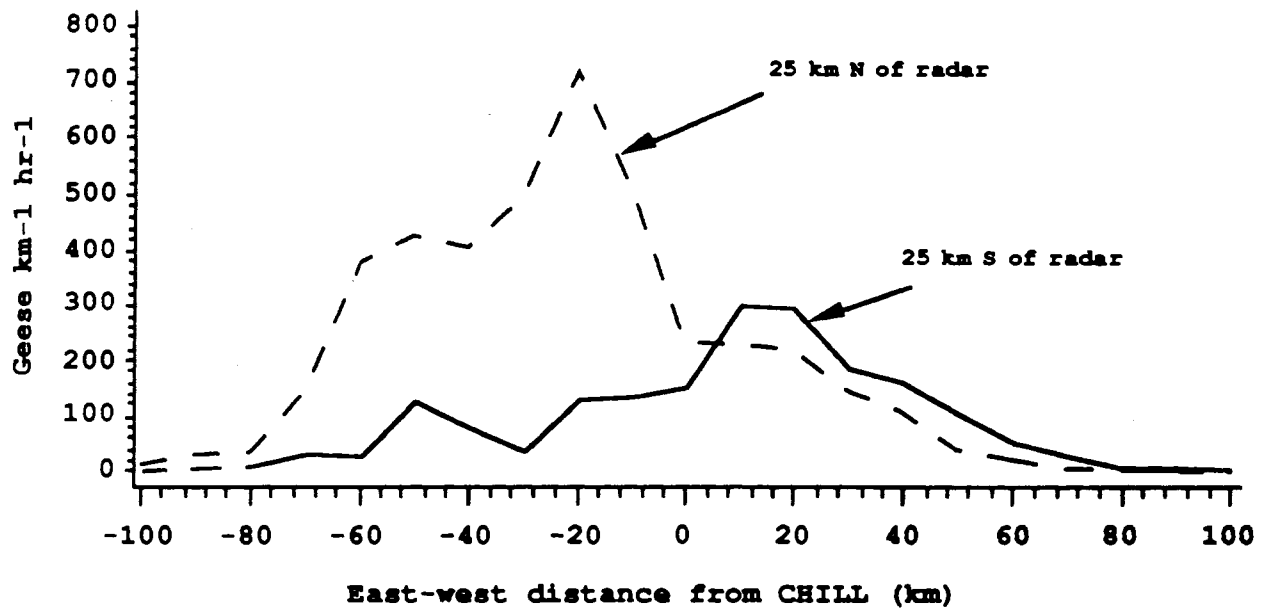


as usually defined is invalid or inaccurate when birds have a scattered or multimodal distribution of track, it is quite appropriate for these well-directed goose migrations.

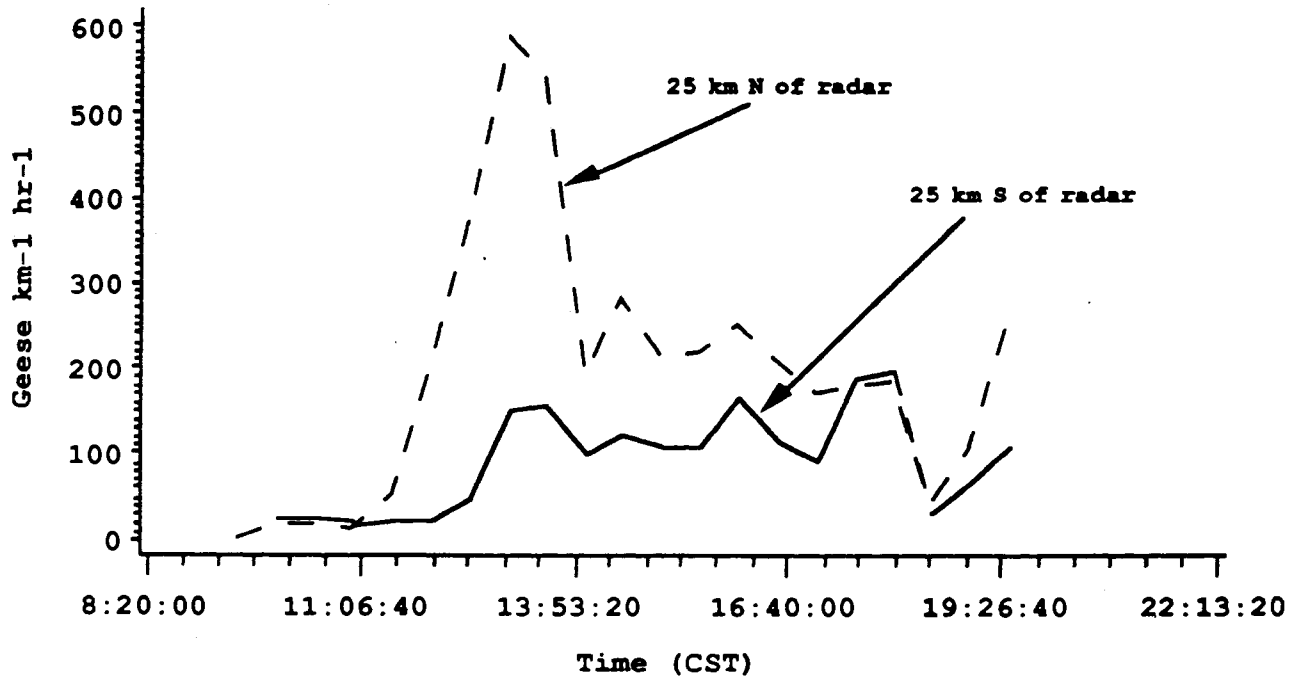
To measure MTR for the Canada Goose data, two E-W line segments were positioned at 25 km N and 25 km S of CHILL. The lines extended to 100 km E and 100 km W of CHILL, at which distance only low concentrations of geese were detected. Paths of duration less than 4 volumes were omitted from this analysis, as a conservative measure designed to minimize counting ground targets as geese. MTRs along the lines are shown in the following figures of MTR along the two lines summed over the entire data-collection period (top) and MTR summed along the north line in 30-min intervals (bottom).

Some noteworthy points, many of which are also evident on PPI images:

- More and especially larger flocks were registered N than S of CHILL. Mean MTR N of CHILL on this date:  $158 \text{ geese km}^{-1} \text{ hr}^{-1}$ ; S of CHILL:  $73 \text{ geese km}^{-1} \text{ hr}^{-1}$ . More favorable ground clutter and fewer obstructions N of CHILL certainly explains at least part of this effect.
- This is a dense migration of large birds. At  $(-20,25) \text{ km}$  (NW of CHILL), average MTR was 712, or about 4-5 flocks of average size  $\text{km}^{-1} \text{ hr}^{-1}$ , over the 11.3 hr period.
- The generally SSE-ward track of the geese shows in the offset peaks, W of CHILL to the N and E of CHILL to the S.
- To the N, a shallow notch in the curve at  $X=-40 \text{ km}$  reflects the "valley" in TOT\_REF visible on the PPIs.
- To the S, a similar shallow notch at  $X=-30 \text{ km}$  represents an obstruction to the radar beam at azimuth= $228^\circ$ .



Migration traffic rate of Canada Geese on 15 Dec 1989. Numbers of geese are computed by estimating flock size from TOT\_REF, summing the estimated geese flying through each 10-km section of two lines drawn 25 km N of the radar and 25 km S of the radar, and dividing by the 10-km section length.



Time course of Canada Goose migration during CHILL observations on 15 Dec 1989. Calculations were performed similar to the previous figure, except that flocks were binned into 30-min time periods. The last period was shorter than 30 min and is not included in the plot.

- Echoes fall off to nearly 0 outside 100 km. At this range and at the arbitrary 25-km N-S distance chosen for the analysis, the radial component of groundspeed for geese travelling S diminishes to about  $6 \text{ ms}^{-1}$ , in the region where anti-clutter filtering and Doppler velocity thresholding begin to come into play, so that part of this fall-off in geese at 100 km is artifact.

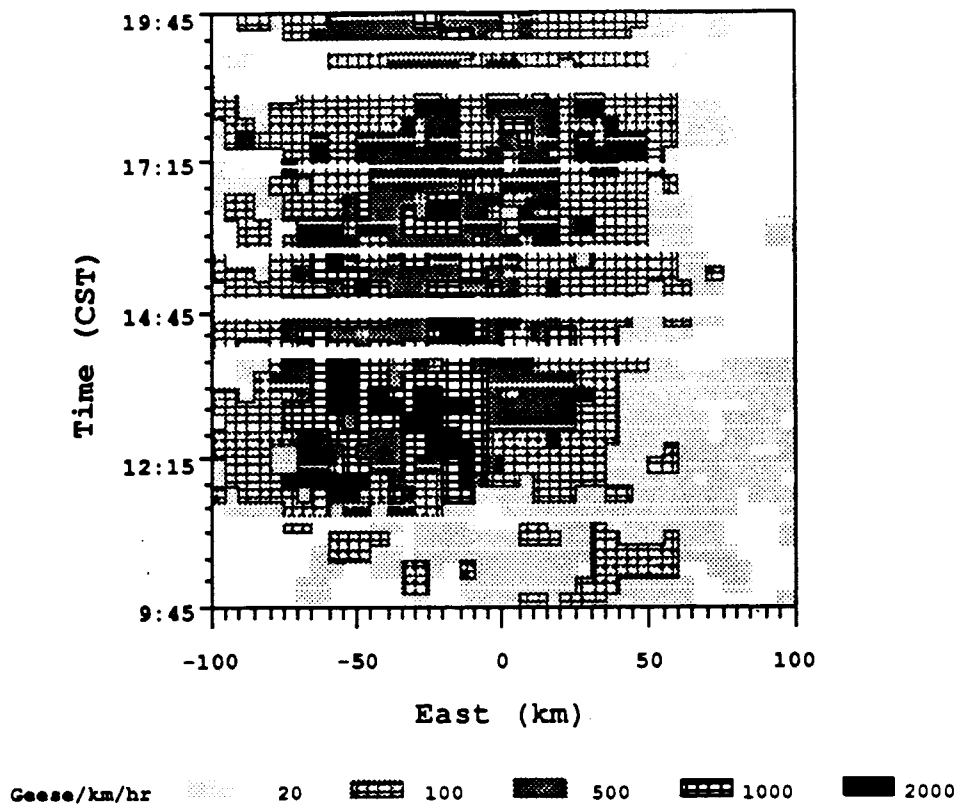
The following figure replots MTR N of CHILL in three dimensions with numbers of geese indicated by levels of shading. In this figure peak (as opposed to average) densities of geese are seen to be thousands of birds  $\text{km}^{-1} \text{kr}^{-1}$  and a gradual eastward drift in the longitude at which the geese pass by.

Integrating the curves gives an estimate of the total number of geese in paths of duration  $> 2$ :

N of CHILL:  $4.7 \times 10^4$

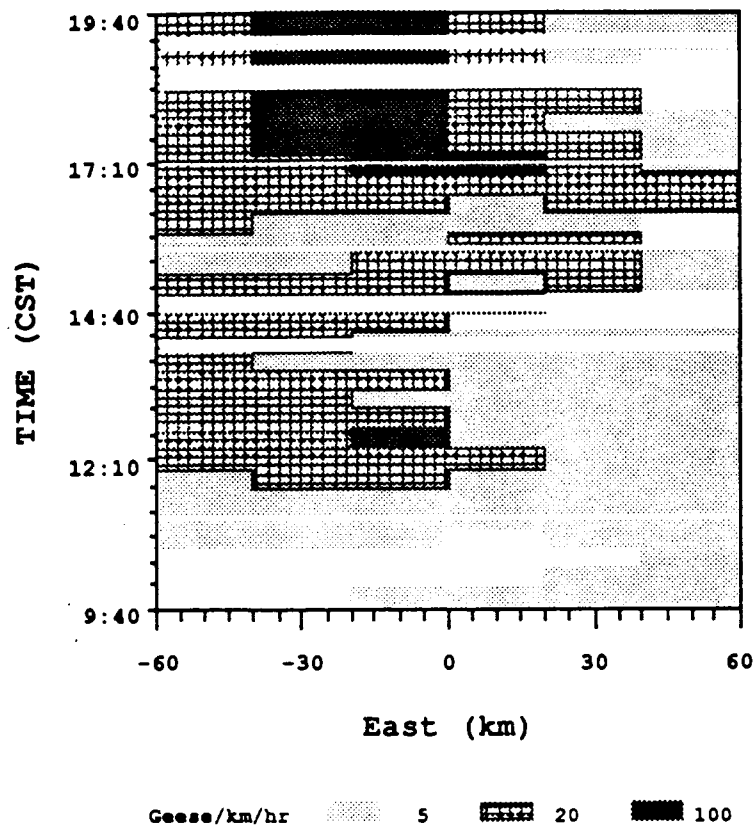
S of CHILL:  $2.1 \times 10^4$

The larger estimate represents about 10% of the MVP movement reported, that is, of the increment to the southern Illinois MVP goose count between 11 Dec and 16 Dec 1989. Most of the other 90% are probably geese that flew outside of the data collection period of ca. 10 hrs, that took other route(s) than near CHILL, or that were in the many paths of duration  $< 3$  excluded from the analysis. In addition, CHILL was not operating continuously for the period and some or many flocks "winked out" along the arbitrary 100 km line and were not detected on CHILL.



Migration Traffic Rate on 15 Dec 1989. MTR is estimated along a line 25 km north of CHILL during the ca. 10-hr data-collection period. Passage rate of Canada Geese is indicated by darkness of shading and data are binned into 0.5 km x 15 min intervals. Horizontal white areas indicate gaps in data collection.

Principal features of the plot, discussed in the text, are a temporal peak in passage about 13:00 and channeling of the geese into a flyway whose position shifted eastward during the course of the day.



MTR as in previous figure but 100 km N of CHILL, in a window  $\pm 60$  km in east-west dimension, and with coarser resolution in space and time. The estimated number of geese is lower largely because the low-flying geese are not in line-of-sight to CHILL.

The strong temporal peak seen on the 25-km figure at 13:00 appears here, attenuated, about 45 min earlier. And an evening movement out of Wisconsin is streaming over Pontiac IL as CHILL operations cease at 19:57.

Some geese appear to have departed their Wisconsin stopover in at least one pulse or wave, as evidenced by the clear peak in goose numbers around 13:00 crossing the line 25 km N of CHILL. Long paths (N=572 in this analysis of the pulse) that were 25 km N of CHILL at 1300 had a median groundspeed of 87 km hr<sup>-1</sup>. One traditional concentration of MVP geese in fall migration is Horicon NWR, Wisconsin, about 377 km distant from CHILL at about 354° (Craven, et al. 1986). Extrapolating backward to a hypothesized synchronous departure from Horicon, the pulse of geese would have departed about 4.1 hr earlier, at about 0900. These paths had a median track of 171°, which differs by only about 3° (0.4 S.D.) from the straight line from Horicon NWR to CHILL.

Extrapolating back in analogous fashion from the ca. 11:20 increase of geese 25 N of CHILL, the geese would have begun to depart Horicon at about 0715, or within a few minutes of local civil sunrise at Horicon NWR.

Alternatively, pulse(s) might have been produced if geese departed synchronously from widely dispersed geographic locations to the N and if one of those locations (e.g. Horicon NWR) had a high density of geese. This alternative seems less likely because the flyway was narrowly concentrated E-W on 15 Dec 1989.

Although data collection ended at 1957, migration continued. Before CHILL operations ceased a new pulse of geese appeared 100 km N of CHILL after 1715. Based on arguments similar to those advanced in the above discussion of the 1300 peak, this was an apparent late afternoon or evening departure from southern Wisconsin. Of course no comparison of the relative magnitude of daytime vs. nighttime MVP migratory movements can be made with these few data.

## Acknowledgements

Special thanks are due to Jeffrey Short, who had the idea, and Frank Bellrose, who provided a hard act to follow. Special thanks also to Daniel Halkin, Dave Mattox, Douglas B. Quine, George Swenson III, Bob Szafoni, and Greg Tillman, who exercised special talents for long hours in pursuit of birds on radar in connection with this project.

Many other colleagues, students, and employees were indispensable to the project in many ways. Their participation, and in many cases the generous cooperation of their organizations, made the project possible: Charles Alexander, Bill Anderson, Liz Anderson, Paul Bartels, Steve Bautista, Ellen Brewer, Kris Bruner, Dave Brunkow, Andy Caron, Tom Choy, Randy Cetin, Bob Coblentz, Bill Cochran, Jim Cochran, Nancy Covey, Tud Crompton, Tim Crum, Chris Davies, Russ DeFusco, Robb Diehl, Bob Dogan, Jim Evans, Glen Eveland, Barbara Frase, Spiros Geotis, Ken Glover, Larry Gross, Beverly Hubert, Pat Kennedy, Bob Kull, Avery Lambert, Charles Lasner, Dave Lesney, Paul Lester, Vance Mansur, Jim McNamara, Ron Merritt, Paul Mitchell, Cindy Mueller, Gene Mueller, Rich Murnan, Jerry Nespor, Jim Nissen, Tim O'Bannon, Paul Pomes, Arlo Raim, Ron Rinehart, Steve Rich, Scott Robinson, Chris Rohl, Glen Sanderson, Arno Schriefer, Jim Seets, Alan Siggia Trina Simpson, Dale Sirmans, Rod Snell, Don Staggs, George Swenson Jr., Mike Thompson, Joe Ward, Dick Warner, Bill Wheeler, Todd White, Mark Whitney, Richard Whitton, Willard Airport Control Tower at Savoy, Illinois, Sue Wood, Jerry Wray, John Wright, Dan Zimmerman and Dusan Zrnica.

My apologies to anyone I may have omitted by mistake.

## Literature Cited

- Able, K. and S. Gauthreaux, Jr. 1975. Quantification of nocturnal passerine migration with a portable ceilometer. *Condor* 77:92-96.
- Achtemeier, G. L. 1992. Grasshopper response to rapid vertical displacements within a clear air boundary layer as observed by Doppler radar. *Environ Entomol* 21:921-938.
- Achtemeier, G. L., B. Ackerman, L. K. Hendrie, M. E. Irwin, R. P. Larkin, N. Liquido, E. A. Mueller, R. W. Scott, W. Steiner and D. J. Voegtlin. 1987. The pests and weather project. ILENR/RE-AQ-87-1, Illinois Department of Energy and Natural Resources, Energy and Environmental Affairs Division.
- Alerstam, T. 1990. Ecological causes and consequences of bird orientation. *Experientia* 46:405-414.
- Allen, H. and L. Young. 1982. An annotated bibliography of avian communal roosting. Washington Department of Game,
- American Ornithologists' Union. 1983. Check-list of North American birds. American Ornithologists' Union, Lawrence, Kansas.
- Ansorge, V., K. Hammerschmidt and D. Todt. 1992. Communal roosting and formation of sleeping clusters in Barbary Macaques (*Macaca Sylvanus*). *Am J Primatol* 28:271-280.
- Babcock, K. M., D. D. Humburg and D. A. Graber. 1990. Goose management: the Mississippi Flyway perspective. Pp. 312-320 in *Transactions 55th North American Wildlife and Natural Resources Conference*.
- Beerwinkle, K. R., J. A. Witz and P. G. Schleider. 1993. An automated, vertical looking, X-band radar system for continuously monitoring aerial insect activity. *Trans ASAE* 36:965-970.
- Bellrose, F. C. 1981. Migration speeds of three waterfowl species. *Wilson Bulletin* 93:121-124.
- Black, C. 1941. Ecological and economic relations of the crow, with special reference to Illinois. Thesis, University of Illinois, Urbana, Illinois.
- Blokpoel, H. 1970. A further attempt to forecast bird migration Over Cold Lake, Alberta. *Field Note* No. 54,
- Blokpoel, H. 1976. Bird hazards to aircraft. Clarke, Irwin, & Co., Ltd., Ottawa, Canada.
- Bogler, P. 1990. Radar principles with applications to tracking systems. John Wiley and Sons, New York.
- Caccamise, D. and J. Fischl. 1985. Patterns of association of secondary species in roosts of



- European Starlings and Common Grackles. *Wilson Bulletin* 97:173-182.
- Caccamise, D., L. Lyon and J. Fischl. 1983. Seasonal patterns in roosting flocks of Starlings and Common Grackles. *Condor* 85:464-481.
- Clements, J. 1989. Illinois facts 1989. Clements Research II, Dallas TX.
- Clergeau, P. 1990. Flocking behaviour of Starlings (*Sturnus vulgaris*) during the day: a gradual gathering to the roost. *J. Ornithol.* 131:458-460.
- Craven, S. R., G. A. Bartelt, D. H. Rusch and R. E. Trost. 1986. Distribution and movement of Canada Geese in response to management changes in East Central Wisconsin, 1975-81. Technical Bulletin No. 158, Department of Natural Resources.
- Crum, T. D. and R. L. Alberty. 1993. The WSR-88D and the WSR-88D Operational Support Facility. *Bulletin of the American Meteorological Society* 74:1669-1687.
- Crum, T. D., R. L. Alberty and D. W. Burgess. 1993. Recording, archiving, and using WSR-88D data. *Bulletin of the American Meteorological Society* 74:645-653.
- Defusco, R. P., R. P. Larkin and D. B. Quine. 1986. Bird hazard warning using next generation weather radar. Pp. 135-148 in *Proceedings of the 18th Bird Strike Committee Europe*.
- Doviak, R. J. and D. S. Zmric. 1984. Doppler radar and weather observations. Academic Press, Orlando, Florida.
- Dunning, J. B. 1992. CRC handbook of avian body masses. CRC Press, Boca Raton, FL.
- Eastwood, E. 1967. Radar ornithology. Methuen & Co., London.
- Eastwood, E., G. Isted and G. Rider. 1962. Radar Ring Angels and the Roosting Behavior of Starlings. *Proceedings of the Royal Society of London* B156:242-267.
- Evans, W. R. 1994. Nocturnal flight call of Bicknells Thrush. *Wilson Bull* 106:55-61.
- Feare, C. 1984. The starling. Oxford University Press, Oxford.
- Gauthreaux, S., Jr. 1969. A portable ceilometer technique for studying low-level nocturnal migrations. *Bird-Banding* 40:309-320.
- Gauthreaux, S. A., Jr. 1974. A Conference on the Biological Aspects of the Bird/Aircraft Collision Problem, Clemson University, Clemson, S.C., 5-7 February, 1974. 536 pp.
- Gauthreaux, S. A., Jr. 1992. The use of weather radar to monitor long-term patterns of trans-gulf migration in spring. Pp. 96-100 in Hagan, J. M., III and D. W. Johnston, eds. *Ecology and conservation of neotropical migrant landbirds*.
- Graber, R. R., J. W. Graber and E. L. Kirk. 1971. Illinois birds: Turdidae. *Illinois Natural History Survey Biological Notes* 75:1-44.
- Graber, R. and W. Cochran. 1959. An audio technique for the study of nocturnal migration of

- birds. *Wilson Bulletin* 71:220-236.
- Graber, R. and W. Cochran. 1960. Evaluation of an Aural Record of Nocturnal Migration. *Wilson Bulletin* 72:253-273.
- Greenstone, M. H. 1990. Meteorological determinants of spider ballooning: the roles of thermals vs. the vertical windspeed gradient in becoming airborne. *Oecologia* 84:164-168.
- Greenstone, M. H. 1991. Aerial dispersal of arthropod natural enemies: altitudinal differences in taxonomic distribution of dispersers. Pp. 104-106 in Tenth conference on biometeorology and aerobiology and the special session on hydrometeorology.
- Guli, D. 1986. Polarization diversity in radars. *Proceedings of the IEEE*. 74:245-269.
- Harper, W. G. 1959. Roosting movements of birds and migration departures from roosts as seen by radar. *Ibis* 101:201-208.
- Hunt, F. R. 1975. Automatic radar equipment to determine bird strike probability part I. Night-time passerine migration. Field Note no. 69, National Research Council of Canada.
- Isaminger, M. A. 1992. Birds mimicking microbursts on 2 June 1990 in Orlando, Florida. DOT/FAA/NR-91/10, Project Report ATC-184, Federal Aviation Administration.
- Klazura, G. E. and D. A. Imy. 1993. A description of the initial set of analysis products available from the NEXRAD WSR-88D system. *Bulletin of the American Meteorological Society* 7:1293-1311.
- Lack, D. and G. C. Varley. 1945. Detection of birds by radar. *Nature* 156:446.
- Larkin, R. and L. Eisenberg. 1978. A method for automatically detecting birds on radar. *Bird-Banding* 49:172-181.
- Larkin, R. and D. Thompson. 1980. Flight speeds of birds observed with radar: Evidence for two phases of migratory flight. *Behavioral Ecology and Sociobiology* 7:301-317.
- Larkin, R. P. 1982a. The potential of the NEXRAD radar system in reducing bird/aircraft hazards. Rep. Final Report Contract Number F5ESCG20900001, U. S. Air Force, AFESC.
- Larkin, R. P. 1982b. Spatial distribution of migrating birds and small-scale atmospheric motion. Pp. 28-37 in Papi, F. and H.-G. Wallraff, eds. *Avian Navigation*. Springer-Verlag, New York.
- Larkin, R. P. 1990. Report on bird hazard algorithm. Grant Agreement 14-16-0009-87-1221, U.S. Fish and Wildlife Service.
- Larkin, R. P. 1991a. Flight speeds observed with radar, a correction: slow "birds" are insects. *Behav. Ecol. Sociobiol.* 29:221-224.
- Larkin, R. P. 1991b. Sensitivity of NEXRAD algorithms to echoes from birds and insects. Pp. 203-205 in 25th International Conference on Radar Meteorology.

- Larkin, R. P. and D. B. Quine. 1987. Report on bird movement data. Report of Contract DACA-86-D-001 by the U. S. Army Construction Engineering Research Laboratory.
- Larkin, R. P. and D. B. Quine. 1988. Recognizing bird targets on next generation weather radar. Pp. in Proceedings of the 19th Bird Strike Committee Europe. BSCE, Madrid, Spain.
- Larkin, R. P. and D. B. Quine. 1989. Report on bird hazard algorithm. Grant Agreement 14-16-0009-87-1221, U.S. Fish and Wildlife Service.
- Marti, C. and F. Heiniger. 1987. [use of thermal imagers in field ornithology]. Ornithol. Beob. 84:67-69.
- Mueller, E. A. and R. P. Larkin. 1985. Insects observed using dual-polarization radar. Journal of Atmospheric and Oceanic Technology 2:49-54.
- Mueller, E. A. 1989. Description of the CHILL radar system. Pp. 609-614 in 24th Conference on Radar Meteorology.
- Mueller, E. A., P. C. Kennedy and D. A. Brunkow. 1989. CHILL radar data analysis guide. Illinois State Water Survey Miscellaneous Publication 109:1-29.
- Newman, R. J. and G. H. Lowery. 1964. Selected quantitative data on night migration in autumn. Special publications of the Museum of Zoology, Louisiana State University 3:1-39.
- NEXRAD Joint System Project Office. 1981. Next Generation Weather Radar Joint Operational Requirements.
- Nisbet, I. C. T. and W. H. Drury, Jr. 1969. A migration wave observed by moon-watching and at banding stations. Bird-Banding 40:243-254.
- Peach, W. J., D. P. Hodson and J. A. Fowler. 1992. Variation in the Winter Body Mass of Starlings *Sturnus vulgaris*. Bird Study 39:89-95.
- Peltier, J. T. 1989. A study of ground clutter suppression at the CHILL Doppler weather radar. Masters thesis, University of Illinois at Champaign-Urbana. 169 pp.
- Quine, D. B. and R. P. Larkin. 1987. Draft report on bird movement data and NEXRAD system. Contract 14-16-0009-87-1221, U.S. Fish and Wildlife Service.
- Rabb, R. L. and G. G. Kennedy. 1979. Movement of highly mobile insects: Concepts and methodology in research. Department of Entomology, N. Carolina State University, Raleigh, North Carolina.
- Richardson, W. J. 1990. Timing of bird migration in relation to weather: updated review. Pp. 78-101 in Gwinner, E., ed. Bird Migration. Springer-Verlag, Berlin.
- Riley, J. R. 1989. Remote sensing in entomology. Ann. Rev. Entomol. 34:247-271.
- Rinehart, R. E. 1991. Radar for meteorologists. Department of Atmospheric Sciences, Grand

Forks, North Dakota.

- Samuel, M. D., D. H. Rusch, K. F. Abraham, M. M. Gillespie, J. P. Prevett and G. W. Swenson. 1991. Fall and winter distribution of Canada Geese in the Mississippi Flyway. *Journal of Wildlife Management* 55:449-456.
- Seliga, T. 1980. Dual polarization radar. *Nature* 285:191-192.
- Sirmans, D. 1988. NEXRAD suppression of land clutter echo due to anomalous microwave propagation - Part I. NEXRAD JSPO, Norman, OK.
- Skolnik, M. I. 1970. Radar handbook. McGraw-Hill, New York.
- United States General Accounting Office. 1989. Reducing risks to military aircraft from bird collisions. Rep. Test and Evaluation GAO/NSIAD-89-127, Legislation and National Security Subcommittee, Committee on Government Operations, House of Representatives.
- Tacha, T. C., A. Woolf, W. D. Klimstra and K. F. Abraham. 1991. Migration patterns of the Mississippi Valley population of Canada Geese. *J. Wildl. Manage.* 55:94-102.
- Tye, A. 1993. Diurnal activity centers and information centers - A need for more critical study. *Wilson Bulletin* 105:368-372.
- United States Naval Observatory. 1987-1990. Almanac for computers. Nautical Almanac Office, Washington, D.C.
- Vaughn, C. 1985. Birds and insects as radar targets: a review. *Proc. IEEE* 73:205-227.
- Williams, T. C. and J. M. Williams. 1969. Bat hazards to aircraft: detection by radar. In *Proceedings of the world conference on bird hazards to aircraft*, Kingston, Ontario, pp. 307-320.
- Wolf, W. W., C. R. Vaughn, R. Harris and G. M. Loper. 1993. Insect Radar Cross-Sections for Aerial Density Measurements and Target Classification. *Trans ASAE* 36:949-954.

## Appendix I. Glossary and acronyms for NEXRAD Bird Hazard Algorithm

[See also the more technical glossaries in Rinehart, (1991) and Bogler (1990).]

**A-scope**: A fundamental radar display presenting the strength of radar echo vertically and the range horizontally, along the radar beam.

**ACC**: Air Combat Command

**Aerosol**: A suspension of fine droplets in air.

**AFGL**: Air Force Geophysics Laboratory. The site at Sudbury, MA, where one of the NEXRAD prototype radars is located.

**Air speed**: Synonymous with Flight speed, q.v. Also called True Air Speed.

**Aliasing**: Doppler velocity wraparound, causing targets fast receding to appear to be approaching or vice versa. Aliasing is an inevitable property of the way Doppler measurements are performed. It appears at a certain, defined Doppler speed (Nyquist velocity) above which the radar cannot measure speed unambiguously. Its occurrence can be minimized and its existence detected and corrected. The Nyquist velocity can be changed (in present-generation radars) only by using a different radar frequency or trading off other specifications.

**AMC**: Air Mobility Command

**Amplitude**: In this report, radar echo amplitude is used virtually synonymously with intensity and reflectivity. It is the amount of energy reflected back to the radar from a given target and is a function of the size of the target, the orientation of the target if it is not spherical, and especially of the range of the target.

**Anomalous Propagation**: Ducting or bending of radar signals due to inhomogeneities in the atmosphere. Anomalous propagation is commonly produced by refraction in temperature and humidity inversions at night; in such situations it is common, rather than as unusual as its name implies. It usually has the effect of making targets, especially low ones, visible on the radar

at distances where the earth's curvature would be expected to rule out their appearance.

**Aspect:** The direction a radar target is facing relative to the radar. Aspect is commonly measured by examining the amplitude of radar echo returned from a target as the target is rotated around through 360°.

**Azimuth:** Compass bearing measured from 0° to 360° relative to true north.

**AWS:** The USAF Air Weather Service

**Backscatter:** Energy redirected at least partly back along the path from which it came. Backscatter includes both specular (mirror-like) reflection and more complicated and realistic models of ways in which microwave energy interacts with targets such as birds and weather.

**Base data:** The fundamental (and most detailed) data from the RDA that are available to NEXRAD algorithms. Presently available base data are Base Reflectivity, Base Velocity, and Base Spectral Width.

**BASH:** Bird Aircraft Strike Hazard Team, operating out of Tyndall, Air Force Base, Florida.

**Beamwidth:** The angle subtended by a radar beam. Specifically, the azimuthal beamwidth is the number of degrees over which the radiated radar energy is at least half that in the center of the beam, where the energy is maximal.

**Blackbird:** The term is usually used loosely and includes European Starlings, Common Grackles, Redwings, Brown-headed Cowbirds, and blackbirds of the genus Euphagus. These species are of similar size and often roost together.

**Boresight:** Sighted along or near the center of the beam of a pencil-beam radar.

**BSCE:** Bird Strike Committee Europe, the most important international organization concerned with bird/aircraft collision problems.

**CAPPI:** Constant Altitude Planned Position Indicator. A display like a PPI (see below), but actually synthesized from several PPI's to show data only from a certain altitude stratum.

**Centroid:** The position taken to represent the position (central tendency) of an echo segment. The

NEXRAD Storm Centroids algorithm computes the centroid in three dimensions from gates weighted by reflectivity. The flock paths algorithm in this report computes a centroid in similar fashion but in only the XY dimension.

Circular polarization: Polarization in which, effectively, a 360° sweep of polarization is achieved.

Circular polarization has unique properties when scattering off flat objects ("sides of barns") and spherical objects not large with respect to the wavelength.

CHILL: A prototype NEXRAD radar system originally built in cooperation by the University of Chicago and the University of Illinois. Until early 1990 CHILL was operated by the Illinois State Water Survey and was located in Champaign County, Illinois.

Clear air: A hypothetical construct used by radar meteorologists, roughly synonymous with "cloudless". "Clear air echoes" are radar echoes coming from regions of the sky with no visible meteorological scatterers. The term implies that what is returning echo is not visible. Birds and insects are common causes of clear air echoes, along with dust and inhomogeneous distributions of refractive index in the atmosphere. NEXRAD scan strategies include clear air modes, in which the antenna rotation rate is decreased to increase the effective sensitivity of the radar to faint echoes.

Clutter: Targets that cause radar echos but are not useful signals. Sometimes clutter obscures the targets being observed. See also Ground Clutter.

Convergence: A meteorological situation in which air rises and is replaced by air moving in horizontally from more than one direction.

Cross section: A relative measure of the size of point targets, in units of area. Cross section of birds does not always vary monotonically with physical measures of size, such as the number of birds in a flock or the size of a single bird target.

dBZ: The common logarithm of reflectivity relative to 1 mm /m . dBZ is a standard measure of the reflectivity of meteorological (water) targets.

**C-band**: 5-cm radar wave length used by some weather radars. See also S-band.

**dB**: see Decibel

**dBm**: Power relative to 1 milliwatt, expressed in decibels.

**dBZ**: A decibel measure of water content of cloud (Z). It is designed to measure precipitation potential and to be independent of range.

**Decibel**: A ratio between two quantities, expressed in a logarithmic fashion:  $10 \cdot \log_{10}(a/b)$ .

**Decision Sum**: A means of incorporating several factors quantitatively in a yes-or-no decision. In a decision sum, the factors are scaled so that they take the same unit, then summed, perhaps first by weighting the factors. The decision sum is compared against a threshold or ranked with another decision sum arrived at the same way.

**Diel**: A 24-hour interval. Diel includes diurnal (daytime) and nocturnal (nighttime).

**Doppler Speed**: Speed measured using the Doppler Effect. Doppler speed of a target, one of the primary products of NEXRAD, is always measured along a straight line from the observer to the target, therefore it is always measured along a radial from a radar. Only if a target is directly approaching or receding from the radar is the Doppler speed equal to the actual ground speed of the target. The Doppler Effect is an apparent change in frequency of a wave train resulting from relative motion of the source of the wave energy, in this case, the target reflecting microwave energy.

**Doppler velocity**: In general usage, Doppler velocity is synonymous with Doppler speed.

**Dot Echo**: Dot echoes arise from targets that are effectively point targets in space; the targets are smaller than the resolution cell of the radar being used. Individual birds or compact flocks of birds will be dot echoes as viewed by the NEXRAD radar system.

**Echo segment**: A group of gates at the same elevation, treated as a unit for analysis. Gates in an echo segment are contiguous, or nearly contiguous, depending on the algorithm used to group them together.



**8 mm tape:** A serial magnetic recording medium widely used for backup purposes and, in the case of NEXRAD Level II archives, for recording large amounts of data. The lowest grade of 8 mm tape is used in video camcorders. 8 mm tape as a computer medium is evolving rapidly at the present time (1993).

**Elevation:** The vertical angle of the radar beam, with the horizon as 0° and the zenith as 90°.

**Exabyte:** The brand name of 8 mm tape drives, used for archiving Level II NEXRAD data. Although this situation may change, Exabyte is presently the only manufacturer of 8 mm tape drives. Exabyte Corp. also resells the 8 mm tape medium.

**FFT:** Fast Fourier Transform. A procedure for generating frequency spectra, sometimes also used for generating correlations. This common digital technique is useful in analyzing Doppler signals.

**Flight speed:** Speed relative to the air through which the bird is flying. "Air speed" or "True air speed" is the pilot's term for Flight Speed.

**Firmware:** Software that is built into electronic equipment. In general, it is distinguished from ordinary software by being coded in a very low-level language or in binary, by being tailored to be small and run fast, and to perform quite specialized functions, often being written for a specific application and running only on a specific model of processor.

**Gate:** see Range Gate

**Gate spacing:** The interval between one sample and the next along a radial; the effective range resolution of a pulsed radar. It is engineered in microseconds but ordinarily stated in meters or kilometers.

**GPG:** A 3-cm tracking radar unit operated by the Illinois State Natural History Survey for the purpose of studying flying animals. This unit has been modified from a military radar designed to track aircraft in fire-control work.

**Ground Clutter:** Targets on or near the ground generating unwanted radar echoes. These include

topographic features, trees, buildings, ocean waves, automobiles, and other moving or stationary targets.

**Ground speed:** Speed of travel relative to the ground. See also Flight Speed.

**Ground Truth:** Data establishing the identity and other properties of a radar target, obtained by direct visual observation from the ground or by other persuasive means.

**Heading:** Angle of a flying animal's progress through the air. It is assumed that the heading is the direction an animal's body is pointed. The heading is one component of velocity relative to the air, flight speed is the other component.

**Main bang:** The image of the transmitted pulse of a radar appearing in the received signal. The Main Bang prevents data from being taken very close to the radar.

**Micro 5:** The model of computer that will eventually be employed in NEXRAD RPG's and RDA's.

**Microburst:** A quick, local downflow of air from a cloud. The archetypical microburst hazardous to aviation consists of a downdraft that strikes the ground and is deflected outward in all directions. A naive pilot landing or taking off into a microburst will want to decrease power and/or nose down to compensate for the increased airspeed and lift of the outflow region; when the slowed aircraft then enters the downdraft, it will lose altitude dangerously fast.

**Mosaicking:** Combining information from more than one geographically separate radar unit to produce a map of the total area covered by the radar units, and possible areas of overlap.

**MVP:** The Mississippi Valley Population of Canada Geese, one of about 11 major races and populations. MVP geese winter in southern Illinois and parts of adjacent states.

**NCDC:** National Climatic Data Center, the only official archiving organization of the Department of Commerce. NCDC will be responsible for archiving data from the WSR-88D.

**NCP:** Normalized Coherent Power, a correlation coefficient that increases with Signal/Noise ratio.

**NEXRAD:** The Next Generation Weather Radar, WSR-88D, presently in production and designed to provide a modern national network of operational weather radars.

**NOTAM:** Notice To AirMen, a warning of a specific situation. Pilots check for these before flying.

**NWS:** National Weather Service, an agency of the Department of Commerce.

**Nyquist frequency (or velocity):** The lowest Doppler frequency (or velocity) that reaches the phase ambiguity at  $\text{phase}=180^\circ$ , at which the sign of the radar-measured Doppler velocity reverses and it is said to "wrap around". See also Aliasing.

**OSE:** NEXRAD Operational Support Facility, in Norman OK.

**Paramax:** The company with a contract to convert A.E.L. into runnable code.

**Passerine:** Birds of the order Passeriformes; most passerines are songbirds and many small birds that fly long distances in the United States are passerines.

**Point target:** Synonymous with Dot Echo, q.v.

**Polarization:** The rotational angle of transverse waves. The NEXRAD system uses horizontal polarization, which reflects energy better from horizontally-oriented targets than from vertically-oriented ones. Examples of horizontally-oriented targets will be birds flying tangential to the radar, falling water droplets, and snowflakes.

**Polarization diversity:** Refers to the ability of a radar to transmit and receive several different polarizations, and usually to the ability to transmit one polarization and receive the echo at the same and/or a different polarization. ZDR, q.v., is the garden variety of polarization diversity.

**PPI:** The maplike Plan Position Indicator display, common to most radar systems with rotating antennae. In a PPI display the radar is commonly located at the center and the display projects intensity, Doppler, or other information around the radar with North at the top of the display. The PPI display presents images as they appear along the radar beam at whatever elevation the radar beam is situated during the antenna's rotation through  $360^\circ$ . At elevations above  $0^\circ$ , targets more distant from the center of the display will therefore be higher in altitude above the radar.

**Pulse Length:** The length of a brief pulse of radar energy, measured in time (microseconds) or in distance (meters).

**PRF:** See Pulse Repetition Frequency

**PRT:** Pulse Repetition Time, 1/PRF.

**Pulse Repetition Frequency:** Number of transmitted pulses of microwave energy per second, expressed in Hertz.

**Pulse Volume:** The 3-dimensional size of a radar pulse traveling through space. Its length is the pulse length. For a pencil-beam radar such as NEXRAD, the diameter of the pulse volume will be identical to the beam width of the radar, measured in degrees. The size of the pulse volume measured in linear units such as meters will increase linearly with distance from the radar. Generally, targets within the pulse volume will reflect radar energy at the azimuth, elevation, and range nominally specified by the center of the pulse volume.

**Pulse Width:** Same as pulse length. Isn't that odd?

**PUP:** Principle User Processor--part of the NEXRAD system. As presently envisioned, a PUP will have two functions: it will receive processed radar information from the RPG and will display this information in an interactive fashion to people using the NEXRAD system. In addition, the PUP will thus be the point of interaction between NEXRAD users, both human and automatic, and the rest of the NEXRAD system.

**Radar cross section:** See Cross section.

**Radar Product:** A useful output of NEXRAD. Reflectivity, Doppler, and spectral width are the three primary products.

**Radial:** The series of range gates that are sampled at one antenna position, also called a "ray". Actually, the radar usually slews continuously and more than one sample is taken, so a radial commonly refers to the mean or nominal azimuth/elevation at which a temporally-grouped series of range gates are sampled.

**Range:** Straight-line distance from the radar to the target. By "range" is usually meant "slant range", not distance over the ground.

**Range Gate:** A short interval of range during which a near-instantaneous sample of incoming radar echo is sampled. In practice, "gate" is often used to indicate the data obtained from one pulse volume, summed over a short series of radar pulses at nominally one azimuth.

**Range Height Indicator:** A radar display of altitude above the ground vertically versus distance over the ground horizontally. An RHI display shows a vertical slice of space at a fixed azimuth.

**Range unfolding:** see Unfolding

**RDA:** Radar Data Acquisition--part of the NEXRAD system. The RDA is the "front end" of the NEXRAD WSR-88D, including the antenna, radar transmitter and receiver, and pre-processing elements and antenna control devices.

**Real Time:** Activities are in real time if they occur fast enough to influence the events to which they are responsive. In the case of bird hazard monitoring, real time operation will be operation in which a developing bird hazard can be detected and information relayed to the pilot in time to possibly modify the flight pattern to reduce the risk.

**Reflectivity:** The amount of radar energy scattered from the target back toward the radar. See amplitude, and dBZ. (See [Rinehart, 1991 #2220] for a more precise but, in ordinary meteorological usage less common, definition for reflectivity.)

**Resolution Cell:** See pulse volume

**RHI:** Range Height Indicator. A display showing height, (altitude) vertically and distance from the radar horizontally, along a radius. The origin, the radar, is commonly at the left bottom of such a display.

**Ring Angel:** A distinct and unique pattern of radar echoes produced by a blackbird roost from which birds are departing in early morning. On a calm morning, the echoes expand symmetrically from a point at the roost in all directions, usually generating waves that have the appearance of

pond water into which a stone has been dropped.

**RMS:** Route Mean Square.

**RPG:** The Radar Product Generator section of NEXRAD. The RPG is a computer of considerable power receiving information from the RDA and exporting this information to the PUP under control of its own programs and of requests from the PUP. The RPG is commonly co-located with the RDA or at least located no more than a kilometer or so from it.

**S-band:** The radio frequency band of NEXRAD and many other weather radars, with a nominal wavelength of about 10 cm .

**Scan:** Usually synonymous in weather radar with with a volume scan, but not always.

**Second Trip:** Second trip echoes do not make two trips. Rather, they are echoes from targets further distant than are meant to be detected from a given radar pulse; they occur so long after a given pulse that the following radar pulse has already been generated. Therefore, they appear at much shorter range than they actually are. Second trip echoes are often, but not always, easily distinguishable on radar displays.

**Shear:** In the most common meteorological usage, shear refers to variation in wind velocity with altitude above the ground.

**Shorebird:** Charadriiform birds; they commonly frequent the seashore and other open habitats and are small-to moderate-sized birds with longish legs and narrow bills. They characteristically fly in densely-packed flocks and include plovers, sandpipers, and similar birds.

**Sidelobe:** Radar energy that is concentrated at a different angle from the antenna position. Sidelobes from ground clutter, geese, and other strong or close echoes are often important but those from fainter targets are usually too weak to interfere with the main lobe's echo. The most important sidelobes for meteorological radars are usually those within 2-3° degrees off the nominal antenna position and those at 90° or greater, spilling around the edges of the antenna.

**Signature:** See wing-beat signature.

S/N: The ratio of Signal to Noise. Higher values indicate a purer signal; in information-theoretic terms 1.0 indicates the minimum detectable signal.

Slant Range: see Range

Sounding: A balloon-launch to obtain data on the horizontal wind and other data.

Spectral Width: The amount of variation in the velocities of the targets in a Doppler signal. The spectral width can be thought of as the second moment of the Doppler signal, the first moment being the Doppler velocity. The ideal radar pulse is transmitted as a single frequency and, due primarily to the radial motion of the targets, it returns with that frequency shifted but also broadened into a spectrum of different frequencies, partly or mostly due to variation in the radial motions of the targets in the pulse volume. Spectral width attempts to characterize the width of that spectrum.

Sweep: As applied to current operational NEXRAD, it is one 360° rotation of the antenna at constant elevation. One such sweep generates one PPI image.

σ: See Cross section.

Target: Something that generates a radar echo.

TDR: see TDWR

TDWR: Terminal Doppler Weather Radar. Doppler radars similar in some ways to NEXRAD but configured for detailed observation around commercial airfields. These radars rotate faster than WSR-88D's and use faster pulse rates and closer gate spacing. An FAA project.

Track: Direction of travel relative to the earth. See also Heading.

True Air Speed: See Flight Speed.

TWS: Track-while-scan, a technique of following multiple targets from a scanning radar antenna without feedback, by matching echoes received in successive scans.

Unfolding (Range unfolding): Attempting to correct for second-trip echoes, q.v. Range unfolding is done on the WSR-88D by devoting a low-elevation scan to sampling at a PRF designed to be

so low that even the most distant echoes from a given pulse return before the next pulse is transmitted, then using that special scan to recognize and correct for possible second-trip echoes in subsequent scans.

**Universal format:** A specification for arranging radar data on computer tape so that it can be read by a different ("foreign") computer system. In practice, this laudable goal is seldom met due to advances in technology and lack of a certification mechanism for the format.

**USFWS:** United States Fish and Wildlife Service

**VAD:** The Velocity Azimuth Display, which is a display of the radial speed (Doppler speed) versus azimuth. When the radar unit is surrounded by a field of birds or meteorological targets all moving in the same direction, the VAD looks like a sine wave whose amplitude is proportional to the ground velocity of the targets, whose phase indicates their ground direction, whose variation from a pure sine wave indicates the variability of the Doppler speeds, and whose offset from 0 RMS is (under certain assumptions) related to vertical velocity or convergence.

**Variance:** A measure of the variability in the Doppler Signal; closely associated with the spectral width parameter in the NEXRAD specifications.

**VCP:** Volume Coverage Pattern, the programmed antenna motions in azimuth and elevation that comprise a volume scan.

**Velocity:** A 2- or 3-dimensional vector of change in position with time. Commonly, velocity is thought of in the horizontal plane and has the components of angular direction and linear speed. However, sometimes "velocity" is used when "speed" is actually more appropriate.

**Volume or Volume Scan:** The volume of space scanned by continuously rotating the radar in azimuth and incrementing or decrementing the elevation about once per rotation, so that a three-dimensional space is sampled. Also, the data resulting from one such scan.

**Waterfowl:** Ducks, geese, and swans. Sometimes large wading birds, pelicans, cormorants, and



similar birds are included when "waterfowl" is used.

**Wave Length:** The distance between crests of the wave-like electromagnetic energy emitted by microwave radars. Radar wave lengths range from millimeters to a few tens of centimeters.

Wave length is the inverse of frequency.

**Wind direction:** The direction of the wind, relative to the ground, at a certain time and height.

Meteorologists always measure the direction from which the wind is blowing, whereas in work with flying birds it is often more natural to specify the direction toward which the wind is blowing (to compare with the direction toward which the animal is flying). It is best to specify the reference for wind direction each time.

**Wind profile:** A plot of wind direction and speed as it differs with altitude.

**Wind speed:** The speed of the wind, relative to the ground, at a certain time and height.

**Wing beat signature:** A record of echo amplitude (or one of its derivatives) as a function of time, showing rapid changes in radar cross section due to changes in the shape and aspect of the bird(s) during flight. Although often used, the term is misleading for two reasons. First, not only the wings, but also tilting of the body, rhythmic changes in the conformation of the chest musculature, and other effects undoubtedly contribute to the observed "signature"--for small birds illuminated at S-band or L-band, the wings themselves may not even be very important. Second, the term was coined to parallel aircraft "target signatures", which are used by military radars to identify specific models of aircraft from their radar echoes. However identification of bird species from radar echoes is rarely achieved, at least in situations with a long list of possible species that could generate radar echoes.

**WORM:** Write Once, Read Many. A voluminous computer storage medium on which each block of data may be written only once. As long-term storage devices rotating optical WORMs are losing ground to new tape and other devices.

**Wraparound (Doppler):** See Aliasing.

**WSR-88**: See NEXRAD. The "88" refers to its year of official birth, 1988, and the "D" to the fact that it is a Doppler radar.

**ZDR**: Characterizes the "horizontalness" or "verticalness" of a target. ZDR is measured by transmitting a horizontally-polarized radar pulse at a target, then transmitting a vertically-polarized pulse at the target, and finally subtracting the echoes resulting from the two pulses. This differential reflectivity will be positive for targets that reflect more horizontal than vertical energy.

## Appendix II. English and scientific names

American Crow	<i>Corvus brachyrhynchos</i>
American Robin	<i>Turdus migratorius</i>
Brewer's blackbird*	<i>Euphagus cyanocephalus</i>
Brown-headed Cowbird*	<i>Molothrus ater</i>
Canada Goose	<i>Branta canadensis</i>
Common Grackle*	<i>Quiscalus quiscula</i>
egret	several genera of Ardeidae
European Starling*	<i>Sturnus vulgaris</i>
Great-tailed Grackle	<i>Quiscalus mexicanus</i>
heron	Ardeidae
Red-wing Blackbird*	<i>Agelaius phoeniceus</i>
Rusty Blackbird*	<i>Euphagus carolinus</i>
Snow Goose	<i>Chen caerulescens</i>

---

\* These species, which look similar from a distance and commonly roost together, are often together called "blackbirds". In this document, the quotation marks are retained to denote "blackbirds" in this broad sense.

### Appendix III. The radar equation

The relationship of the echo signal received by the radar to the distance and size of the target are given by the radar equation:

$$\sigma = \frac{(4\pi)^3 \cdot R^4 \cdot P_r}{P_t \cdot G^2 \cdot \lambda^2}$$

Symbol	Units	1989 CHILL value of constants	
$\sigma$	m <sup>2</sup>		Radar cross section at wavelength $\lambda$
R	m		Slant range to target
$P_r$	W		Receiver signal from the echo
$P_t$	W	58.5 dB re 1 W	Radar transmitter power
G	--	42 dB	Antenna gain at wavelength $\lambda$
$\lambda$	m	0.1	Wavelength (S-band)
RC	km, mW	72.58 dB	Radar Constant (Doviak and Zmic 1984)

Decibel calculation of receiver power from weather radar reflectivity is given by:

$$P_r = \text{reflectivity} - \text{RC} - 20 \cdot \log_{10} (R/1000) - 30$$

Appendix IV. Software for emulation of WSR-88D by research radars.

```
      SUBROUTINE EMULATE_NEXRAD (  LENGTH,
*                                AZ,
*                                REF, VEL, SW, SN,
*                                REFGATE, VELGATE, SWGATE,
*                                REFBIN1, REFINBINN,
*                                VELBIN1, VELINBINN,
*                                SWBIN1, SWINBINN,
*                                SNBIN1, SNINBINN,
*                                RNL,
*                                REF_MISSING_DATA, VEL_MISSING_DATA,
*                                SW_MISSING_DATA, SN_MISSING_DATA,
*                                SW_HERE,
*                                SN_HERE,
*                                RADAR_CONST,
*                                FILTERED,
*                                NSIZE,
*                                NREF, NVEL, NSW,
*                                REFOUT, VELOUT, SWOUT,
*                                NEXRAD_STRING,
*                                EM_NEX_VERSION,
*                                T_CN
*                                )
```

```
C +-----
C
C EMULATE_NEXRAD.FOR Outputs new REF, VEL, and SW arrays after NEXRADizing
C
C Program family:   Harness
C For use by:      Public
C Keywords:        NEXRAD,radar
C Author:          Ron Larkin
C
C Complete Description:
|   NEXRADizing is the process of making data from a garden-variety research
| radar look as if they had come from a NEXRAD WSR-88. Thus, we may use
| data from various research radars to emulate data from NEXRAD itself in
| developing bird algorithms.
|
| Functions of this routine:
|   Sets the maximum range to 230 km if it exceeds that in the input data.
|   Applies a primitive notch filter to reduce low-VEL ground return, if
|   the data are now known to be filtered already.
|   Performs the Censor Strong Point Clutter function of the NEXRAD PSP.
|   Converts REF from INGATE m to 1000 m bins (whatever research radar
|   to NEXRAD short pulse).
```

| Converts VEL and SW from INGATE m to 250 m bins.

|

| FORTRAN 77 for VAX/VMS. Ron Larkin, March 1988.

C

C Logicals used:

C none

C

C Files used:

C none

C

C Special Notes:

| Reference:

| Computer program development specification for signal processing program.

| (B5, CPCI Number 02), NEXRAD JSPO Specification Number DV1208261B,

| Part 1 of Two Parts, 29 Feb 1988. See 3.2.1, especially 3.2.1.2 and

| parallel sections on VEL and spectral width.

| This file contains EMULATE\_NEXRAD per se and several captive routines

| thereof. Presently, EMULATE\_NEXRAD is called only by XLT\_NXRD\_UFRAY

| in CAT\_COPY.

|

|-----

|

| Restrictions:

| Gate spacing (m):

| NEXRAD REF 1000 m

| " VEL 250 m

| " SW 250 M

| Assumes we are working entirely in Short Pulse, not Long Pulse

| On output, data start at bin 1; the flexibility afforded by BIN1

| will have been lost.

| In the CALL statement to this routine, output arrays are

| allowed to be the same arrays as the input arrays. Because we

| use internal scratch arrays anyway, this is not a problem but

| will wreak havoc if the internal structure of this program is

| changed.

| Treats only REF, VEL, and (if available) SW. Other fields such as

| ZDR and P3 are left with their INGATE gate spacing;

| the various gate spacings are handled correctly down the line anyway.

| New dBZ to dBM code tested only on CHILL data so far (10 May 90).

| See further restrictions on the notch filter in NOTCH\_FILTER subroutine.

| Note that Dale Sirmans mentioned that Strong Point Censor may be switched off

| when operating the WSR-88.

|-----

|

C Modification History:

C Date Person Version Modification

C

-----

- \* 28 Sep 88 R.L. Add SW\_HERE argument & functionality.
- \* 30 Nov 88 R.L. Add notch filtering, clutter map.
- \* 10 Apr 89 D.M. Revise to new NEXRAD spec DV1208261B
- \* 27 Jun 89 D.M. Add signal/noise array for Huntsville data
- \* May 90 RL Add arguments for SN, SN\_HERE, SN\_MISSING\_DATA,  
 SNBIN1, SNINBINN and FILTERED, activate SN logic,  
 rearrange arguments.
- \* Oct-Nov 90 R.L. Finish May 90 modifications, taking advantage of  
 revised XLT\_READ\_DFLT5 & omnipresent Radar Constant.
- \* 10 Dec 90 RL 2 Added 2 arguments to report 'NEXRAD' and  
 EMULATE\_NEXRAD version.
- \* 8 Jan 91 RL 2 Added check to make sure radar constant is reasonable.
- \* 30 Jan 91 RL 2 Corrected SIGMA in NOTCH\_FILTER; was 0.2 now 1.5.
- \* 31 Jan 91 RL 3 Upped SIGMA to 3.0 after trying 17 May 85 0331 MIT data  
 Then moved SIGMA out to a lookup file.
- \* 3 Feb 91 RL 4 Moved MAX\_NOTCH\_DEPTH out to the lookup file; had been  
 a constant=60 dB.

C - - - - -

IMPLICIT NONE

C+

! Input arguments:

INTEGER	LENGTH	! Size of input arrays
REAL	AZ	! Azimuth in deg, as in BABEL_COMMON
REAL	REF(LENGTH)	! Reflectivity, dBm
REAL	VEL(LENGTH)	! Velocity m/s
REAL	SW(LENGTH)	! Spectral width, m/s
REAL	SN(LENGTH)	! Signal/noise for each gate in dB (to ! check this I used XLT_UFEXAM on ! Huntsville tape).
REAL	REFGATE	! REF gate spacing (m) (assume SN same)
REAL	VELGATE	! VEL gate spacing (m)
REAL	SWGATE	! Width gate spacing (m)
INTEGER	REFBIN1	! Bin where valid REF data start
INTEGER	REFINBINN	! Last bin having valid REF data
INTEGER	VELBIN1	! Bin where valid VEL data start
INTEGER	VELINBINN	! Last bin having valid VEL data
INTEGER	SWBIN1	! Bin where valid SW data start
INTEGER	SWINBINN	! Last bin having valid SW data
INTEGER	SNBIN1	! Bin where valid SN data start
INTEGER	SNINBINN	! Last bin having valid SN data
REAL	RNL	! Receiver noise level, in dBm ! If array SN is missing (i.e. if ! SN_HERE=.FALSE.), is used to fill ! the array
REAL	REF_MISSING_DATA	! Value to use for ref missing data
REAL	VEL_MISSING_DATA	! Value to use for vel missing data

REAL	SW_MISSING_DATA	! Value to use for sw missing data
REAL	SN_MISSING_DATA	! Value to use for sn missing data
LOGICAL	SW_HERE	! T if spectral width is available.
LOGICAL	SN_HERE	! T if SN array is available
REAL	RADAR_CONST	! Radar constant
LOGICAL	FILTERED	! T if data already filtered so that ! the NEXRAD notch filter is not ! required to be emulated.
INTEGER	NSIZE	! Size of VEL & SW output arrays. ! Should be (230*1000)/250 for ! VEL & SW, I think.

! Output arguments:

INTEGER	NREF	! No. of last NEXRAD bin in REF
INTEGER	NVEL	! No. of last NEXRAD bin in VEL
INTEGER	NSW	! No. of last NEXRAD bin in SW
REAL	REFOUT(NSIZE)	! Output array of REF ! Can cut size to (NSIZE/4) only ! after BABEL modifies its ! pointers. See Restrictions.
REAL	VELOUT(NSIZE)	! Output array of VEL ! It's legal for these to be the ! same as the input arrays, if ! they are long enough.
REAL	SWOUT(NSIZE)	! Output array of SW
CHARACTER*(*)	NEXRAD_STRING	! 'NEXRAD' or blank
INTEGER	EM_NEX_VERSION	! Version no. of this subroutine
REAL	T_CN	! Threshold for censoring REF, in dB ! A guess: T_CN=30 dB (14 Mar ! 88). Set it to 0 to switch off ! strong point clutter censoring.

C -

! Local storage:

LOGICAL	FIRST_CALL	! T if once-only code should execute
DATA FIRST_CALL /.TRUE./		
SAVE FIRST_CALL		
LOGICAL	POINT	! Function returns T if a point target
CHARACTER*80	B	! Buffer for ASCII input
CHARACTER*(*)	PARAMETER_FILE	! File where filter and other control ! parameters are kept.
PARAMETER (PARAMETER_FILE='[LOOKUP.TRANSLATE_RDR]EMULATE_NEXRAD.DAT')		
CHARACTER	ROUTIN*(*)	! Name of this routine
PARAMETER (ROUTIN='EMULATE_NEXRAD')		
INTEGER	DEV	! Device for reading parameters
INTEGER	I	! Index



```

INTEGER          J          ! DO loop index.
INTEGER          k_em_nex_version ! Version of this subroutine
PARAMETER (k_em_nex_version=4)    ! Up this after significant mods.
INTEGER          LOGICAL_UNIT ! Returns next avail L.U.N.
INTEGER          N          ! DO loop index.
INTEGER          NSN        ! Last valid element in array SNA
INTEGER          NUSED      ! N used in computation of km REf
INTEGER          OUTSIZE    ! Computes size of output array
INTEGER          REFBINN    ! Last bin having valid data
INTEGER          SNBINN     ! SNINBINN after MAXKM call
INTEGER          SWBINN     ! SWINBINN after MAXKM call
INTEGER          WORKN      ! Max size of working arrays
PARAMETER (WORKN=1025)      ! Max we expect from a research radar
INTEGER          VELBINN    ! VELINBINN after MAXKM call

REAL            CSPA(WORKN) ! Censored Surveillance Power Array
REAL            DB          ! Function to do 10*log(x)
REAL            GATE        ! INGATE for internal use
REAL            MAXKM        ! Function computes max. NEXRAD range
REAL            MAXNEXKM     ! Max. range used (km),
PARAMETER (MAXNEXKM=230.0) ! see Restrictions, in comments
REAL            MAX_NOTCH_DEPTH ! Read from parameter file, used in
                                ! NOTCH_FILTER, q.v. Must be +.
REAL            MW          ! Function converts dBm to mW
EXTERNAL        MW
REAL            NGATE       ! Gate spacing (m) for NEXRAD:
PARAMETER (NGATE=250.0)    ! see Restrictions, below
REAL            NOISE(1025) ! Noise level in dBm
                                ! (dimension is arbitrarily large)
INTEGER          PCDET(0:WORKN) ! Point clutter detection array
DATA PCDET(0),PCDET(WORKN) /2*0/
REAL            REF_MAXKM    ! Range of last gate (km)
REAL            RNLMW_FIXED ! Receiver noise level in mW
                                ! Calculated only if .NOT. SN_HERE.
REAL            SIGMA        ! For NOTCH_FILTER. q.v. and also
                                ! [LOOKUP.TRANSLATE_RDR]*.DAT
REAL            SN_MAXKM     ! Range of last gate in SN (km)
REAL            RNL_MW(WORKN) ! Radar noise level in mW
REAL            SPSA(WORKN)  ! Surveillance Power Sum Array
REAL            SWA(WORKN)   ! SW in NEXRAD bins
REAL            SW_MAXKM     ! Range of last gate (km)
REAL            TRATIO       ! T_CN expressed as a ratio
REAL            UNITY        ! Null function; returns argument
EXTERNAL        UNITY
REAL            VELA(WORKN)  ! Velocity in NEXRAD bins
REAL            VEL_MAXKM    ! Range of last gate (km)

```

```

IF (FIRST_CALL) THEN
  DEV = LOGICAL_UNIT(DEV)
  OPEN (unit=DEV, status='OLD', readonly,
&      file=PARAMETER_FILE)
  CALL NEXT_LINE (B, DEV)
  READ (B,'(F)')      SIGMA
  IF (SIGMA .LT. 0.0) THEN
    CALL CRASH (ROUTIN,'SIGMA is negative',PARAMETER_FILE)
  ELSE IF (SIGMA .EQ. 0.0) THEN
    TYPE *, 'SIGMA is 0 in ', PARAMETER_FILE
  END IF
  CALL NEXT_LINE (B, DEV)
  READ (B,'(F)')      T_CN
  IF (T_CN .LT. 0.0) THEN
    CALL CRASH (ROUTIN,'T_CN is negative',PARAMETER_FILE)
  END IF
  CALL NEXT_LINE (B, DEV)
  READ (B,'(F)')      MAX_NOTCH_DEPTH
  IF (MAX_NOTCH_DEPTH.LT.0.0) THEN
    CALL CRASH (ROUTIN,'MAX_NOTCH_DEPTH is negative',PARAMETER_FILE)
  END IF
  CLOSE (unit=DEV)
  FIRST_CALL = .FALSE.
END IF

```

! Check radar constant for reasonableness

```

IF (RADAR_CONST.LT.40.0 .OR. RADAR_CONST.GT.120.0) THEN
  CALL RCRASH (ROUTIN,'Radar constant unreasonable',RADAR_CONST)
END IF

```

! Check gate spacings of input arrays to be sure they are reasonable.

```

CALL CHECK_GATE (REFGATE, 'REFGATE', ROUTIN)
CALL CHECK_GATE (VELGATE, 'VELGATE', ROUTIN)
IF (SW_HERE) THEN
  CALL CHECK_GATE (SWGATE, 'SWGATE', ROUTIN)
END IF

```

! (SN is assumed to have the same gate spacing as REF.)

! Compute the max extent in distance of each array. Also computes the

! BINN (last filled bin on output) for each array, making sure it is

! not over the max extent.

```

REF_MAXKM = MAXKM (REFBIN1, REFINBINN, REFBINN, REFGATE, MAXNEXKM)
VEL_MAXKM = MAXKM (VELBIN1, VELINBINN, VELBINN, VELGATE, MAXNEXKM)
IF (SW_HERE) THEN
  SW_MAXKM = MAXKM (SWBIN1, SWINBINN, SWBINN, SWGATE, MAXNEXKM)
END IF

```

```

IF (SN_HERE) THEN
  SN_MAXKM = MAXKM (SNBIN1, SNINBINN, SNBINN, REFGATE, MAXNEXKM)
ELSE
  SN_MAXKM = REF_MAXKM
END IF

```

```

! Compute the size of the 3 output arrays. Note that NREF may change
! later in conversion to NEXRAD because present spec is 1 km in RA.
NREF = OUTSIZE (REF_MAXKM, NGATE, NSIZE, 'REF', ROUTIN)
NVEL = OUTSIZE (VEL_MAXKM, NGATE, NSIZE, 'VEL', ROUTIN)
IF (SW_HERE) THEN
  NSW = OUTSIZE (SW_MAXKM, NGATE, NSIZE, 'SW', ROUTIN)
END IF
IF (SN_HERE) THEN
  ! Compute the size of the RNL_MW array.
  NSN = OUTSIZE (SN_MAXKM, NGATE, NSIZE, 'SN', ROUTIN)
ELSE
  NSN = NREF
END IF

```

! Convert:

```

! REF to milliwatts at 250 m gate spacing,
! VEL to 250 m gate spacing,
! SW to 250 m gate spacing,
! SN to mW at 250 m gate spacing, if SN is present.
CALL SPACE_GATES (REFGATE, NGATE, REFBIN1, REFBINN,
  * NREF, WORKN, REF, SPSA, MW, REF_MISSING_DATA)
CALL SPACE_GATES (VELGATE, NGATE, VELBIN1, VELBINN,
  * NVEL, WORKN, VEL, VELA, UNITY, VEL_MISSING_DATA)
IF (SW_HERE) THEN
  CALL SPACE_GATES (SWGATE, NGATE, SWBIN1, SWBINN,
  * NSW, WORKN, SW, SWA, UNITY, SW_MISSING_DATA)
END IF
IF (SN_HERE) THEN
  ! Convert signal/noise ratio to noise itself in dB
  DO J = SNBIN1, SNINBINN
    NOISE(J) = REF(J) - SN(J)
  END DO
  ! Now re-bin if needed and convert noise level to milliwatts
  CALL SPACE_GATES (REFGATE, NGATE, SNBIN1, SNBINN,
  * NSN, WORKN, NOISE, RNL_MW, MW, SN_MISSING_DATA)
ELSE
  ! Use a constant S/N ratio
  IF (RNL.EQ.REF_MISSING_DATA) THEN
    CALL RCRASH(ROUTIN, 'RNL=missing-data yet no s/n data either', RNL)
  END IF
  RNLMW_FIXED = MW(RNL)

```

```

DO J = 1,NSN
  RNL_MW(J) = RNLMW_FIXED
END DO
END IF

```

```

IF (.NOT. FILTERED) THEN
  ! Apply a primitive notch filter to decrease low-VEL clutter targets
  CALL NOTCH_FILTER (REF_MISSING_DATA, VEL_MISSING_DATA, SIGMA,
    MAX_NOTCH_DEPTH, AZ, WORKN, NREF, SPSA, NVEL, VELA )
END IF

```

```

! Zero array PCDET
DO N = 1,NREF
  PCDET(N) = 0
END DO

```

```

IF (T_CN .GT. 0) THEN

```

```

  ! Censor strong point clutter.

```

```

  ! Convert T_CN to a ratio.
  TRATIO = MW(T_CN)

```

```

  ! Set a 1 in each element of PCDET for which REF sticks up above REF
  ! on either side by T_CN dB.

```

```

DO N = 3,NREF-2
  IF (POINT(SPSA,
2      N,
3      N-2,
4      TRATIO,
5      RNL_MW(N-2),
6      REF_MISSING_DATA)) THEN
    IF (POINT(SPSA,
2      N,
3      N+2,
4      TRATIO,
5      RNL_MW(N+2),
6      REF_MISSING_DATA)) THEN
      PCDET(N) = 1
    END IF
  END IF
END IF
END DO

```

```

  ! Compute P(N) (for short-pulse mode), using PCDET array
  CALL CENSOR (WORKN, PCDET, NREF, SPSA, CSPA, REF_MISSING_DATA)
  CALL CENSOR (WORKN, PCDET, NREF, VELA, VELOUT, VEL_MISSING_DATA)
  IF (SW_HERE) THEN

```

```

        CALL CENSOR (WORKN, PCDET, NREF, SWA, SWOUT, SW_MISSING_DATA)
    END IF

ELSE

    ! Merely copy the arrays.
    DO J = 1,NREF
        CSPA(J) = SPSA(J)
        VELOUT(J) = VELA(J)
        SWOUT(J) = SWA(J)
    END DO

END IF

! Compute REF output array by combining into 1 km bins, a 4-to-1 compression
I = 1
DO J = 1,NREF,4
    REFOUT(I) = 0
    NUSED = 0
    DO N = J, MIN(J+3,NREF)
        IF (CSPA(N).NE.REF_MISSING_DATA) THEN
            NUSED = NUSED + 1
            REFOUT(I) = REFOUT(I) + CSPA(N)
        END IF
    END DO
    IF (NUSED.GT.0) THEN
        REFOUT(I) = REFOUT(I) / FLOAT(NUSED)
    ELSE
        REFOUT(I) = REF_MISSING_DATA
    END IF
    I = I + 1
END DO
NREF = I-1

! Convert ref back to dBm, unless a bin is missing data.
DO N = 1,NREF
    IF (REFOUT(N).NE.REF_MISSING_DATA) THEN
        IF (REFOUT(N).EQ.0) THEN
            IF (SN_HERE) THEN
                REFOUT(N) = DB(RNL_MW(N))
            ELSE
                REFOUT(N) = RNL          ! We expect never to reach here
            END IF
        ELSE
            REFOUT(N) = DB(ABS(REFOUT(N))) * SIGN(1.0,REFOUT(N))
        END IF
    END IF
END IF

```

END DO

NEXRAD\_STRING = 'NEXRAD'    ! Signals conversion complete  
EM\_NEX\_VERSION = k\_em\_nex\_version    ! Local version number returned.

RETURN  
END ! Of EMULATE\_NEXRAD subroutine

.....

SUBROUTINE CENSOR (WORKN, PCDET, NREF, A, B, MISSING\_DATA )

! Censor strong point targets as described in the above reference.  
! Note that we skip elements 1,2, and (1 and 2 from the end). Later,  
! because they are zero, these elements will be filled with the radar noise  
! level. I asked O.S.F. about this and nobody could tell me what the  
! firmware does with these bins on the end.

IMPLICIT NONE

! Input arguments:

INTEGER	WORKN	! For dimensioning PCDET
INTEGER	PCDET(0:WORKN)	! 0 if ok, 1 if point-target
INTEGER	NREF	! Last valid data in A & B
REAL	A(NREF)	! Input array
REAL	B(NREF)	! Output array
REAL	MISSING_DATA	! Signals no-data-here

! Local storage:

INTEGER	CGOTO	! For computed go-to
INTEGER	N	! Loop index

! Check NREF first for sufficient size.

IF (NREF.LE.5) THEN  
  TYPE \*, 'NREF = ', NREF, ' WORKN=', WORKN  
  STOP 'NREF too small in subr. CENSOR'  
END IF

DO N = 3,NREF-3

  CGOTO = PCDET(N-1)\*4 + PCDET(N)\*2 + PCDET(N+1) + 1  
  GO TO (7,1,2,3,4,5,6,7), CGOTO  
  PAUSE 'CGOTO out of bounds'

1        B(N) = A(N-1)  
      GO TO 10

2        IF (A(N-2).EQ.MISSING\_DATA) THEN  
          B(N) = A(N+2)

```

        ELSE IF (A(N+2).EQ.MISSING_DATA) THEN
            B(N) = A(N-2)
        ELSE
            B(N) = 0.5*A(N-2) + 0.5*A(N+2)
        END IF
        GO TO 10

3      IF (A(N-2).EQ.MISSING_DATA) THEN
            B(N) = A(N+3)
        ELSE IF (A(N+3).EQ.MISSING_DATA) THEN
            B(N) = A(N-2)
        ELSE
            B(N) = 0.5*A(N-2) + 0.5*A(N+3)
        END IF
        GO TO 10

4      B(N) = A(N+1)
        GO TO 10

5      B(N) = A(N)
        GO TO 10

6      IF (A(N-3).EQ.MISSING_DATA) THEN
            B(N) = A(N+2)
        ELSE IF (A(N+2).EQ.MISSING_DATA) THEN
            B(N) = A(N-3)
        ELSE
            B(N) = 0.5*A(N-3) + 0.5*A(N+2)
        END IF
        GO TO 10

7      B(N) = A(N)

10     CONTINUE
        END DO

```

RETURN

END ! of subroutine CENSOR

.....

SUBROUTINE CHECK\_GATE (GATE, VARIABLE, ROUTIN)

! Check gate-spacing for reasonableness.

IMPLICIT NONE

REAL            GATE            ! Gate spacing in meters

```

CHARACTER*(*)    VARIABLE    ! Name of this variable GATE
CHARACTER*(*)    ROUTIN      ! Name of the calling routine

```

```

IF (GATE.LT.10.0 .OR. GATE.GT.1500.0) THEN
  TYPE *, VARIABLE, ' restricted to 10-1500 m in ', ROUTIN, GATE
  STOP 'Fatal error'
END IF
RETURN
END ! of subroutine CHECK_GATE

```

```

*****
REAL FUNCTION MAXKM (BIN1, INBINN, BINN, GATE, MAXNEXKM)

```

```

! Compute how far an array extends in range.

```

```

IMPLICIT NONE

```

```

! Input arguments:

```

```

INTEGER          BIN1          ! Bin where valid data start
INTEGER          INBINN        ! Last bin having valid data
REAL             GATE          ! Gate spacing (m)
REAL             MAXNEXKM      ! Max. range used (km)

```

```

! Output arguments:

```

```

INTEGER          BINN          ! Output last bin

```

```

MAXKM = (INBINN-BIN1+1) * GATE / 1000.0

```

```

! Check for (unlikely) RA>230 km

```

```

IF (MAXKM.GT. MAXNEXKM) THEN
  TYPE *, 'Truncating range at ', MAXNEXKM, ' km'
  BINN = BIN1 + ((MAXNEXKM*1000.0) / GATE) -1
  MAXKM = MAXNEXKM
ELSE
  BINN = INBINN
END IF

```

```

RETURN
END ! of function MAXKM

```

```

*****
REAL FUNCTION MW (X)

```

```

! Convert dBm to milliwatts. Also converts any value in dB to a ratio, of
! course.

```

```

IMPLICIT NONE

```



REAL            X            ! A dBm value

MW = 10.0\*\*(X/10.0)

RETURN

END ! of Function MW

.....  
..

SUBROUTINE NOTCH\_FILTER (REF\_MISSING\_DATA, VEL\_MISSING\_DATA, SIGMA,  
MAX\_NOTCH\_DEPTH, AZ, N, NREF, REF, NVEL, VEL )

! If first call, construct a notch filter to emulate the NEXRAD filter that  
! removes low velocity targets within the region of ground clutter typical  
! for this date. If a clutter map file exists, apply the filter to a  
! radial of data.  
! Ron Larkin, Nov. 1988. FORTRAN 77 for VAX.

! References:

! NEXRAD JSPO. 1984. NEXRAD Technical Requirements (NTR).  
! NEXRAD JSPO. 1986a. Critical Item Development Specification for receiver/  
! signal processor. Specification number DVI1208254D, 21 April 1986.  
! NEXRAD JSPO. 1986b. Computer Program Development Specification for signal  
! processing program. Sepcification number DVI1208261B, 25 May 1986.  
! Sirmans, D. 1987. NEXRAD suppression of land clutter echo due to anomalous  
! microwave propagation - Part I. Prepared for JSPO, revised April 1988.

! Restrictions:

! -- It doesn't check to see if CHILL (for instance) has already decluttered  
! the image. At this time (30 Nov 88) Dave Brunkow is planning to  
! install a clutter filter in the SP-20 processor; data collected some-  
! time in the near future should have one or more header fields to  
! show whether a clutter-filter has been applied at the CHILL.  
! -- The clutter map as currently implemented is simple, merely operating  
! out to a certain range and then stopping.  
! -- No Clutter Filter 2 (a reflectivity filter, JSPO 1986a 3.1.2.3 ), is  
! implemented yet. Only Clutter Filter 1 is implemented now.  
! -- A file assigned to logical symbol CLUTTER\_MAP determines which ray  
! file is used for removing ground clutter. If no file is assigned to  
! this file OR IF THE PROGRAM CANNOT READ THIS FILE FOR ANY REASON,  
! no clutter filtering is performed.  
! -- Uses a crude filter, not a full 5-pole elliptical one. See  
! comments near Statement Function FILT\_DB below.  
! -- 28-jun-89 dm CHANGED SIGMA FROM 2.0 TO 0.2  
! -- 30 Jan 91 RL Changed SIGMA back from 0.2 to 2.0, damnit. Thence to 1.5.

! -- 11 Jun 92 RL Now reports CLUTTER\_MAP logical & permits defining it w/ PAUSE

IMPLICIT NONE

! Arguments

REAL	REF_MISSING_DATA	! Input. Value to use for missing data
REAL	VEL_MISSING_DATA	! Input. Value to use for missing data
REAL	SIGMA	! Notch half-width in m/s (here equals ! an s.d.)
REAL	MAX_NOTCH_DEPTH	! Input. Max depth of notch filter in ! dB, a positive value. 60 dB was ! insufficient for 17 May 85 MIT data.
REAL	AZ	! Input. AZ in degrees cf. BABEL_COMMON
INTEGER	N	! Input. Length of array arguments
INTEGER	NREF	! Input. No. of filled elements
INTEGER	NVEL	! in REF and VEL arrays.
REAL	REF(N)	! I/O. Reflectivity along 1 radial ! in mW. Assumed to be in ! 250 m bins with range=0 ! at Bin 1.
REAL	VEL(N)	! I/O. Velocity along 1 radial ! in m/s, spaced like REF.

! Local storage

CHARACTER*50	CLUTTER_FILE	! Translation of CLUTTER_MAP
CHARACTER*(*)	ROUTIN	! Name of this routine
PARAMETER (ROUTIN='NOTCH_FILTER')		
CHARACTER*50	TRANSLATE_LOGICAL	! Function returns result of DEFINE
LOGICAL	FIRST_CALL	! T the 1st time this routine is called
DATA FIRST_CALL/.TRUE./		
SAVE FIRST_CALL		
LOGICAL	MAP_EXISTS	! T if a clutter map file was found.
INTEGER	MAX_VEL	! Max velocity in (m/s)*10
PARAMETER (MAX_VEL=500)		
INTEGER	BIGGEST_J	! As far as we need to go out a radial
INTEGER	DEV	! Device for reading the clutter map
INTEGER	I	! Argument to statement function
INTEGER	INDEX	! Pointer into velocity lookup table
INTEGER	J	! DO loop index
INTEGER	JAZ	! Integer azimuth, bounded to be sure ! it'll point into KM_LIST array.
INTEGER	LOGICAL_UNIT	! Function returns next avail. L.U.N.
INTEGER	LASTBIN(0:359)	! Last bin where ground clutter occurs
INTEGER	MINUS_BLANKS	! Function returns col. of last nonblank
INTEGER	NUM_AZS	! Number of azimuths in clutter file
INTEGER	POTENTIAL_KM	! Outer edge of clutter file patch in km
REAL	FILT_DB	! Statement function to perform filtering

```

REAL      MW           ! Function converts dB to a ratio
REAL      SCALE_FACTOR ! Scales filter so 0 m/s is -60 dB
REAL      TERM1        ! First term in filter function
REAL      VLOOK(0:MAX_VEL) ! Lookup table for velocities; here is
                           ! where the filter function lives.

```

```

! Function to perform the filtering operation. Given a velocity
! in (m/s)*10, it returns a decibel value by which to reduce a signal.
! Note that the NEXRAD NTR specifies a 5-pole elliptical filter. However,
! we still (Nov 1988) don't have an up-to-date copy of the JSPO 1986a document
! and therefore the exact specs for the filter and its notch width are up
! in the air. So we use a simpler filter that will serve for now, a literal
! Gaussian function with mean=0 m/s and s.d.=SIGMA.
! TERM1 is computed in-line, below.

```

```

      FILT_DB(I) = TERM1 * EXP(-0.5*((REAL(I)/10.0)/SIGMA)**2 )

```

```

IF (FIRST_CALL) THEN

```

```

  CLUTTER_FILE = TRANSLATE_LOGICAL('CLUTTER_MAP')

```

```

  J = MINUS_BLANKS(CLUTTER_FILE)

```

```

  IF (J.EQ. 0) THEN

```

```

    TYPE *, 'CLUTTER_MAP is undefined.'

```

```

    TYPE *, 'If you leave it undefined, filtering will be skipped'

```

```

    PAUSE 'Define it if you like, then type CONTINUE'

```

```

  ELSE

```

```

    TYPE *, ' CLUTTER_MAP is assigned to: ', CLUTTER_FILE(1:J)

```

```

  END IF

```

```

  ! Attempt to open a file describing the ground clutter

```

```

  DEV = LOGICAL_UNIT(DEV)

```

```

  OPEN (unit=DEV, file='CLUTTER_MAP', readonly, status='OLD',
    *      ERR=800)

```

```

  MAP_EXISTS = .TRUE.

```

```

  GO TO 801

```

```

800  MAP_EXISTS = .FALSE.

```

```

  TYPE *, ' Clutter map file not found, or protection wrong.'

```

```

  TYPE *, ' No clutter filtering will be performed.'

```

```

801  CONTINUE

```

```

  IF (MAP_EXISTS) THEN

```

```

    ! Read that clutter filter from DIR$PATCH:

```

```

    ! READ_RAY_FILE could be used here except it carries too much
    ! baggage in the form of INCLUDE files & calls.

```

```

    READ (DEV,'(I6)') NUM_AZS

```

```

    IF (NUM_AZS.LE.0 .OR. NUM_AZS.GT.360) THEN

```

```

      CALL ICRASH (ROUTIN,'Number of azimuths bad',NUM_AZS)

```

```

    END IF

```

```

    DO J = 1,NUM_AZS

```

```

      READ (DEV,'(I4,4X,I4)') JAZ, POTENTIAL_KM

```

```

        IF (JAZ.LT.0.OR.JAZ.GT.359) THEN
            CALL ICRASH (ROUTIN,'Bad azimuth',JAZ)
        END IF
        LASTBIN(JAZ) = (POTENTIAL_KM-1) * 4
    ENDDO
    CLOSE (unit=DEV)

    IF (SIGMA .GT. 0.0) THEN
        ! Construct 1st term for filter function above.
        TERM1 = 1.0 / (SIGMA*SQRT(2.0*3.1416))
        ! Scale the filter so VEL=0 is cut by -60 dB
        SCALE_FACTOR = -MAX_NOTCH_DEPTH / FILT_DB(0)
        DO J = 0,MAX_VEL
            VLOOK(J) = MW(FILT_DB(J)*SCALE_FACTOR)
        END DO
    ELSE
        ! No notch filtering.
        DO J = 0,MAX_VEL
            VLOOK(J) = 1
        END DO
    END IF
END IF
FIRST_CALL = .FALSE.
END IF

```

```

IF (MAP_EXISTS) THEN
    JAZ = MIN(359,MAX(0,NINT(AZ)))
    J = 1
    BIGGEST_J = MIN(NVEL, LASTBIN(JAZ))
    DO WHILE (J .LE. BIGGEST_J)
        IF (VEL(J).NE.VEL_MISSING_DATA .AND.
-         REF(J).NE.REF_MISSING_DATA)
-         THEN
            ! Construct a pointer into the VEL lookup table
            INDEX = MIN(MAX_VEL,ABS(NINT(VEL(J)*10.0)))
            ! Attenuate REF by this filter value
            REF(J) = REF(J) * VLOOK(INDEX)
        END IF
        J = J + 1
    END DO
END IF

```

```

RETURN
END ! of subroutine NOTCH_FILTER

```

\*\*\*\*\*

```

INTEGER FUNCTION OUTSIZE (MAXK, GATE, SIZE, NAME, ROUTIN)

```

! Compute the size of an output array.

IMPLICIT NONE

! Input arguments:

REAL	MAXK	! Max range in km
REAL	GATE	! Gate spacing for this parameter
INTEGER	SIZE	! How big OUTSIZE may become
CHARACTER(*)	NAME	! Name of this field
CHARACTER(*)	ROUTIN	! Name of the calling routine

! Local storage:

INTEGER	NTEMP	! Holds result for checking
---------	-------	-----------------------------

NTEMP = MAXK \* (1000.0/GATE)

IF (NTEMP.GT.SIZE) THEN

TYPE \*, 'Computed size (', NTEMP,') > array size (', SIZE

\*, '), in ', NAME, 'called by ', ROUTIN

TYPE \*, 'Gate depth argument=', GATE, ' m.'

TYPE \*, 'Max range=', MAXK, ' km.'

STOP 'Fatal error'

ELSE

OUTSIZE = NTEMP

END IF

RETURN

END ! of function OUTSIZE

.....

LOGICAL FUNCTION POINT (A, N1, N2, TRATIO, RNLMW, MISSING\_DATA)

! Returns true if N1 is a point target

! Input arguments:

REAL	A (*)	! Array of data
INTEGER	N1	! Index of numerator of the comparison
INTEGER	N2	! Index of denom. of the comparison
REAL	TRATIO	! Min amplitude of a point that ! will be suppressed
REAL	RNLMW	! Receiver noise level in mW
REAL	MISSING_DATA	! Signals no-data-here

! Local storage

REAL	V1	! Numerator of the comparison
------	----	-------------------------------

REAL	V2	! Denom. of the comparison
------	----	----------------------------

V1 = A(N1)

```

IF (V1.EQ.MISSING_DATA) THEN
  POINT = .FALSE.
ELSE
  IF (A(N2).EQ.MISSING_DATA .OR. A(N2).EQ.0) THEN
    V2 = RNLMW
  ELSE
    V2 = A(N2)
  ENDIF
  POINT = V1/V2 .GT. TRATIO
END IF

```

```

RETURN
END ! of function POINT
.....

```

#### SUBROUTINE SPACE\_GATES

```

* (RGATE, NGATE, BIN1, BINN, N, BN, A, B, F, MISSING_DATA )

```

! Array A is a radial from a research radar, gate spacing RGATE within  
! the bounds checked by CHECK\_GATE. Move it into array B at the NEXRAD  
! gate spacing, NGATE, which can be less, the same, or greater than RGATE.  
! The assumptions about the input data made by this routine are several and  
! should really be spelled out in comments.

IMPLICIT NONE

! Input arguments:

REAL	RGATE	! Gate spacing for research radar, m.
REAL	NGATE	! Gate spacing for NEXRAD radar, m.
INTEGER	BIN1	! 1st valid element of A
INTEGER	BINN	! Last valid element of A
INTEGER	N	! Last valid element of array B
INTEGER	BN	! Length of array B
REAL	A (*)	! Input array from research radar
REAL	F	! Passed function name
REAL	MISSING_DATA	! Bad-data flag

! Output arguments:

REAL	B(BN)	! Output array, NEXRAD spacing
------	-------	--------------------------------

! Local storage:

INTEGER	COUNT(2000)	! Number of research bins in each ! NEXRAD bin.
INTEGER	ENDLOOP	! End-range for Do loop
INTEGER	HOWFAR	! No. bins over which to look for ! data to be duplicated.
INTEGER	I,J	! Loop counters
INTEGER	PREV_GOOD_BIN	! Most recent bin w/ valid data
INTEGER	TOOFAR	! Span for initial missing data

```

PARAMETER (TOOFAR=-100)           ! An absurdly large distance.
REAL      NM                      ! Distance on NEXRAD radar, m.
REAL      RM                      ! Distance on research radar, m.

```

```

! Distribute array A into array B, summing or skipping bins as needed.
! Ignore missing data in Array A. Missing data flags will be recreated
! in array B in a later step.

```

```

IF (RGATE.LT.NGATE) THEN

```

```

    DO J = 1,N                      ! Zero arrays for N's and sums
        COUNT(J) = 0
        B(J) = 0.0
    END DO
    J = 1                          ! Sum
    NM = 0.0
    RM = 0.0
    DO I = BIN1,BINN
        IF (RM.GT.NM) THEN
            NM = NM + NGATE
            J = J + 1
            IF (J.GT.N) THEN
                GO TO 300          ! We have overextended the
                                !   output array.
            END IF
        END IF
        IF (A(I).NE.MISSING_DATA) THEN ! Missing data will be filled
            B(J) = B(J) + F(A(I)) ! in below when averaging.
            COUNT(J) = COUNT(J) + 1
        END IF
        RM = RM + RGATE
    END DO
    DO I = 1,J                      ! Average
        IF (COUNT(J).GT.0) THEN
            B(J) = B(J) / COUNT(J)
        ELSE
            B(J) = MISSING_DATA
        END IF
    END DO

```

```

ELSE IF (RGATE.EQ.NGATE) THEN

```

```

    DO I = BIN1,BINN
        IF (A(I).NE.MISSING_DATA) THEN
            B(I) = F(A(I))
        ELSE
            B(I) = MISSING_DATA
        END IF
    END DO

```

END DO

ELSE !RGATE > NGATE

```
  I = 1
  J = 0
  NM = 0.0
  RM = RGATE
  DO WHILE (I.LE.BINN)
    DO WHILE (NM.LT.RM)
      J = J + 1
      IF (A(I).NE.MISSING_DATA) THEN
        B(J) = F(A(I))
      ELSE
        B(J) = MISSING_DATA
      END IF
      NM = NM + NGATE
    ENDDO
    RM = RM + RGATE
    I = I + 1
  ENDDO
```

END IF

IF (N.GT.0) RETURN ! omitting code below!?

! Perform one of the following depending on gate spacing ratio:  
! (1) Average 1 or more research radar bins together to make 1 NEXRAD bin,  
! if research bins were smaller or the same (e.g. AFGL, CHILL).  
! (2) Carry a research radar bin forward 1 or more bins, if research bins  
! were coarser (e.g. MIT).  
! Where missing data create gaps too large to fill with research radar  
! data, fill with MISSING\_DATA.

```
300  HOWFAR = RGATE/NGATE
      IF (COUNT(1).NE.0) THEN    ! 1st bin is a special case
        B(1) = B(1) / REAL(COUNT(1))
      ELSE
        ENDLOOP = 1 + HOWFAR
        IF (ENDLOOP.GE.2) THEN
          DO J = 2,ENDLOOP    ! Look for a valid element to stick here
            IF (COUNT(J).GT.0) THEN
              B(1) = B(J) / REAL(COUNT(J))
              GO TO 400
            END IF
          ENDDO
```



```

        END IF
        B(1) = MISSING_DATA
400    CONTINUE
    END IF
    IF (B(1).EQ.MISSING_DATA) THEN
        PREV_GOOD_BIN = TOOFAR
    ELSE
        PREV_GOOD_BIN = 1
    END IF

    DO J = 2,N                ! Now do the rest of the bins.
        IF (COUNT(J).GT.0) THEN
            B(J) = B(J) / REAL(COUNT(J))
            PREV_GOOD_BIN = J
        ELSE
            ! This bin is empty; RGATE must exceed NGATE
            IF (J.GE. PREV_GOOD_BIN+HOWFAR) THEN
                B(J) = MISSING_DATA
            ELSE
                B(J) = B(J-1)    ! Replicate previous bin
            END IF
        END IF
    END DO

    RETURN
    END ! of subroutine SPACE_GATES
.....

REAL FUNCTION UNITY (X)

! A null function to complement FUNCTION MW for the other parameters.

IMPLICIT NONE

REAL      X                ! A dBm value

UNITY = X

RETURN
END ! Of function UNITY

```

## Appendix V. Adaptable parameters

The following parameters are associated with their "working values", some of which will need to be adjusted according to changing needs such as experience with additional species of birds, site-specific requirements, and user requirements.

---

### Adaptable Parameters: **Migrating Birds Algorithm**

Mnemonic	Working value	Description
DropThU	3.5 km	Maximum radial or azimuthal distance with signal below RefThL, beyond which a new echo segment is started.
MinRange	3 km	Minimum range used in algorithm
NgateThL	2	Minimum number of gates for an echo segment.
NSegThL	3	Minimum number of echo segments in an echo component.
NTargTypes	5	Number of types of targets to classify.
RefThL	-8 dBZ	Lower threshold for REF of flying animals

---

### Adaptable Parameters: **Roosting Birds Algorithm**

Mnemonic	Working value	Description
AccInit	15	Initial accumulator threshold, used on the first roost, if any, located in a image, then replaced (modified upward or downward) by an adaptive procedure. This parameter influences computational speed but has little influence upon results.
AccThL	1	Lowest permitted value for AccThresh, below which the search for roosts is ended.
Annulus	0.4	A disc ((1+Annulus) X RoostRadius) in radius is cleared around each roost immediately after it is located, so that cells in the disk cannot contribute to subsequent roosts in that volume scan.

BirdFltSpd	20 m/s	Expected speed of a bird in still air, used in determining the angle over which to search for circle centers--the Hubble Constant of the Roosting Birds Algorithm. See Meinertzhagen (1955), Harper (1959).
ChuckRef	0.15	Proportion of reflectivities to discard when estimating total reflectivity of a roost. Discards ChuckRef/2 cells from the top end of the reflectivity distribution and ChuckRef/2 from the bottom end.
FootPrint	4 km	Minimum distance a roost may be from another roost previously found in the current volume scan. Any closer roost is not counted, but the echoes that comprise it cannot contribute to further roosts.
InterRoost	MaxRad	Minimum XY distance between different roosts on successive scans or mornings.
MaxNRoost	4	Maximum number of roosts in one sweep. In fact, the algorithm has not found more than 3 roosts in a sweep in data examined thus far.
MaxRad	20 km	Maximum possible circle radius for birds. In future, it may be profitable to scale MaxRad according to the sizes of known roosts at a site.
MaxRange	160 km	Maximum slant range at which useful data on roost departures may be acquired. This value gets its present value from roosts observed at KOUN in Oklahoma.
MaxWind	10 m/s	Maximum wind speed for algorithm to run. Also determines the range of direction(s) a bird echo with a given VEL could be travelling.
MinCoverage	2%	Coverage in a circle below this value causes the circle not to qualify as a roost and the algorithm to stop processing the current sweep. Coverage is defined as the area of the circle divided by the area of the cells in the circle that qualify as bird echoes.
MinNcirc	40	Minimum total number of circles to search for a roost. The maximum number of circles used by the algorithm is presently hardwired at 4,000.
QuitThL	8 dBZ	Smallest roost-candidate accepted as a roost. Algorithm stops for this scan when TotRef<QuitThL is reached. 8 to 9 dBZ presently appears to be an appropriate value.

ReduceAcc	0.6	Proportion by which AccInit is reduced if too few circles are found.
RefThL	3 dBZ	Lower threshold for reflectivity of a gate
RefThU	60 dBZ	Upper threshold for reflectivity of a gate
RoostLife	8 days	A known roost is dropped if it is not found in this many days.
SumDist	0.25 km	Distance in XY across which radii are summed.
SWThU	7 m/s	Upper limit of spectral width for roosting birds
VelThL	5 m/s	Lower threshold for velocity of a gate
VelThU	28 m/s	Upper threshold for velocity of a gate in calm air. May exceed the Nyquist velocity after wind-unwrapping of Doppler velocity.
WindAdj	7 m/s	Value added to Doppler velocity in determining the angle over which to search for circle centers.

---

#### Adaptable Parameters:    **Flocks of Waterfowl Algorithm**

Mnemonic	Working value	Description
AgeThL	3 scans	Lower threshold for path length.
AreaCor	160 km	Correction constant to correct minimum area of echo segments for influence of range.
BirdVel	70 km hr <sup>-1</sup>	Nominal flight speed of waterfowl
BunchSizThU	12	Maximum BunchSize before BunchSize is artificially reduced.
ContinRefThU	12 km ?	Maximum radial extent of continuous REF in a waterfowl echo segment.
DeltaDThU	10 ms <sup>-1</sup>	Rejection criterion for DELTA_D when BunchSize > BunchSizThU
DeltSpdThL	120 km hr <sup>-1</sup>	Minimum delta estimated flight speed to consolidate together two echo segments in sweeps with different elevations. Species-specific flight speed + 2 S.D.s is used as the value.
GapThL	5 min	Longest gap in continuous PPI volume scan data.

HeightThL	0.15 km	Lowest waterfowl migration, AGL.
HeightTHU	?	Highest waterfowl migration, AGL
MeasWt <sub>1</sub> - MeasWt <sub>4</sub>	1.0	Weights used with the four decision-sum measures.
NGateThL	4	Minimum number of gates for an echo segment.
PerimThU	180	Maximum perimeter size of an echo segment, in gates.
RadDistThU	1 km	Maximum radial distance between gates in the same echo segment.
RefThL	0.5 dBZ	Lower threshold for REF
SearchThU	150 km hr <sup>-1</sup>	Maximum distance from the tip of the wind vector to look for a match.
SWThU	10 ms <sup>-1</sup>	Upper threshold for spectral width of a gate. This value may be too high.
TotRefA	-0.39	 N geese = 10(TotREfA + TotRefB*TotRef)
TotRefB	0.067	
VelThU <sup>1</sup>	4 ms <sup>-1</sup>	Upper threshold for Doppler speed
VelThL <sup>1</sup>	-4 ms <sup>-1</sup>	Lower threshold for Doppler speed
WgtSWThU	7 ms <sup>-1</sup>	Upper threshold for weighted average spectral width. This value may be too high.

---

<sup>1</sup> VEL thresholds will depend on clutter filter characteristics during operation.